

NEW IDEAS FOR YUKAWA INTERACTIONS  
AND THE ORIGIN OF MASS

By

Zeke Murdock  
Bachelor of Arts in Liberal Arts  
St. John's College  
Santa Fe, NM, USA  
2003

Submitted to the Faculty of the  
Graduate College of  
Oklahoma State University  
in partial fulfillment of  
the requirements for  
the Degree of  
DOCTOR OF PHILOSOPHY  
July, 2011

NEW IDEAS FOR YUKAWA INTERACTIONS  
AND THE ORIGIN OF MASS

Dissertation Approved:

Dr. Satya Nandi

---

Dissertation Advisor

Dr. Kaladi Babu

---

Dr. Flera Rizatdinova

Dr. Birne Binegar

---

Dr. Mark E. Payton

Dean of the Graduate College

## ACKNOWLEDGMENTS

In my time studying physics at Oklahoma State University I have had the great privilege to have lengthy discussions with so many individuals. These discussions have extensively shaped my knowledge and understanding of particle physics. I am grateful to my professors, Dr. Nandi, Dr. Babu, Dr. Khanov, and Dr. Rizatdinova for holding weekly seminars that exposed me to the ideas that are on the frontier of particle physics. They have always been patient and understanding as I learned. In spite of the large classes that they are responsible for, they have always been available to help me when I stopped by their office for clarification of these difficult ideas.

The postdocs here have also made themselves amazingly available to me. Santosh Rai and Zurab Tavartkiladze were immensely helpful in much of the work in this document. They sat with me and explained the intricate details of laborious calculations with great patience, even as they juggled their own projects and problems.

I have had the great fortune to share the high energy office with some fantastic minds. I can't possibly count the number of times that I went to Ben Grossmann's desk to ask him for help with a problem that I was working on. I've never met anyone else in my life that is so willing to help people understand difficult problems. He also collaborated with me on the work in chapter 5. I have had many fruitful discussions with the other students here as well. Julio, Abdelhamid Albaid, Steven Gabriel, Ayon Patra, Sakhi Khan, and Leo Meng have all helped me many times with difficulties that I have had.

I thank Dr. Joe Lykken for collaborating with Dr. Nandi and myself in the work of chapter 3. The Department of Energy has provided the financial support for my

time as a research assistant at OSU. Before becoming an RA, the Department of Physics was gracious enough to provide me with a teaching assistantship for my first three years in the program.

Finally, Thank you to the members of my committee for taking the time and effort to be a part of this process. Especially Dr. Binengar who graciously accepted to join my committee at the last minute when my previous outside member was not available. Of course, Dr. Nandi has been immeasurably helpful to me. I haven't been the easiest person to advise, but he has worked with me every step of the way, pushing and driving me to the place that I am now.

## PREFACE

This dissertation is based on 5 papers I have written in collaboration with various authors as listed below. Three have been published and 2 are submitted for publication. These are mostly based on introducing new ideas for the Yukawa sector of the Standard Model and exploring how these ideas can be tested experimentally in high energy colliders.

- \* Z. Murdock, S. Nandi and Z. Tavartkiladze, “Perturbativity and a Fourth Generation in the MSSM,” *Phys. Lett. B* **668**, 303 (2008).
- \* J. D. Lykken, Z. Murdock and S. Nandi, “A light scalar as the messenger of electroweak and flavor symmetry breaking,” *Phys. Rev. D* **79**, 075014 (2009).
- \* B. N. Grossmann, Z. Murdock and S. Nandi, “Neutrino Masses from Fine Tuning,” *Phys. Lett. B* **693**, 274 (2010).
- \* Z. Murdock, S. Nandi and S. K. Rai, “Non-renormalizable Yukawa Interactions and Higgs Physics,” *arXiv:1010.1559 [hep-ph]*.
- \* B. N. Grossmann, Z. Murdock and S. Nandi, “Fermion Mass Hierarchy from Symmetry Breaking at the TeV Scale,” *arXiv:1011.5256 [hep-ph]*.

# TABLE OF CONTENTS

Chapter	Page
<b>1 INTRODUCTION</b>	<b>1</b>
1.1 The Standard Model . . . . .	1
1.2 Particle Content . . . . .	1
1.3 Electroweak Symmetry Breaking . . . . .	3
1.3.1 Gauge Invariance . . . . .	3
1.3.2 Spontaneous Symmetry Breaking . . . . .	5
1.3.3 The Higgs Mechanism . . . . .	7
1.3.4 $SU(2) \times U(1)$ Symmetry Breaking . . . . .	9
1.4 The Yukawa Sector . . . . .	11
1.5 CKM Matrix . . . . .	12
1.6 Extensions of the Standard Model . . . . .	13
1.7 Modifying the Yukawa Sector . . . . .	15
<b>2 NON-RENORMALIZABLE YUKAWA INTERACTIONS AND HIGGS PHYSICS</b>	<b>17</b>
2.1 Introduction . . . . .	17
2.2 Formalism . . . . .	18
2.3 Phenomenological implications . . . . .	20
2.3.1 Higgs decays . . . . .	20
2.3.2 Higgs productions and signals: implications at the Tevatron . . . . .	21
2.3.3 Higgs productions and signals: implications for the LHC . . . . .	23
2.4 Other implications . . . . .	24

<b>3</b>	<b>A LIGHT SCALAR AS THE MESSENGER OF ELECTROWEAK AND FLAVOR SYMMETRY BREAKINGS</b>	<b>27</b>
3.1	Introduction . . . . .	27
3.2	Model and formalism . . . . .	30
3.2.1	Fermion masses and CKM mixing . . . . .	32
3.2.2	Yukawa interactions and FCNC . . . . .	34
3.2.3	Higgs sector and the $Z'$ . . . . .	35
3.3	Phenomenological Implications: Constraints from existing data . . . .	36
3.3.1	$K^0 - \bar{K}^0$ mixing . . . . .	37
3.3.2	$D^0 - \bar{D}^0$ mixing . . . . .	37
3.3.3	Other rare processes . . . . .	37
3.3.4	Constraint on the mass of $s$ . . . . .	38
3.3.5	Constraint on the mass of the $Z'$ . . . . .	38
3.4	Phenomenological Implications: New physics signals . . . . .	39
3.4.1	Higgs signals . . . . .	39
3.4.2	Top quark physics . . . . .	44
3.4.3	$Z'$ physics . . . . .	44
3.4.4	$B_s^0 \rightarrow \mu^+ \mu^-$ . . . . .	45
3.4.5	Vectorlike fermions, productions and decays . . . . .	46
3.5	UV Completion . . . . .	47
3.5.1	Two generation model . . . . .	47
3.5.2	Three generation model . . . . .	51
3.6	Conclusion . . . . .	58
3.7	Extension of the Model . . . . .	60
<b>4</b>	<b>PERTURBATIVITY AND A FOURTH GENERATION IN THE MSSM</b>	<b>61</b>
4.1	Introduction . . . . .	61

4.2	Theoretical Bounds and Some Implications . . . . .	64
4.2.1	Bounds from Tree Level Unitarity . . . . .	64
4.2.2	Bounds from Perturbative RGE . . . . .	65
4.2.3	Implications for Higgs Physics . . . . .	67
4.3	The Model with Perturbative UV Completion . . . . .	68
4.4	Conclusions . . . . .	74
<b>5</b>	<b>NEUTRINO MASSES FROM FINE-TUNING</b>	<b>75</b>
5.1	Introduction . . . . .	75
5.2	Model and the formalism . . . . .	77
5.2.1	Our model . . . . .	77
5.2.2	Higgs potential . . . . .	78
5.2.3	Mixing between the light and heavy neutrinos . . . . .	79
5.3	Phenomenological implications . . . . .	83
5.3.1	LEP constraints . . . . .	83
5.3.2	Higgs decays and Higgs signals . . . . .	83
5.3.3	$ZH \rightarrow \nu\bar{\nu}b\bar{b}$ Search at Tevatron . . . . .	86
5.3.4	$N_R$ Decays via Charged Higgs . . . . .	86
5.4	Conclusions . . . . .	87
<b>6</b>	<b>CONCLUSIONS</b>	<b>89</b>
	<b>BIBLIOGRAPHY</b>	<b>91</b>



## LIST OF TABLES

Table		Page
3.1	Yukawa and gauge couplings of $h$ and $s$ . . . . .	40
3.2	Charge assignments in the two generation model for the scalar fields $H$ , $S$ , $F$ , and the SM quark fields $q_{3L}$ , $q_{2L}$ , $u_{3R}$ , $u_{2R}$ , $d_{3R}$ , and $d_{2R}$ . Also listed are the color triplet weak doublet heavy quark pairs $Q_{iL}$ , $Q_{iR}$ and the color triplet weak singlet heavy quark pairs $U_{iL}$ , $U_{iR}$ , $D_{iL}$ , $D_{iR}$ . . . . .	48
3.3	Charge assignments in the three generation model for the scalar fields $H$ , $S$ , $F_i$ , the SM quark fields $q_{iL}$ , $u_{iR}$ , $d_{iR}$ , and the heavy quark pairs $Q_{iL}$ , $Q_{iR}$ , $U_{iL}$ , $U_{iR}$ , $D_{iL}$ , $D_{iR}$ . . . . .	54
5.1	Solution values for the matrix $m_D$ . . . . .	81
5.2	Mixing angles between the light neutrinos (subscripts 1, 2, 3) and the heavy neutrinos (subscripts 4, 5, 6). . . . .	82
5.3	Collider Searches for $m_h = 120\text{GeV}$ . . . . .	86
5.4	Decay Rates for $N_R$ , $M_N = 80\text{ GeV}$ , $M_h = 120\text{ GeV}$ . . . . .	87

## LIST OF FIGURES

Figure		Page
2.1	Illustrating the branching ratios for Higgs decays in (a) SM and (b) new model as a function of its mass. We have used the package HDECAY [10] to calculate the Higgs decay modes. . . . .	20
2.2	Illustrating how the Tevatron bound on SM Higgs applies on the Higgs boson in our model. . . . .	22
2.3	Illustrating $\sigma \times BR$ for the SM Higgs and in our model for the decay modes $\tau\tau, \gamma\gamma$ and $WW$ at LHC with a center-of-mass energy of 7 TeV. . . . .	23
2.4	Cross section for double Higgs production through gluon gluon fusion for the SM Higgs (dashed) and for the Higgs in our model (solid) at LHC with a center-of-mass energy of 7 and 14 TeV. . . . .	26
3.1	Branching ratio of $h \rightarrow 2x$ , for $\theta=0$ and $\alpha=1$ [10]. . . . .	41
3.2	Branching ratio of $h \rightarrow 2x$ , for $\theta=20^\circ$ and $\alpha=1$ . . . . .	42
3.3	Branching ratio of $h \rightarrow 2x$ , for $\theta=26^\circ$ and $\alpha=1$ . . . . .	42
3.4	Branching ratio of $h \rightarrow 2x$ , for $\theta=40^\circ$ and $\alpha=1$ . . . . .	43
3.5	Branching ratio of $h \rightarrow 2x$ including $h \rightarrow ss$ and $h \rightarrow Z'Z'$ where $m_{Z'} = 40$ GeV and $m_s = 100$ GeV. Here $\alpha = 1$ . . . . .	45
3.6	Branching ratio of $s \rightarrow 2x$ including $s \rightarrow Z'Z'$ where $m_{Z'} = 40$ GeV. Here $\alpha = 1$ . . . . .	46
3.7	The Feynman diagram associated with Eq. (3.18) . . . . .	51
3.8	The Feynman diagram associated with Eq. (3.20) . . . . .	51
3.9	The Feynman diagram associated with Eq. (3.22) . . . . .	51

3.10	The Feynman diagram associated with Eq. (3.26) . . . . .	52
4.1	Plotting allowed quark masses using $3\sigma$ limits of $S$ and $T$ in green. Superimposed in red are constraints from all 3 parameters, $S$ , $T$ , and $U$ , while more wide, green, area corresponds to the analysis with ig- noring $U$ . Here, $M_h = 115$ GeV, $m_{\tau'} = 150$ GeV, and $m_{\nu'} = 100$ GeV. $(\Delta S, \Delta T, \Delta U)$ for the leptons are (0.01, 0.045, 0.11). . . . .	63
4.2	Plotting $\tan\beta$ vs. $\Lambda$ , the scale at which $y_{b'}$ becomes non-perturbative. For masses we took the lowest allowed values from Eq. 4.1. . . . .	66
4.3	Diagrams generating Yukawa couplings $\lambda_{t'}$ , $\lambda_{b'}$ and $\lambda_{\tau'}$ . . . . .	73
4.4	Plots at left hand side: running of Yukawa couplings $\lambda_t$ , $\lambda_{t'}^{(1)}$ , $\lambda_{b'}^{(1)}$ and $\lambda_{\tau'}^{(1)}$ . Right hand side: running of couplings $\lambda_U$ , $\lambda_D$ , $\lambda_D'$ , $\lambda_E$ . . . . .	73
5.1	Branching ratio of $h \rightarrow 2x$ . . . . .	84
5.2	Branching ratio of $h \rightarrow 2x$ with the coupling between $N_R$ and $\nu_L$ , $y = \frac{1}{7}$	85
5.3	Decay modes of $N_R$ . . . . .	85

## CHAPTER 1

### INTRODUCTION

#### 1.1 The Standard Model

The Standard Model of particle physics has proven to be a very successful model of the subatomic world. It is labeled by the symmetry group  $SU(3)_C \times SU(2)_L \times U(1)_Y$ . So much information is packed into that short expression, yet it is difficult to truly understand what it means without quite a bit of explanation. In order to understand it, let us look first at the particle structure of the Standard Model.

#### 1.2 Particle Content

The Standard Model includes within it a total of six flavors of quarks, six leptons, twelve force carrying particles, and the yet to be discovered missing piece: the Higgs boon. The quarks make up most of the matter that we see around us in our daily lives. The bound state of two up quarks and one down quark makes a proton, while two down quarks and an up quark make a neutron. Protons and neutrons form the nucleus of atoms with electrons orbiting in various patterns. The electron is a lepton and provides us with the electricity we need to power all the fantastic devices of this technological age in which we live. The electron, up quark, and down quark, along with the electron neutrino make up the first generation of particles in the standard model. This first generation is replicated at least two times with searches for a possible fourth generation still in progress at the Tevatron at Fermilab, and the Large Hadron Collider (LHC) at CERN. This replication is very curious. Why is it that there is a

muon and tau lepton that have the same quantum numbers as the electron, but are much heavier ( $m_\tau \sim 3500m_e$ )? Why are there two extra generations of quarks that do not compose any of the visible matter in the universe? The Standard Model does not answer these questions, and we will try to address them later in this document by proposing extensions to the current theory.

While the quarks and leptons make up the visible matter content of the universe, the way in which they interact is dictated by the four known fundamental forces. These forces have associated particles that act as the carriers of the forces. The simplest and most well-known is the photon which governs the electromagnetic interaction. The  $W$  and  $Z$  bosons discovered at CERN in the early 1980s are the force carriers of the weak interaction that governs radioactive decay processes. Together these interactions are unified to make the electroweak interaction represented by the symmetry  $SU(2)_L \times U(1)_Y$ . This symmetry was discovered by Glashow, Weinberg and Salam and correctly predicted the discovery of the  $W$  and  $Z$  bosons. Electroweak symmetry is the core of what we now call the Standard Model. It is a symmetry that is broken spontaneously giving us the  $U(1)_{em}$  symmetry of electromagnetism containing the familiar positive and negative charges of static electricity. Electroweak symmetry is broken via the Higgs mechanism that will be discussed below.

The third interaction is the strong force represented by the symmetry group  $SU(3)_C$ . This interaction holds together the quarks inside of the proton and neutron. The  $C$  stands for color as the charges of this interaction are named red, green, and blue. The carriers of this force are the gluons. While there is only one photon, a  $W^+$ , a  $W^-$  and one  $Z$ , there are 8 different flavors of gluons characterized by their different colors. The strong force has not been unified with the electroweak force, but there are attempts to do so in Grand Unified Theories (GUTs).

The fourth interaction is gravity. The graviton would be the carrier of the gravitational force, but we have not yet found it because the gravitational force is so

much weaker than the other three forces. Finding such a particle would allow us to construct a quantum theory of gravity and thus complete our picture of the known forces in the universe. Gravity is not included as part of the Standard Model, but the goal is to unify it with the other forces someday.

### 1.3 Electroweak Symmetry Breaking

The Standard Model combines the electromagnetic and weak interaction in the gauge symmetry,  $SU(2)_L \times U(1)_Y$  where  $U(1)_Y$  is called hypercharge symmetry. The Higgs Mechanism breaks this symmetry to  $U(1)_{em}$  and generates mass for the W and Z bosons which are the carriers of the weak force. This explains why the photon is massless while the mediators of the weak force are massive. The breaking of this symmetry generates a new massive particle called the Higgs boson. It has yet to be discovered, but limits have been put on its mass by experiments at the Tevatron and LEP. We know that if it in fact exists,  $m_h > 114$  GeV from LEP, and from the Tevatron the mass range, 155 – 172 GeV is excluded. In order to understand the Higgs mechanism we will first discuss gauge invariance.

#### 1.3.1 Gauge Invariance

Demanding gauge invariance is similar to demanding that the laws of physics should remain unchanged under a coordinate transformation. Take for example the Dirac Lagrangian for a fermino  $\psi$ :

$$\mathcal{L} = i\bar{\psi}\gamma^\mu\partial_\mu\psi - m\bar{\psi}\psi. \quad (1.1)$$

Consider now the  $U(1)$  symmetry transformation,

$$\psi \rightarrow e^{iq\alpha}\psi,$$

where  $q$  is the charge of the fermion under this symmetry and  $\alpha$  is an arbitrary parameter. If  $\alpha$  and  $q$  are unchanged under the derivative  $\partial_\mu$ , then the Lagrangian

remains unchanged, therefore the physics should remain the same. This is referred to as a global gauge transformation as it is the same everywhere in space and time. If instead  $\alpha$  were a function of the space-time coordinate  $x_\mu$ , then the Lagrangian would no longer be invariant. Such a transformation is referred to as a local gauge transformation as the function  $\alpha(x_\mu)$  varies in space and time. If we now demand that the Lagrangian remain invariant under such a local transformation, interesting things happen. Applying the transformation  $\psi \rightarrow e^{iq\alpha(x_\mu)}\psi$  to the Lagrangian above causes us to pick up an extra unwanted term:

$$\mathcal{L} \rightarrow \mathcal{L} - q[\partial_\mu \alpha(x_\mu)]\bar{\psi}\gamma^\mu\psi. \quad (1.2)$$

If we want our Lagrangian to be invariant under such a local gauge transformation, we will need to add something to cancel out the extra term that appears. In order to do this, let us introduce a new field  $A_\mu$  that transforms as

$$A_\mu \rightarrow A_\mu + \partial_\mu \alpha(x_\mu). \quad (1.3)$$

With this field we can add a new term to equation 1.1 so that it becomes:

$$\mathcal{L} = i\bar{\psi}\gamma^\mu\partial_\mu\psi - m\bar{\psi}\psi + q\bar{\psi}\gamma^\mu\psi A_\mu. \quad (1.4)$$

The additional term will cancel out the unwanted term of Eq. 1.2. This Lagrangian is now invariant under a local gauge transformation. Now there is a new field  $A_\mu$ , and we must write all terms in the Lagrangian that are allowed by this local gauge transformation. It is immediately evident that we cannot write a mass term such as  $m^2 A_\mu A^\mu$  as it would not be invariant under the transformation rule of equation 1.3. This means that the new field must be massless. We can however write a term like  $F^{\mu\nu} = \partial^\mu A^\nu - \partial^\nu A^\mu$  that *is* invariant under equation 1.3. Now if we put all the pieces together for our final Lagrangian we have:

$$\mathcal{L} = i\bar{\psi}\gamma^\mu\partial_\mu\psi - m\bar{\psi}\psi + q\bar{\psi}\gamma^\mu\psi A_\mu - \frac{1}{4}F^{\mu\nu}F_{\mu\nu}. \quad (1.5)$$

In this equation  $F_{\mu\nu}$  is the familiar field strength tensor of electrodynamics. The second to last term describes how the field  $A_\mu$  interacts with the field  $\psi$ , with the charge strength  $q$ . It should be clear now that the field  $A_\mu$  is the photon. It is quite remarkable that by requiring local gauge invariance in the Dirac Lagrangian we have generated the photon and the interactions that make up electrodynamics. This process works very well for electrodynamics because the photon is massless. However as seen above with the transformation rule of equation 1.3 we cannot write a mass term. This creates problems for the weak theory where the  $W$  and  $Z$  bosons are both massive particles. The solution to this comes from the Higgs mechanism and spontaneous symmetry breaking.

It is important to note that the local gauge transformation we have considered in this section involves a  $U(1)$  symmetry as the function  $e^{iq\alpha(x_\mu)}$  is a 1 dimensional “matrix”. This is how we have generated electrodynamics whose interactions are governed by a  $U(1)_{em}$  symmetry. When considering the weak interaction, our transformation will involve the 2 dimensional Pauli matrices as the weak interaction is associated with an  $SU(2)$  symmetry.

In this section we have discussed a pedagogical way to understand local gauge invariance, but for later sections it is important to note that we could have done the same thing by promoting the derivative in equation 1.1 to the covariant derivative as:

$$D_\mu = \partial_\mu + iqA_\mu, \tag{1.6}$$

keeping in mind how  $\psi$  and  $A_\mu$  transform as described above.

### 1.3.2 Spontaneous Symmetry Breaking

Spontaneous symmetry breaking happens when a symmetric theory collapses to a particular asymmetric state. A very simple example is if we can imagine a perfectly cylindrical pencil that is sharpened and made to stand on its point. While the initial



state is symmetric, at some point the pencil will fall choosing a particular direction thus becoming assymmetric.

In quantum field theory the Goldstone model is a simple example of spontaneous symmetry breaking. The Lagrangian for the Goldstone model is:

$$\mathcal{L} = \partial^\mu \phi^* \partial_\mu \phi - \mu^2 |\phi|^2 - \lambda |\phi|^4. \quad (1.7)$$

The field  $\phi$  is a complex scalar field that is invariant under the global gauge transformation  $\phi \rightarrow e^{iq\alpha} \phi$ . As above this is a  $U(1)$  symmetry. In classical Lagrangian mechanics, the Lagrangian is written as  $\mathcal{L} = T - V$ , where  $T$  represents all the kinetic energy terms and  $V$  represents the potential energy terms. Equation 1.7 has a similar form with:

$$\begin{aligned} T &= \partial^\mu \phi^* \partial_\mu \phi \\ V &= \mu^2 |\phi|^2 + \lambda |\phi|^4, \end{aligned}$$

where  $V$  represents the potential energy of the field  $\phi$ . In order for  $V$  to be bounded from below and have a ground state,  $\lambda$  must be positive. The sign of  $\mu^2$  can be either positive or negative. If  $\mu^2 > 0$  we can plot  $V(\phi)$  and we will have a paraboloid with a minimum at zero. This means that the vacuum expectation value or ground state of  $\phi$  is zero, or  $\langle 0 | \phi | 0 \rangle = 0$ . This global minimum means that the theory cannot exhibit spontaneous symmetry breaking.

The case of  $\mu^2 < 0$  is much more interesting for the task at hand. If we plot  $V(\phi)$  we will get a surface that is commonly described as a mexican hat potential with an unstable, local maximum at  $\phi = 0$ . There will also be a circle of minimum where  $\phi = \sqrt{\frac{-\mu^2}{2\lambda}}$ . This value can be easily found in the standard way by setting  $\frac{\partial V}{\partial \phi} = 0$ . Now the vacuum expectation value of  $\phi$  is non-zero:

$$\langle 0 | \phi | 0 \rangle = \sqrt{\frac{-\mu^2}{2\lambda}} = \frac{v}{\sqrt{2}}, \quad (1.8)$$

where  $v$  will be referred to as the vacuum expectation value or VEV from now on.

Now that we know the VEV, we can express  $\phi$ :

$$\phi(x_\mu) = \frac{v + \sigma(x_\mu) + i\eta(x_\mu)}{\sqrt{2}}, \quad (1.9)$$

where  $\sigma$  and  $\eta$  are fields that simply express  $\phi$  as a deviation from the ground state  $v$ . If we now rewrite the Lagrangian of Eq. 1.7 some important terms cancel (notably the mass term for the field  $\eta$ ):

$$\mathcal{L} = \frac{1}{2}\partial^\mu\sigma\partial_\mu\sigma + \frac{1}{2}\partial^\mu\eta\partial_\mu\eta - \lambda v^2\sigma^2 + \frac{\lambda}{4}(v^4 - \eta^4 - \sigma^4) - v\lambda\eta^2\sigma - \frac{\lambda}{2}\eta^2\sigma^2 - v\lambda\sigma^3 \quad (1.10)$$

Though we have not actually changed the field  $\phi$  in any way, several important things have happened. We have generated a mass term for the real component of the field ( $\sigma$ ) that is  $m_\sigma^2 = 2\lambda v^2$ . By contrast, we have no mass term for the imaginary component ( $\eta$ ),  $m_\eta = 0$ . The massless field  $\eta$  is often referred to as a Goldstone boson. We have generated several quartic and cubic interaction terms. While the original Lagrangian was invariant under a global  $U(1)$  transformation, the field  $\sigma$  does not obey the same transformation due to the cubic term in the Lagrangian. This means that our original symmetry has been spontaneously broken by the vacuum. As a result we have generated a massive boson  $\sigma$  and a massless Goldstone boson  $\eta$ . This is only a basic idea of spontaneous symmetry breaking. When we now combine this method of expanding the field about its VEV with the requirement of local gauge invariance, we get the Higgs mechanism.

### 1.3.3 The Higgs Mechanism

In the last section we demanded that our Lagrangian be invariant under a global transformation. Now we will demand that it be locally gauge invariant. We can start from Eq. 1.7, promote the derivatives to the covariant derivative, and add the interaction term  $F^{\mu\nu}F_{\mu\nu}$  giving us:

$$\mathcal{L} = D^\mu\phi^*D_\mu\phi - \mu^2|\phi|^2 - \lambda|\phi|^4 - \frac{1}{4}F^{\mu\nu}F_{\mu\nu}. \quad (1.11)$$

The covariant derivative is defined above in Eq. 1.6. The field  $\phi$  now transforms under the local transformation:

$$\phi(x_\mu) \rightarrow e^{iq\alpha(x_\mu)}, \quad (1.12)$$

and the vector field  $A_\mu$  transforms as in Eq. 1.3. If we now expand the covariant derivative  $D_\mu$  and use Eq. 1.9 to expand the scalar field  $\phi$  about its VEV we get (omitting the interaction terms for clarity):

$$\mathcal{L} = \frac{1}{2}\partial^\mu\sigma\partial_\mu\sigma + \frac{1}{2}\partial^\mu\eta\partial_\mu\eta - \lambda v^2\sigma^2 - \frac{1}{4}F^{\mu\nu}F_{\mu\nu} + \frac{q^2v^2}{2}A^\mu A_\mu + qvA^\mu\partial_\mu\eta + \text{interaction terms} \quad (1.13)$$

The last term in this equation,  $qvA^\mu\partial_\mu\eta$ , is troublesome as it is not an interaction term or a mass term. We would like to find a parameterization of the field  $\phi$  that avoids this spurious term. What we can do is to use our local gauge transformation of Eq. 1.12 to pick a specific gauge (referred to as the unitary gauge) in which the field  $\phi$  is real. In this way we rotate away the imaginary component of the field  $\phi$  and we have

$$\phi(x_\mu) = \frac{v + \sigma(x_\mu)}{\sqrt{2}}. \quad (1.14)$$

Now if we use this particular choice of gauge in Eq. 1.11 we have:

$$\mathcal{L} = \frac{1}{2}\partial^\mu\sigma\partial_\mu\sigma - \lambda v^2\sigma^2 - \frac{1}{4}F^{\mu\nu}F_{\mu\nu} + \frac{q^2v^2}{2}A^\mu A_\mu + \text{interaction terms} \quad (1.15)$$

An interesting thing has happened. The field  $A_\mu$  has now acquired a mass term,  $m_A = qv$ . What started out as a massless vector field has become a neutral massive vector boson thanks to the combination of local gauge invariance and spontaneous symmetry breaking. This combination is known as the Higgs mechanism. The Lagrangian describes a massive neutral scalar boson,  $\sigma$ , which is now referred to as a Higgs boson. The field  $\eta$ , the complex component of  $\phi$ , has now been absorbed into  $A_\mu$  to give it mass.

In this section we demanded that the complex field  $\phi$  be invariant under a local  $U(1)$  transformation. In the Standard model we start with  $SU(2) \times U(1)$  symmetry and generate mass for the  $W$  and  $Z$  bosons while leaving the photon massless.

### 1.3.4 $SU(2) \times U(1)$ Symmetry Breaking

The Standard Model Lagrangian combines the interaction of the fermions with the gauge bosons and the interactions of the gauge bosons with one another. All of the terms obey electroweak symmetry,  $SU(2) \times U(1)$ . Unfortunately if we were to write explicit mass terms into the Lagrangian for the fermions and gauge bosons, they would violate this symmetry. It is for this reason that we need the Higgs mechanism to introduce a new field that is invariant under electroweak symmetry but also breaks that symmetry thus giving mass to the vector bosons as shown in the last section. As we will see this same field ends up creating mass terms for the fermions. In order for this to work in the Standard Model, our choice of Higgs will be slightly different. If we start with a field  $\phi$  that is a doublet under weak isospin  $SU(2)$  we have:

$$\Phi(x_\mu) = \begin{pmatrix} \phi_1(x_\mu) + i\phi_2(x_\mu) \\ \phi_3(x_\mu) + i\phi_4(x_\mu) \end{pmatrix}. \quad (1.16)$$

The components of this field are complex. The upper component has isospin,  $I_3 = 1/2$  and the lower component,  $I_3 = -1/2$ . This field will transform just as the fermions do under  $SU(2)$ :

$$\Phi(x_\mu) \rightarrow e^{ig\boldsymbol{\tau} \cdot \boldsymbol{\lambda}(x_\mu)/2}, \quad (1.17)$$

where  $\boldsymbol{\tau}$  are the Pauli matrices which are the generators of the  $SU(2)$  group,  $g$  is the coupling constant for  $SU(2)_L$  weak isospin, and  $\boldsymbol{\lambda}(x_\mu)$  is an arbitrary function. The transformation rule for  $\phi$  under  $U(1)_Y$  weak hypercharge is:

$$\Phi(x_\mu) \rightarrow e^{ig'Y\alpha(x_\mu)}, \quad (1.18)$$

where  $Y$  is the hypercharge of the Higgs field and  $g'$  is the coupling strength for  $U(1)_Y$ . Weak hypercharge and weak isospin are related directly to electric charge as  $Q = I_3 + Y$ . Our Higgs Lagrangian will be similar to previous sections except that because  $\Phi$  is a matrix our notation will change slightly:

$$\mathcal{L} = (D^\mu \Phi)^\dagger (D_\mu \Phi) - \mu^2 \Phi^\dagger \Phi - \lambda (\Phi^\dagger \Phi)^2. \quad (1.19)$$

The covariant derivative for  $SU(2) \times U(1)$  is more complicated than in Eq. 1.6 as the symmetry group is larger and has more generators. The covariant derivative is:

$$D_\mu = \partial_\mu + ig\boldsymbol{\tau} \cdot \mathbf{W}_\mu/2 + ig'YB_\mu, \quad (1.20)$$

where  $W^\mu$  is a vector field for  $SU(2)$  with three components and  $B_\mu$  is a vector field for the  $U(1)$  hypercharge symmetry. Following from our methods of the previous section we can use gauge invariance to transform the field  $\Phi$  to the unitary gauge as:

$$\Phi(x) = \frac{1}{\sqrt{2}} \begin{pmatrix} 0 \\ h(x) + v \end{pmatrix}. \quad (1.21)$$

Where  $v$  is the VEV of the field  $\Phi$ . Because our Lagrangian has not changed in a major way, the VEV is still  $v = \sqrt{-\mu^2/\lambda}$ . If we now choose the hypercharge of  $\Phi$  to be  $Y = 1/2$ , then the field  $h$  will be neutral.

Putting all these pieces together we can produce mass terms for the gauge bosons and the Higgs boson,  $h$ . After this process the physical  $W$  and  $Z$  bosons and the photon end up being linear combinations of the  $W_\mu$  and  $B_\mu$  fields:

$$\begin{aligned} A_\mu &= W_\mu^3 \sin \theta_W + B_\mu \cos \theta_W \\ Z_\mu &= W_\mu^3 \cos \theta_W - B_\mu \sin \theta_W \\ W_\mu^\pm &= \frac{1}{\sqrt{2}} (W_\mu^1 \mp iW_\mu^2). \end{aligned}$$

The angle  $\theta_W$  is the weak mixing angle,  $\tan \theta_W \equiv g'/g$ . Its value has been determined experimentally from the measured couplings of the theory,  $g \sin \theta_W = e$ , where  $e$  is the

electromagnetic coupling. After doing all transformations and using the expressions above for  $A$ ,  $Z$  and  $W^\pm$  we obtain for the mass portion of the Lagrangian:

$$\mathcal{L}_{\text{mass}} = \frac{g^2 v^2}{4} W_\mu^+ W^{-\mu} + \frac{g^2 v^2}{8 \cos^2 \theta_W} Z_\mu Z^\mu + \lambda v^2 h^2 \quad (1.22)$$

From this equation we can read off the masses of the  $W$ ,  $Z$ , and Higgs bosons:

$$m_W = \frac{gv}{2}, \quad m_Z = \frac{gv}{2 \cos \theta_W}, \quad m_h = \sqrt{2\lambda v^2} = \sqrt{-2\mu^2}. \quad (1.23)$$

The imaginary parts of the field  $\Phi$  have been “eaten” by the  $W$  and  $Z$  fields to give them their mass. The photon is now massless which makes sense as the  $U(1)_{em}$  symmetry remains unbroken. By comparison, the gauge boson of  $SU(3)_C$ , the gluon, is also massless as that symmetry is unbroken as well.

We have now shown one role that the Higgs boson plays in the Standard Model. Next we will show how it gives mass to the fermions via Yukawa interactions.

## 1.4 The Yukawa Sector

In the previous section we mentioned that the weak hypercharge of the Higgs boson in the Standard Model is  $Y_h = 1/2$ . The hypercharge of the quark doublet,  $q_L = \begin{pmatrix} u^i \\ d^i \end{pmatrix}_L$ , is  $Y_q = 1/6$ , where  $i$  runs from 1 to 3 for the 3 generations. The right handed singlet,  $d_R^i$  has  $Y_d = -1/3$ . For the leptons we have  $l_L = \begin{pmatrix} \nu_e^i \\ e^i \end{pmatrix}_L$ . There is no  $\nu_R$ . We can now construct  $SU(2)_L \times U(1)_Y$  invariant interaction terms for the fermions and the Higgs boson:

$$\mathcal{L}_{\text{Yukawa}} = y_d^{ij} \Phi \bar{q}_L^i d_R^j + y_u^{ij} \tilde{\Phi} \bar{q}_L^i u_R^j + y_e^{ij} \Phi \bar{l}_L^i e_R^j. \quad (1.24)$$

These interactions are referred to as Yukawa interactions. Neutrinos have a very tiny mass, and we could write a Yukawa interaction for the neutrinos if  $\nu_R$  was present, however we have not seen right-handed neutrinos in the laboratory. Another issue

is that we still do not know if the neutrino is a Dirac or Majorana particle. We will discuss the problem of neutrino mass in more depth in chapter 5. The  $y^{ij}$  are dimensionless coupling constants called Yukawa couplings. Here,  $i$  and  $j$  run from 1 to 3 for the three generations, and  $\tilde{\Phi} = i\tau_2\Phi^*$ , where  $\tau_2 = \begin{pmatrix} 0 & -i \\ i & 0 \end{pmatrix}$ . In the unitary gauge,  $\tilde{\Phi} = \frac{1}{\sqrt{2}} \begin{pmatrix} h + v \\ 0 \end{pmatrix}$ . This pulls out the top component of the doublet to produce the correct mass term as,  $\frac{v}{\sqrt{2}}y_u^{11}\bar{u}_L^1u_R^1$ , which would be the mass term for the up quark. One thing to note here is that the size of the Yukawa couplings,  $y_u^{ij}$ , are not determined. This means that while the Higgs boson can give a mass term to the fermions, it cannot predict the size of the mass. We will discuss how to give values to these Yukawa couplings from a higher symmetry in chapter 3.

The Higgs boson serves several purposes in the Standard Model. It breaks electroweak symmetry, gives mass to the gauge bosons, and gives mass to the fermions. There is a little more to the story. The fermion fields as they are represented in Eq. 1.24 are written in the weak basis. In order to convert them to their corresponding mass eigenstates we need to introduce the Cabibbo-Kobayashi-Maskawa (CKM) matrix.

## 1.5 CKM Matrix

The components  $y_d^{ij}v/\sqrt{2} = M_d^{ij}$  make up a  $3 \times 3$  mass matrix for the down type quarks. There is of course a similar matrix  $M_u$  for the up type quarks. These matrices are not diagonal. When we diagonalize the mass matrix we use a biunitary transformation. These two transformation matrices also transform the quarks from the weak interaction eigenstate into their mass eigenstates as in,  $u_R^0 = S_u u_R$  and  $u_L^0 = T_u u_L$  where the superscript zero refers to the mass eigenstate and  $S_u^\dagger M_u T_u = M_u^{\text{diag}}$ . There are different matrices to diagonalize the down type quark mass matrix. In the

charged currents involving the  $W^\pm$  bosons we must make these same transformations. Because the matrices that transform the up quarks into their mass eigenstates are different from the ones for the down quarks, we get a new unitary mixing matrix known as the CKM matrix,  $V_{CKM} = T_u^\dagger T_d$ . This matrix describes the strength of the mixings in the weak sector. Through experiment physicists have measured the central values of this matrix:

$$\begin{pmatrix} V_{ud} & V_{us} & V_{ub} \\ V_{cd} & V_{cs} & V_{cb} \\ V_{td} & V_{ts} & V_{tb} \end{pmatrix} \approx \begin{pmatrix} 0.97428 & 0.2253 & 0.00347 \\ 0.2252 & 0.97345 & 0.0410 \\ 0.00862 & 0.0403 & 0.9991 \end{pmatrix} \quad (1.25)$$

where  $V_{us}$  represents the mixing between the up quark and the strange quark. Just as the Standard Model does not predict the strength of the Yukawa couplings, it does not predict the elements of the CKM matrix. In chapter 3 below we will show a model in which we derive these parameters from a higher symmetry.

## 1.6 Extensions of the Standard Model

The Standard Model has done a great job of describing the vast majority of experimental results. There are phenomena that it does not explain however. While neutrinos were previously thought to be massless, current experiments have shown that they have very tiny masses. Their masses are much much smaller than even the mass of the electron. Another phenomenon that the standard model fails to explain is Dark Matter. About 20% of the matter in the universe is dark matter. Dark because it is electrically neutral and interacts only very weakly with the matter of the standard model. Another common problem is often referred to as the hierarchy problem. The hierarchy problem refers to the fact that when we calculate quantum corrections to the mass of the Higgs boson, we end up with a quadratic divergence. In order to resolve these difficulties as well as some others people propose extensions to the Standard Model. Common examples are Supersymmetry and Extra Dimensions.



Supersymmetry proposes that for each fermion in the Standard Model there is a heavier “superpartner” that is a boson. For every boson there is a superpartner that is a fermion. For example the electron has spin  $1/2$ , it’s superpartner, the selectron, has spin  $0$ . If supersymmetry were an exact symmetry of nature, the superpartners would have the same mass as the Standard Model particles. Since we have not seen them we predict that supersymmetry must be broken at some scale. Currently we hope that the masses of the superpartners are in the TeV range so that we might be able to see them at the LHC. Supersymmetry solves the hierarchy problem because the quantum corrections to the Higgs mass are cancelled between the particles and their scalar superpartners. In addition most supersymmetric theories institute R-parity which forces the lightest supersymmetric particle (LSP) to be stable. In the simplest supersymmetric extension of the Standard model the Minimal Supersymmetric Standard Model (MSSM), this particle is the neutralino (a mixture of the Higgsino, Wino, and Bino). Given the correct couplings and mass for this particle it may be able to account for the dark matter content of the universe. In chapter 4 of this thesis we will discuss extending the MSSM to add a fourth generation of fermions.

Another extension of the Standard model that we will discuss below is a Froggatt-Nielsen mechanism. This is where there is some sort of more complicated interaction involving many particles at a higher scale that we are able to probe with current physics. These higher interactions reduce to the low energy effective theory of the Standard Model. We will use this mechanism along with the introduction of a singlet Higgs in order to generate the fermion masses and mixings of the CKM matrix in chapter 3. In the development of this and above sections, several references were used [1, 2, 3].

## 1.7 Modifying the Yukawa Sector

Now that we have developed what the Higgs boson is and how it interacts with the fermions, our focus will be to modify the existing Yukawa interactions to solve problems of the standard model or simply to question them. We then show how these modifications effect experimental results that may be tested at the LHC or Tevatron. The Yukawa sector of the Standard Model is the least understood. We cannot directly measure the Yukawa couplings, and we have not yet found the Higgs Boson. It is for this reason that modifying the Yukawa sector will be the main focus of this thesis.

In chapter 2 we will discuss how the standard dimension 4 Yukawa interactions of the Standard Model are not the only way to generate mass for the fermions. If for some reason the dimension 4 terms are absent then the fermion masses will come from dimension 6 operators. If this proposal is correct, the most interesting effect is that the phenomenology of Higgs searches at the Tevatron and LHC would be changed. Specifically broadening the exclusion range for the mass of the Higgs boson.

In chapter 3 we will use a Froggatt-Nielsen mechanism to generate the masses and mixings of the quarks in the Standard Model. The Yukawa couplings in this model are all of a similar order. The hierarchy of masses in the Standard Model will be generated through higher order interactions involving vector-like quarks and flavon scalars. The quarks of the standard model are chiral, as they have a left handed doublet and right handed singlet. Our proposal leads to interesting results at colliders if there is any truth to our model. In particular one version of our model allows the  $h \rightarrow \gamma\gamma$  signal to be increased by a factor of 10. This is a very important mode for Higgs discovery at the LHC if the Higgs is light.

In chapter 4 we will work in the framework of the MSSM and add a fourth generation. We will discuss limits on the masses of fourth generation particles based on the perturbativity of their Yukawa couplings. We place very stringent limits on the parameter  $\tan\beta$  and the masses for the 4th generation  $b'$  and  $t'$  quarks. In or-

der to broaden these limits we construct a model in which the Yukawa couplings are modified by the introduction of new heavy vector-like quarks.

In chapter 5 we discuss the problem of neutrino mass. We introduce a new way to give masses to neutrinos by fine tuning the values of two different Yukawa matrices. This allows us to have a right handed neutrino that has a mass of about 100 GeV. This leads to some interesting physics signals at the LHC which we discuss.

## CHAPTER 2

# NON-RENORMALIZABLE YUKAWA INTERACTIONS AND HIGGS PHYSICS

### 2.1 Introduction

The Standard Model (SM) based on the gauge symmetry  $SU(3)_C \times SU(2)_L \times U(1)_Y$  is in excellent agreement with all the current experimental results. However, there are sectors of the SM which are still untested, such as the Higgs sector and the Yukawa sector. In the SM, we have only one Higgs doublet, and we allow the Higgs self interactions up to dimension four to maintain the renormalizability of the theory. In this case, the cubic ( $h^3$ ) and the quartic ( $h^4$ ) interactions of the remaining neutral scalar Higgs field,  $h$  is determined in terms of the Higgs mass,  $M_h$  and the known vacuum expectation value (VEV),  $v$ . Although we know  $v$  experimentally to a very good accuracy, the Higgs mass is still unknown. Hence its presence, as well as the magnitude of its cubic and quartic self interactions are completely untested. The other untested sector of the SM is the Yukawa sector. In the SM, we introduce dimension four Yukawa interactions which give masses to the fermions, and also generate the Yukawa interactions between the Higgs field  $h$  and the fermions. The strength of these Yukawa interactions are completely determined in terms of the fermion masses and  $v$ . However, we do not have any experimental evidence for these interactions being the source of the fermion masses, and the presence of these dimension four Yukawa interactions. Another point to emphasize is that we do not know whether the Higgs boson is elementary or composite. Theories have been formulated in which the Higgs boson is a fermion anti-fermion composite; or more specifically a condensate of the

third family quark and anti-quark [4]. Other possibilities for composite Higgs have also been advocated [5, 6]. Whether the Higgs boson is an elementary particle or composite, the operators of dimension higher than four suppressed by some scale,  $M$  are expected. It has also been pointed out that the presence of dimension six operator in the Higgs potential allows us to have baryogenesis via sphaleron [7], still satisfying the current LEP limit on the Higgs mass.

In this work, we propose an alternate scenario for the Yukawa sector, and explore how to test our predictions experimentally at the Tevatron and LHC. The effects of general dimension six operators in the Higgs sector have been considered and studied before [8]. Also other dimension six operators may appear in SM and a complete list of such operators is collected in Ref. [9]. We consider the case in which the usual dimension four Yukawa interactions are either forbidden by a symmetry, or the corresponding coupling happens to be too tiny to generate the observed values of the fermion masses. In this case, the dominant contribution to the fermion masses, as well as the interactions between the fermions and the Higgs boson will arise from the dimension six effective Yukawa interactions of the form  $(f/M^2)\bar{\psi}_L\psi_R H(H^\dagger H)$ , where  $M$  is the mass scale for the new physics through which such effective interactions are generated. As in the SM, fermion masses are still parameters in the theory, but the Yukawa couplings of the fermions to the Higgs boson are a factor of three larger than the SM. This enhances the production of the Higgs boson, as well as affect its decay branching ratios to various final states. This will have interesting consequences for Higgs signals at the Tevatron and LHC, as well as in the possible future lepton collider.

## 2.2 Formalism

Our model is based on the SM gauge symmetry,  $SU(3)_C \times SU(2)_L \times U(1)_Y$ . We denote the left handed electroweak (EW) quark doublets by  $q_{Li} \equiv (u, d)_{Li}^T$ , and the

right handed EW quark singlets by  $u_{Ri}$  and  $d_{Ri}$ , where the index  $i$  ( $i = 1, 2, 3$ ) represent three fermion families. Then the Yukawa interactions of the fermions with the Higgs boson up to dimension six are given by

$$\begin{aligned} \mathcal{L}_{\text{Yukawa}} = & \bar{q}_L f_u u_R \tilde{H} + \bar{q}_L f_d d_R H + \bar{l}_L f_l e_R H \\ & + \frac{1}{M^2} (\bar{q}_L y_u u_R \tilde{H} + \bar{q}_L y_d d_R H + \bar{l}_L y_l e_R H) (H^\dagger H) + h.c., \end{aligned} \quad (2.1)$$

where the fermion fields represent three families, and  $f_d, f_u$  and  $f_l$  represent three corresponding Yukawa coupling matrices for the dimension four Yukawa interaction while  $y_d, y_u$  and  $y_l$  represent three corresponding Yukawa coupling matrices for the dimension six Yukawa interactions.  $M$  is the mass scale for a new physics which generates these dimension six interactions.

Our proposed scenario is the case in which the dimension four Yukawa couplings,  $f_d, f_u$  and  $f_l$  are either forbidden by a symmetry, or happen to be very tiny to generate the observed fermion masses, and this sector is dominated by dimension six interactions given above. Thus, choosing the couplings  $f$  to be zero, for the fermion mass and the Yukawa coupling matrices, we obtain

$$\begin{aligned} \mathcal{M}_{\text{New}} &= \frac{1}{2\sqrt{2}M^2} y_d (v^3), \\ \mathcal{Y}_{\text{New}} &= \frac{1}{2\sqrt{2}M^2} y_d (3v^2), \end{aligned} \quad (2.2)$$

and similar expressions for the up quark and lepton sector. In contrast, in the usual SM, where we do not include the effective dimension six interactions, we have

$$\mathcal{M}_{\text{SM}} = \frac{1}{\sqrt{2}} f_d (v), \quad \mathcal{Y}_{\text{SM}} = \frac{1}{\sqrt{2}} f_d. \quad (2.3)$$

In our scenario, one can see from Eq. 2.2 that the mass matrices and the corresponding Yukawa coupling matrices are proportional. Hence as in the usual SM, we do not have any Higgs mediated flavor changing neutral current interactions. The important point to note is that in our scenario (for simplicity, we call it the new model), the Yukawa

couplings of the Higgs boson to the fermions are three times larger than those in the SM, whereas the gauge interaction of the Higgs boson remains the same. This will make important differences for Higgs production, and its decay branching ratios as we discuss below.

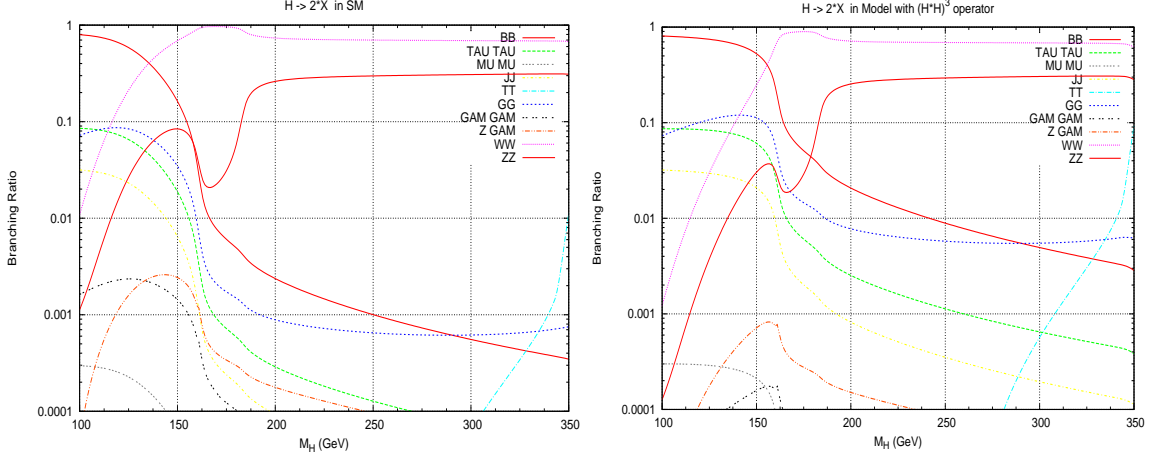


Figure 2.1: Illustrating the branching ratios for Higgs decays in (a) SM and (b) new model as a function of its mass. We have used the package HDECAY [10] to calculate the Higgs decay modes.

## 2.3 Phenomenological implications

### 2.3.1 Higgs decays

In the low Higgs mass range ( $M_h \leq 125$  GeV), the Higgs boson dominantly decays to  $b\bar{b}$  in the SM. This mode is even more dominant in the new model, since the  $hb\bar{b}$  coupling is enhanced by a factor of three compared to the SM. In the SM, the  $b\bar{b}$  to  $WW$  crossover takes place at  $M_h \sim 135$  GeV (see fig. 2.1a), while in our model, this crossover happens at  $M_h \sim 155$  GeV, (see fig. 2.1b). Also, as can be seen from these figures, the  $\gamma\gamma$  branching fraction in our model is suppressed by about a factor of ten compared to the SM. The reason is that in the  $h \rightarrow \gamma\gamma$  decay, the contribution comes

from the  $W$  loop and the top quark loop, and the two contributions are of opposite sign. In our model, because the  $ht\bar{t}$  coupling is enhanced by a factor of three, there is a strong cancelation between the top loop and the  $W$  loop contributions, resulting in the large suppression in the  $\gamma\gamma$  mode. Note that in our model, Higgs couplings to the gauge bosons  $WW$  and  $ZZ$  are unaltered, hence these branching ratios get suppressed compared to the SM as long as  $hb\bar{b}$  is dominant. For heavy Higgs mass range,  $M_h \geq 155$  GeV, the  $WW$  mode starts to dominate, and hence the branching ratio to this mode is very similar to the SM. The same is true for the  $ZZ$  mode. The branching ratio for the  $ZZ$  mode is also essentially the same as the SM for larger mass ranges ( $M_h \geq 185$  GeV).

### 2.3.2 Higgs productions and signals: implications at the Tevatron

Now we discuss Higgs production and the ensuing final state signals in our model and contrast those with the SM. First we consider the Higgs search at the Fermilab Tevatron. For the SM Higgs boson, recent combined analysis by the CDF and D0 collaborations (using  $6.7\text{ fb}^{-1}$  of data) has excluded the SM Higgs mass range from 158 to 175 GeV at 95% confidence level (C.L.) [11, 12]. The dominant production mechanism for the Higgs boson is gluon gluon fusion via the top quark loop. Since in our model, the coupling of the Higgs to the top quark is three times larger, the Higgs production cross sections will be nine times larger than the SM. Higgs production via the gauge interactions to  $Wh$  and  $Zh$  in our model remains the same as in the SM. Combined Tevatron analysis includes the Higgs signals for all channels, and the corresponding backgrounds. Their experimental curve for the observation of the Higgs signals at 95% C.L. over the SM expectation curve as a function of the Higgs mass is shown by the solid curve in fig. 2.2 [12]. The corresponding SM expectation is shown by the horizontal dash-dotted line. As shown by the Tevatron analysis (solid curve), the SM Higgs mass in the range of 158 – 175 GeV is excluded. The corresponding



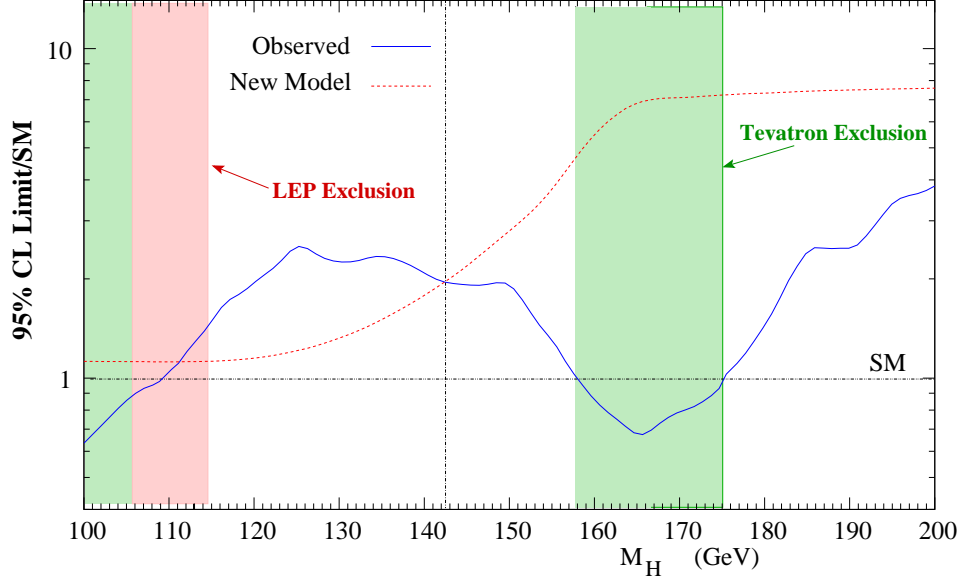


Figure 2.2: Illustrating how the Tevatron bound on SM Higgs applies on the Higgs boson in our model.

exclusion in the low mass range is  $M_h \geq 109$  GeV which falls short of the LEP exclusion of  $M_h \geq 114.4$  GeV [13]. To apply this combined CDF-D0 analysis to our model, we have calculated the  $\sigma_{p\bar{p} \rightarrow h} \times BR(h \rightarrow all)$  included by the Tevatron, and compared those with the SM. The dashed curve in fig. 2.2 shows our results for the ratio of the  $\sigma_{p\bar{p} \rightarrow h} \times BR(h \rightarrow all)$  in our model to the  $\sigma_{p\bar{p} \rightarrow h} \times BR(h \rightarrow all)$  in the SM as a function of the Higgs mass. The intersection of the dashed curve with the solid curve indicates an estimate of the Higgs mass range ( $M_h \gtrsim 142$  GeV) that would be excluded by the present Tevatron analysis in our model.

In the low Higgs mass range, the lower exclusion range increases slightly from  $M_h > 109$  GeV in the SM to  $M_h > 112$  GeV in our model. As the Tevatron luminosity accumulates further, its increased sensitivity to our model will help it study a bigger mass range of the Higgs boson than in the SM. Also, we note that for light Higgs ( $M_h < 130$  GeV), the width of the Higgs boson in our model is larger by a factor of 9 compared to the SM. This can be tested in a possible future muon or  $e^+e^-$  collider.

### 2.3.3 Higgs productions and signals: implications for the LHC

At the LHC, in the SM for large Higgs mass,  $M_h > 150$  GeV, the most promising signals to observe the Higgs boson is via its dominant production through gluon gluon fusion (or  $WW$  fusion), and then its subsequent decays to  $WW$  or  $ZZ$ . In our model, since the dominant Higgs productions via gluon gluon fusion is nine times larger, the Higgs signals will be much stronger. The expectation for the Higgs signals in few of the relevant modes in our model is shown in fig. 2.3 (solid curve), and are compared with the SM expectations (dash-dotted curves) at the LHC for  $\sqrt{s} = 7$  TeV. Note that the cross section times the branching ratio of  $h \rightarrow WW$  in our model is larger than the SM by a factor of  $\sim 3 - 9$  for the Higgs mass range of  $150 - 200$  GeV. The same is true for the  $ZZ$  mode. For the low mass range of the Higgs boson,  $M_h \sim 115 - 130$  GeV, the  $\gamma\gamma$  mode is the most promising in the SM. In our model though, as shown in fig. 3, the signal for the  $\gamma\gamma$  mode is reduced by a factor of  $\sim 3 - 5$  compared to the SM. However, the signal in the  $\tau\tau$  mode is enhanced almost by a factor of nine. Thus in our model, signal in the  $\tau\tau$  mode may be observable at the LHC for the low Higgs mass range with good  $\tau$  ID for the ATLAS and CMS detectors.

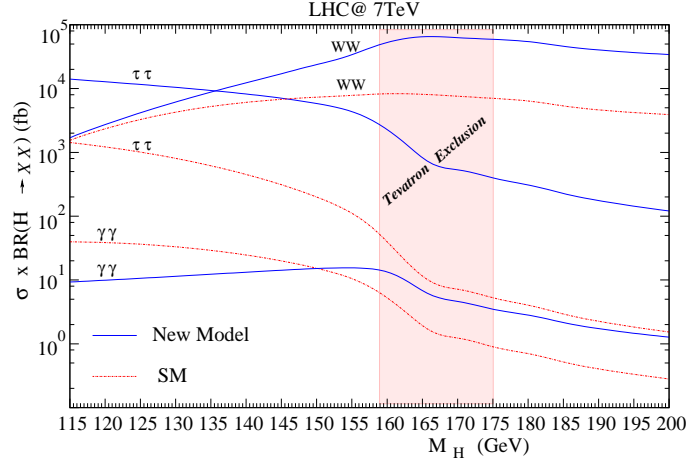


Figure 2.3: Illustrating  $\sigma \times BR$  for the SM Higgs and in our model for the decay modes  $\tau\tau$ ,  $\gamma\gamma$  and  $WW$  at LHC with a center-of-mass energy of 7 TeV.

## 2.4 Other implications

Inclusion of dimension six operators in the Yukawa sector also leads to enhancement in the other modes of Higgs production at colliders. The associated production of a Higgs boson with a heavy quark pair (e.g.  $t\bar{t}h$ ) is enhanced by a factor of 9. The increased event rate would help in improving the sensitivity for the top-Yukawa coupling in this channel at LHC [14, 15].

Another important implication of our model is on double Higgs production at the LHC which can probe the triple Higgs vertex in SM. In the SM, double Higgs production at LHC proceeds through gluon gluon fusion at one-loop level through the top quark dominated *triangle* and *box* diagrams [17, 16, 18]. Due to additional contributions coming from the terms involving the dimension six operators, there is an enhancement in all the vertices involving the Higgs boson in our model. The box contribution is enhanced by a factor of 9 in its amplitude because of two Yukawa vertices, while the triangle contribution is enhanced by a factor of 5, after combining the new Yukawa and triple Higgs vertices (arising from the Higgs potential where we neglect the dimension 4 operator). There is an additional contribution to the amplitude through a new interaction term ( $\bar{f}_L f_R h^2$ ) with a coupling strength of ( $\frac{6im_f\alpha_{EW}}{M_W^2}$ ) where  $m_f$  is the mass of the fermion which leads to a large enhancement of the double Higgs production cross section at LHC. The analytical formula for the double Higgs production in SM can be found in Ref.[17, 18]. To put our results in context we can rewrite the contributions in our model as

$$\begin{aligned} A_{\Delta}^{NP} &= 5 \times A_{\Delta}^{SM} + 2 \times A_{\Delta}^{SM} \frac{\hat{s} - M_h^2}{M_h^2} \\ A_{\square}^{NP} &= 9 \times A_{\square}^{SM} \end{aligned} \tag{2.4}$$

We plot the double Higgs production cross section<sup>1</sup> as a function of the Higgs mass in fig. 2.4 for both the SM as well as our model. Although Eq. 2.4 shows a large en-

---

<sup>1</sup>We use the public code available at <http://people.web.psi.ch/spira/proglist.html>

hancement in the individual contributions, there still is large cancelation between the box and triangle contributions and so the enhancement in the cross section compared to the SM is only at the level of a factor of  $\sim 10$  for low Higgs masses as shown in fig. 2.4 which increases as we go higher in the Higgs mass. Nevertheless it is a substantial increase for the light Higgs mass range and gives a cross section of around  $\sim 300$  fb at LHC with  $\sqrt{s} = 14$  TeV and  $\sim 40$  fb with  $\sqrt{s} = 7$  TeV, respectively for  $M_h \leq 220$  GeV. This can give large enough event rates to study the double Higgs production at LHC.

Finally, let us comment on the scale of new physics,  $M$ . Up to dimension six, we can write the Higgs potential as

$$V_{\text{New}} = -\mu^2(H^\dagger H) + \lambda(H^\dagger H)^2 + \frac{1}{M^2}(H^\dagger H)^3. \quad (2.5)$$

Choosing  $\lambda$  to be zero, the condition for the global minima gives

$$M_h M = \sqrt{3} v^2. \quad (2.6)$$

Using the LEP bound for the Higgs mass,  $M_h > 114$  GeV, from Eq. 2.5, we obtain  $M \leq 1$  TeV. Note the interesting see-saw type relation between the  $M_h$  and  $M$  in Eq. 2.6. Thus if our point of view is correct, we expect the new physics to appear below the TeV scale.

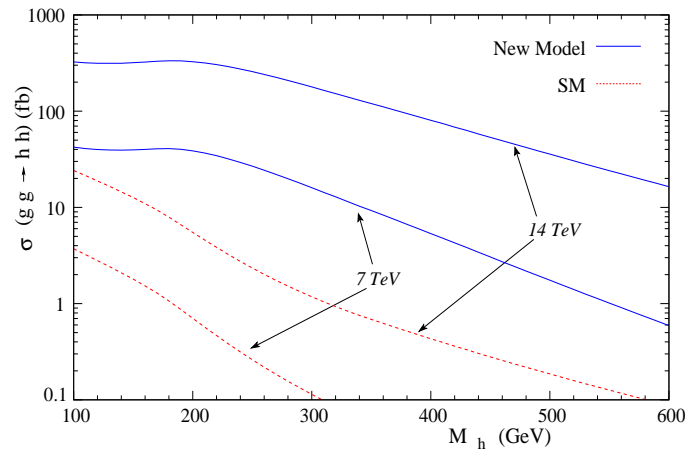


Figure 2.4: Cross section for double Higgs production through gluon gluon fusion for the SM Higgs (dashed) and for the Higgs in our model (solid) at LHC with a center-of-mass energy of 7 and 14 TeV.

## CHAPTER 3

# A LIGHT SCALAR AS THE MESSENGER OF ELECTROWEAK AND FLAVOR SYMMETRY BREAKINGS

### 3.1 Introduction

Explaining the fermion mass hierarchy and mixing pattern is an outstanding challenge of particle physics [20][21][22]. The fermion masses are parameterized by the standard model Yukawa interactions of chiral fermions with a single Higgs doublet. It is technically natural for the dimensionless Yukawa couplings to take small values, since global chiral flavor symmetries are restored (at tree level) in the limit that these couplings vanish, but it is a total mystery why these values are spread over more than five orders of magnitude, in a suggestive pattern of inter-generational and intra-generational hierarchies.

Although the gauge sector of the SM is well established, little is yet known about the Higgs sector. Higgs physics may be much richer than the minimal SM formulation, presenting new dynamics at the TeV scale that will be accessible to experiments at the LHC. Most work on extended Higgs sectors has been motivated by frameworks for understanding the naturalness and hierarchy problem of the SM Higgs boson, but not by the hierarchy problems of the SM flavor sector. One reason is that models that attempt to generate the flavor-breaking patterns of the SM Yukawas from new TeV scale dynamics are strongly constrained by experimental searches for flavor-changing neutral currents (FCNCs) and charged lepton flavor violation (CLFV).

The top quark Yukawa coupling has a value close to one, suggesting that a SM Yukawa coupling is the correct explanation for the top mass. The smallness of the

other Yukawas suggests that some or all of the other quarks and the charged leptons do not couple directly to the electroweak symmetry breaking order parameter, which in the SM is represented by the vacuum expectation value (vev) of the Higgs scalar. Thus a good starting point to construct theories of flavor is to specify a field or mechanism to act as the messenger of electroweak symmetry breaking to the other quarks and leptons.

One simple choice for a messenger is a TeV mass scalar leptoquark, postulated to have a renormalizable coupling between the top quark and the SM leptons [23, 24]. Radiative corrections can then generate a natural hierarchy of fermion masses related to powers of a loop factor.

An even simpler choice for a messenger is an electroweak mass scalar that transforms as a SM singlet and extends the Higgs sector of the SM. In this work, we explore this idea of an extended Higgs sector related to the generation of the fermion mass hierarchy. We present a simple framework where the Higgs doublet  $H$  couples directly to a complex scalar  $S$  that is a SM singlet and is charged under a new local  $U(1)_S$  symmetry carried by a vector boson  $Z'$ . All of the SM fermions are singlets under this new  $U(1)_S$  (apart from small effects from  $Z - Z'$  mixing), which is broken spontaneously at the electroweak scale by the vacuum expectation value of  $S$ .

In our framework the singlet scalar  $S$  is the messenger to SM fermions of both flavor breaking and electroweak symmetry breaking. All SM fermions apart from the third generation quark doublet  $Q_{3L}$  and right-handed top  $u_{3R}$  are assumed to carry a nonzero charge under a gauged chiral flavor symmetry forbidding all SM dimension 4 Yukawa couplings except that of the top quark. We assume that the flavor symmetry is spontaneously broken at a scale  $> 1$  TeV by the vacuum expectation of one or more complex scalar “flavon” fields  $F_i$ . The flavor charges of the SM fermions forbid any dimension 4 couplings to either  $F_i$  or to the Higgs field  $H$ .

We introduce new fermions that are vectorlike under both the SM gauge sym-

metries and  $U(1)_S$ ; these fermions naturally acquire masses  $> 1$  TeV that we will generically denote as  $M$ , and have dimension 4 couplings to both  $F_i$  and to  $H$ . Integrating out these heavy fermions gives higher dimension effective couplings of the SM fermions to  $H$  that replace the role of Yukawa couplings in the SM. These couplings contain explicit flavor breaking in the form of  $\langle F_i \rangle / M$ , which we take to be of order 1, as well as being suppressed by powers of  $S^\dagger S / M^2$ , whose vev we take to be of order  $1/50$ .

In our framework all of the observed SM fermion mass hierarchies are generated from powers of  $\langle S \rangle / M \sim 1/7$ , which is essentially the ratio of the electroweak scale to the TeV scale, often called the “little hierarchy”. We can be agnostic about the source of the little hierarchy itself, since many possibilities have been proposed. The additional challenge of our framework is to achieve simultaneously the appropriate flavon physics at the TeV scale.

Models in our framework have, in addition to the SM particle content, a light singlet scalar  $s$  that mixes with the Higgs boson  $h$ . Exchanges of  $s$  between SM fermions are a new source of FCNC. There is an extra  $Z'$  at the EW scale, but apart from small  $Z - Z'$  mixing effects it does not couple to SM fermions. There may be other  $Z$ 's and one or more flavon scalars at the TeV scale. We predict a host of new heavy fermions around the TeV scale; these are also a source of new FCNC and CLFV effects. We show that flavon charge patterns that reproduce the observed SM fermion masses and mixings also supply enough extra suppression of FCNC and CLFV effects to satisfy current experimental bounds.

In addition to explaining the hierarchy of fermion masses and mixings, models in our framework have many interesting phenomenological implications. Mixing of the singlet  $s$  with the Higgs boson  $h$  can cause large deviations from the SM predictions for the Higgs decay branching fractions, potentially observable at the Tevatron or LHC. The  $s$  particle itself will also be produced at the LHC, and could be confused



with  $h$  if it turns out to be the lightest mass eigenstate. While new FCNC effects are suppressed, we predict contributions to  $D^0-\overline{D}^0$  mixing,  $B_s \rightarrow \mu^+\mu^-$ , and CLFV that are close to the current value or limit. The exotic top quark decays  $t \rightarrow ch$  and  $t \rightarrow cs$  can have branching fractions on the order of  $10^{-3}$ .

Our paper is organized as follows. In section 2, we present the basic outline of our framework. In section 3, we discuss the constraints on the model parameters from the low energy phenomenology. Section 4 contains the phenomenological implications and predictions of the model, especially for the new top decays and Higgs signals at the Tevatron and LHC. In section 5, we outline a possible ultraviolet completion realizing our proposal. Section 6 contains our conclusions and further discussion.

### 3.2 Model and formalism

We extend the gauge symmetry of the SM by a  $U(1)_S$  local symmetry and an additional local flavon symmetry which in the simplest case would be a  $U(1)_F$ . All of the SM fermions are neutral with respect to  $U(1)_S$ , while all of the SM fermions apart from the third generation quark doublet  $q_{3L}$  and right-handed top  $u_{3R}$  are charged under the chiral  $U(1)_F$ . We introduce a complex scalar field  $S$  which has charge 1 under  $U(1)_S$ , is neutral under the flavon symmetry, and is a SM singlet. We also introduce one or more complex scalar fields  $F_i$ , the “flavon” scalars. In the simplest case there would be a single flavon scalar  $F$  that has charge 1 under  $U(1)_F$ , is neutral under  $U(1)_S$ , and is a SM singlet. The Higgs field  $H$  is taken as neutral under  $U(1)_S \times U(1)_F$ . We assume that the flavon charges of the SM fermions are such that only the top quark has an allowed dimension 4 Yukawa interaction.

The  $S$  field is assumed to develop a vev that spontaneously breaks the  $U(1)_S$  symmetry. In frameworks where the little hierarchy between the electroweak scale and the TeV scale is generated, this could occur naturally by extending the Higgs sector to include  $S$ , with a mixed potential. The pseudoscalar component of  $S$  is then

“eaten” to give mass to the  $U(1)_S$   $Z'$  gauge boson. Notice that the vev of  $S$  does not in itself break any of the global flavor symmetries of the Yukawa-less SM;  $S$  is only a messenger of flavor breaking, just as it is also a messenger of electroweak breaking. This is the fundamental distinction that allows  $S$  to exist at the electroweak scale without inducing unacceptably large flavor violating effects.

The flavon scalars  $F_i$  are assumed to develop vevs that spontaneously break the local flavon symmetry at the TeV scale, with the pseudoscalar components of the  $F_i$  eaten to give the flavon gauge bosons mass. To preserve the little hierarchy, we assume that the direct mixing between the  $F_i$  and the extended Higgs sector is negligible.

In this framework the Yukawa interactions of the lighter quarks and leptons are replaced by higher dimension operators that couple these fermions to  $H$ ,  $S$ , and the  $F_i$ . As we will show later in an explicit example, these can be generated as effective couplings by integrating out new heavy fermions at the TeV scale. These effective couplings should respect all of the SM gauge symmetries, as well as  $U(1)_S$  and the flavon symmetries. In particular, the  $U(1)_S$  charged field  $S$  can only appear as powers of  $S^\dagger S/M^2$ , where  $M$  denotes a generic TeV scale parameter. Powers of  $F_i/M$  and  $F_i^\dagger/M$  can also appear, but the exact form depends on the flavon charge assignments of the SM fermions. Since we will assume that vevs of the  $F_i$  are of order  $M$ , we can absorb the  $F_i/M$  dependence into the dimensionless complex couplings  $h_{ij}$ , where  $i, j$  are generation labels; all these couplings we will then take to be of order 1.

The observed SM fermion mass hierarchy is generated from the following low energy effective interactions:

$$\begin{aligned}
\mathcal{L}^{\text{Yuk}} = & h_{33}^u \bar{q}_{3L} u_{3R} \bar{H} + \left( \frac{S^\dagger S}{M^2} \right) (h_{33}^d \bar{q}_{3L} d_{3R} H + h_{22}^u \bar{q}_{2L} u_{2R} \bar{H} + h_{23}^u \bar{q}_{2L} u_{3R} \bar{H} + h_{32}^u \bar{q}_{3L} u_{2R} \bar{H}) \\
& + \left( \frac{S^\dagger S}{M^2} \right)^2 (h_{22}^d \bar{q}_{2L} d_{2R} H + h_{23}^d \bar{q}_{2L} d_{3R} H + h_{32}^d \bar{q}_{3L} d_{2R} H + h_{12}^u \bar{q}_{1L} u_{2R} \bar{H} + h_{21}^u \bar{q}_{2L} u_{1R} \bar{H} \\
& + h_{13}^u \bar{q}_{1L} u_{3R} \bar{H} + h_{31}^u \bar{q}_{3L} u_{1R} \bar{H}) + \left( \frac{S^\dagger S}{M^2} \right)^3 (h_{11}^u \bar{q}_{1L} u_{1R} \bar{H} + h_{11}^d \bar{q}_{1L} d_{1R} H \\
& + h_{12}^d \bar{q}_{1L} d_{2R} H + h_{21}^d \bar{q}_{2L} d_{1R} H + h_{13}^d \bar{q}_{1L} d_{3R} H + h_{31}^d \bar{q}_{3L} d_{1R} H) + h.c.
\end{aligned} \tag{3.1}$$

Note that the above interactions are very similar to those proposed in reference [25], except our interactions involve suppression by powers of  $\left(\frac{S^\dagger S}{M^2}\right)$ , instead of  $\left(\frac{H^\dagger H}{M^2}\right)$ . We will refer to this as the Babu-Nandi texture. The hierarchy among the fermion masses and mixings are obtained from a single small dimensionless parameter,

$$\epsilon \equiv \frac{v_s}{M}, \tag{3.2}$$

where  $v_s$  is the vev of  $S$ . As was shown in [25], a good fit to the observed fermion masses and mixings is obtained with  $\epsilon \sim 0.15$ . The couplings  $h_{ij}$  are all of order one; the largest coupling needed is  $h_{23}^u = 1.4$ , while the smallest coupling needed is  $h_{22}^u = 0.14$ .

The Babu-Nandi texture is not unique, and it does not predict any precise fermion mass relations, since there are slightly more unspecified order 1 parameters than there are Yukawa parameters in the SM.

### 3.2.1 Fermion masses and CKM mixing

The gauge symmetry of our model is the usual  $SU(3)_c \times SU(2)_L \times U(1)_Y$  of the SM, plus two additional local symmetries:  $U(1)_S$  and the flavon symmetry. The SM symmetry is broken spontaneously by the usual Higgs doublet  $H$  at the electroweak scale. We assume that the extra  $U(1)_S$  symmetry is also broken spontaneously at the electroweak scale by a SM singlet complex scalar field  $S$ . The flavon symmetry,  $U(1)_F$

in the simplest case, is broken spontaneously above a TeV by a SM singlet scalar flavon field  $F$ . The pseudoscalar part of the complex scalar field  $S$  is absorbed by the  $Z'$  gauge boson  $U(1)_S$  to get its mass. Thus after symmetry breaking the remaining scalars at the electroweak scale are neutral bosons  $h$  and  $s$ . Parameterizing the Higgs doublet and singlet in the unitary gauge as

$$H = \begin{pmatrix} 0 \\ \frac{h}{\sqrt{2}} + v \end{pmatrix} \quad S = \left( \frac{s}{\sqrt{2}} + v_s \right), \quad (3.3)$$

with  $v \simeq 174$  GeV, and defining an additional small parameter

$$\beta \equiv \frac{v}{M}, \quad (3.4)$$

we obtain, from eqs. (3.1-3.4) the following mass matrices for the up and down quark sector:

$$M_u = \begin{pmatrix} h_{11}^u \epsilon^6 & h_{12}^u \epsilon^4 & h_{13}^u \epsilon^4 \\ h_{21}^u \epsilon^4 & h_{22}^u \epsilon^2 & h_{23}^u \epsilon^2 \\ h_{31}^u \epsilon^4 & h_{32}^u \epsilon^2 & h_{33}^u \end{pmatrix} v, \quad M_d = \begin{pmatrix} h_{11}^d \epsilon^6 & h_{12}^d \epsilon^6 & h_{13}^d \epsilon^6 \\ h_{21}^d \epsilon^6 & h_{22}^d \epsilon^4 & h_{23}^d \epsilon^4 \\ h_{31}^d \epsilon^6 & h_{32}^d \epsilon^4 & h_{33}^d \epsilon^2 \end{pmatrix} v. \quad (3.5)$$

The charged lepton mass matrix is obtained from  $M_d$  by replacing the couplings  $h_{ij}$  appropriately. Note that these mass matrices are the same as in [25], and as was shown there, good fits to the quark and charged lepton masses, as well as the CKM mixing angles are obtained by choosing  $\epsilon \sim 0.15$ , and all the couplings  $h_{ij}$  of order one. To leading order in  $\epsilon$ , the fermion masses are given by

$$\begin{aligned} (m_t, m_c, m_u) &\simeq (|h_{33}^u|, |h_{22}^u| \epsilon^2, |h_{11}^u - h_{12}^u h_{21}^u / h_{22}^u| \epsilon^6) v, \\ (m_b, m_s, m_d) &\simeq (|h_{33}^d| \epsilon^2, |h_{22}^d| \epsilon^4, |h_{11}^d| \epsilon^6) v, \\ (m_\tau, m_\mu, m_e) &\simeq (|h_{33}^\ell| \epsilon^2, |h_{22}^\ell| \epsilon^4, |h_{11}^\ell| \epsilon^6) v, \end{aligned} \quad (3.6)$$

while the quark mixing angles are

$$\begin{aligned}
|V_{us}| &\simeq \left| \frac{h_{12}^d}{h_{22}^d} - \frac{h_{12}^u}{h_{22}^u} \right| \epsilon^2, \\
|V_{cb}| &\simeq \left| \frac{h_{23}^d}{h_{33}^d} - \frac{h_{23}^u}{h_{33}^u} \right| \epsilon^2, \\
|V_{ub}| &\simeq \left| \frac{h_{13}^d}{h_{33}^d} - \frac{h_{12}^u h_{23}^d}{h_{22}^u h_{33}^d} - \frac{h_{13}^u}{h_{33}^u} \right| \epsilon^4.
\end{aligned} \tag{3.7}$$

Generically all of the  $h_{ij}$  can be nonvanishing, but in a particular ultraviolet (UV) completion flavon charge conservation may push some of them to higher order in  $\epsilon$  or to vanish altogether. However from (3.6) and (3.7) we see that the Babu-Nandi texture is rather robust: the only flavor off-diagonal couplings needed to reproduce the observed mixings are one or more of  $h_{12}^d$ ,  $h_{12}^u$ , one or more of  $h_{23}^d$ ,  $h_{23}^u$ , and one or more of  $h_{13}^d$ ,  $h_{13}^u$ ; the rest can either vanish or appear at higher order in  $\epsilon$ .

### 3.2.2 Yukawa interactions and FCNC

Our model has flavor changing neutral current interactions in the Yukawa sector. Using eqs.(1-4), the Yukawa interaction matrices  $Y_u^h$ ,  $Y_d^h$ ,  $Y_u^s$ ,  $Y_d^s$  for the up and down sector, for  $h^0$  and  $s^0$  fields are obtained to be

$$\sqrt{2}Y_u^h = \begin{pmatrix} h_{11}^u \epsilon^6 & h_{12}^u \epsilon^4 & h_{13}^u \epsilon^4 \\ h_{21}^u \epsilon^4 & h_{22}^u \epsilon^2 & h_{23}^u \epsilon^2 \\ h_{31}^u \epsilon^4 & h_{32}^u \epsilon^2 & h_{33}^u \end{pmatrix}, \quad \sqrt{2}Y_d^h = \begin{pmatrix} h_{11}^d \epsilon^6 & h_{12}^d \epsilon^6 & h_{13}^d \epsilon^6 \\ h_{21}^d \epsilon^6 & h_{22}^d \epsilon^4 & h_{23}^d \epsilon^4 \\ h_{31}^d \epsilon^6 & h_{32}^d \epsilon^4 & h_{33}^d \epsilon^2 \end{pmatrix}, \tag{3.8}$$

with the charged lepton Yukawa coupling matrix  $Y_\ell$  obtained from  $Y_d$  by replaing  $h_{ij}^d \rightarrow h_{ij}^\ell$ .

$$\sqrt{2}Y_u^s = \begin{pmatrix} 6h_{11}^u \epsilon^5 \beta & 4h_{12}^u \epsilon^3 \beta & 4h_{13}^u \epsilon^3 \beta \\ 4h_{21}^u \epsilon^3 \beta & 2h_{22}^u \epsilon \beta & 2h_{23}^u \epsilon \beta \\ 4h_{31}^u \epsilon^3 \beta & 2h_{32}^u \epsilon \beta & 0 \end{pmatrix}, \quad \sqrt{2}Y_d^s = \begin{pmatrix} 6h_{11}^d \epsilon^5 \beta & 6h_{12}^d \epsilon^5 \beta & 6h_{13}^d \epsilon^5 \beta \\ 6h_{21}^d \epsilon^5 \beta & 4h_{22}^d \epsilon^3 \beta & 4h_{23}^d \epsilon^3 \beta \\ 6h_{31}^d \epsilon^5 \beta & 4h_{32}^d \epsilon^3 \beta & 2h_{33}^d \epsilon \beta \end{pmatrix} \tag{3.9}$$

with the charged lepton Yukawa coupling matrix  $Y_\ell$  obtained from  $Y_d$  by replaing  $h_{ij}^d \rightarrow h_{ij}^\ell$ .

There are several important features that distinguish our model from the proposals in [25, 26, 27]:

i) Note, from eqs.(3.5) and (3.8), in our model, the Yukawa couplings of  $h$  to the SM fermions are exactly the same as in the SM. This is because the fermion mass hierarchy in our model is arising from  $\left(\frac{S^\dagger S}{M^2}\right)$ . This is a distinguishing feature of our model from that proposed in [25, 26] where the Yukawa couplings of  $h$  are flavor dependent, because the hierarchy there arises from  $\left(\frac{H^\dagger H}{M^2}\right)$ .

ii) In our model, we have an additional singlet Higgs boson whose couplings to the SM fermions are flavor dependent as given in eq. (3.9). Again, this is because the hierarchy in our model arises from  $\left(\frac{S^\dagger S}{M^2}\right)$ . In particular,  $s^0$  does not couple to the top quark, and its dominant fermionic coupling is to the bottom quark. This will have interesting phenomenological implications for the Higgs searches at the LHC.

iii) We note from eq. (3.5-3.8) that the mass matrices and the corresponding Yukawa coupling matrices for  $h$  are proportional as in the SM. Thus there are no flavor changing Yukawa interactions mediated by  $h$ . However, this is not true for the Yukawa interactions of the singlet Higgs as can be seen from eqs. (3.5) and (3.9). Thus  $s$  exchange will lead to flavor violation in the neutral Higgs interactions.

### 3.2.3 Higgs sector and the $Z'$

The Higgs potential of our model, consistent with the SM and the extra  $U(1)_S$  symmetry, can be written as

$$V(H, S) = -\mu_H^2(H^\dagger H) - \mu_S^2(S^\dagger S) + \lambda_H(H^\dagger H)^2 + \lambda_S(S^\dagger S)^2 + \lambda_{HS}(H^\dagger H)(S^\dagger S) \quad (3.10)$$

Note that after absorbing the three components of  $H$  in  $W^\pm$  and  $Z$ , and the pseudoscalar component of  $S$  in  $Z'$ , we are left with only two scalar Higgs,  $h^0$  and  $s^0$ .

The squared mass matrix in the  $(h^0, s^0)$  basis is given by

$$\mathcal{M}^2 = 2v^2 \begin{pmatrix} 2\lambda_H & \lambda_{HS}\alpha \\ \lambda_{HS}\alpha & 2\lambda_S\alpha^2 \end{pmatrix}, \quad (3.11)$$

where  $\alpha = v_s/v$ .

The mass eigenstates  $h$  and  $s$  can be written as

$$\begin{aligned} h^0 &= h \cos \theta + s \sin \theta, \\ s^0 &= -h \sin \theta + s \cos \theta, \end{aligned} \quad (3.12)$$

where  $\theta$  is the mixing angle in the Higgs sector.

In the Yukawa interactions discussed above, as well as in the gauge interactions involving the Higgs fields, the fields appearing are  $h^0$  and  $s^0$ , and these can be expressed in terms of  $h$  and  $s$  using eq. (3.12).

The mass of the  $Z'$  gauge boson is given by

$$m_{Z'}^2 = 2g_E^2 v_s^2 \quad (3.13)$$

Note that the  $Z'$  does not couple to any SM particles directly. Its coupling with the neutral scalar Higgs  $s$  also vanishes. The  $Z'$  coupling to the SM particles will be only via dimension six or higher operators. Such couplings will be generated by the vectorlike fermions in the model to be discussed in section 5.

### 3.3 Phenomenological Implications: Constraints from existing data

In this section, we discuss the constraints on our model from the existing experimental results. As can be seen from eq. (3.9), the exchange of  $s$  gives rise to tree level FCNC processes. This will cause  $K^0 - \bar{K}^0$  mass splitting,  $D^0 - \bar{D}^0$  mixing,  $K_L \rightarrow \mu^+ \mu^-$ ,  $B_s^0 \rightarrow \mu^+ \mu^-$ , as well as contributions to the electric dipole moment (EDM) of neutron and electron, and other rare processes that we discuss below.

### 3.3.1 $K^0 - \bar{K}^0$ mixing

In our model, this arises from the tree level  $s$  exchange between  $d\bar{s}$  and  $\bar{s}d$ , and is proportional to  $\beta^2\epsilon^{10}$ . Taking  $\beta \sim \epsilon \sim 0.15$ , and the values of the couplings  $h_{12}^d$  and  $h_{21}^d$  to be of order 1, the contribution to  $\Delta m_K^{\text{Higgs}} \simeq 10^{-16}$  to  $10^{-17}$  GeV, for an  $s$  mass of 100 GeV. The experimental value of  $\Delta m_K$  is  $3.5 \times 10^{-15}$  GeV [36]. Thus, since the contribution goes like  $m_s^{-4}$ ,  $s$  can be much lighter than 100 GeV. Note that  $\epsilon = v_s/M$  is fixed to be  $\sim 0.15$  to explain fermion mass hierarchy and the CKM mixing. However,  $\beta = v/M$  is a parameter in our model. Although the  $\Delta m_K$  constraint allows a somewhat larger value of  $\beta$ , we shall see that  $D^0 - \bar{D}^0$  mixing constrains  $\beta \sim \epsilon$ .

### 3.3.2 $D^0 - \bar{D}^0$ mixing

This contribution is again due to the tree level  $s$  exchange between  $u\bar{c}$  and  $\bar{u}c$ , and is proportional to  $\beta^2\epsilon^6$ , and hence is enhanced compared to  $\Delta m_K$ . Again, taking the couplings  $h_{12}^u$  and  $h_{21}^u$  to be of order one and  $\beta \sim \epsilon$ , we get  $\Delta m_D \sim 10^{-14}$  GeV for  $m_s = 100$  GeV. This is to be compared with the current experimental value of  $1.6 \times 10^{-14}$  GeV [36, 28]. Thus  $\Delta m_D$  gives a much stronger restriction on the model parameters.  $\beta$  can not be much larger than  $\epsilon$ , and  $s$  can not be much lighter than 100 GeV. If our proposal is correct, an electroweak singlet scalar should be observed at the LHC.

### 3.3.3 Other rare processes

In our model, tree level  $s$  exchange between  $d\bar{s}$  and  $\mu^+\mu^-$  will contribute to  $K_L \rightarrow \mu^+\mu^-$ . This contribution is proportional to  $\beta^2\epsilon^{10}$ , and leads to a contribution to this branching ratio  $\sim 10^{-14}$  for  $\beta \sim \epsilon$  and  $m_s \sim 100$  GeV. This is very small compared to the current experimental value of  $\sim 6.9 \times 10^{-9}$  [36]. Similarly, the contribution to the other rare processes such as  $K_L \rightarrow \mu e$ ,  $K \rightarrow \pi \bar{\nu} \nu$ ,  $\mu \rightarrow e \gamma$ ,  $\mu \rightarrow 3e$ ,  $B_d - \bar{B}_d$  mixing,



etc are several orders of magnitude below the corresponding experimental limits.

### 3.3.4 Constraint on the mass of $s$

Experiments at LEP2 have set a lower limit of 114.4 GeV for the mass of the SM Higgs boson. This is due to the nonobservation of the Higgs signal from the associated production  $e^+e^- \rightarrow Zh$ . In our model, since the singlet Higgs can mix with the doublet  $h$ , there will be a limit for  $m_s$  depending on the value of the mixing angle,  $\theta$ . For  $\sin^2 \theta \geq 0.25$ , the bound of 114.4 applies also for  $m_s$  [29]. However,  $s$  can be lighter if the mixing is small.

### 3.3.5 Constraint on the mass of the $Z'$

We have assumed that the extra  $U(1)$  symmetry in our model is spontaneously broken at the EW scale. But the corresponding gauge coupling,  $g_E$  is arbitrary and hence the mass of  $Z'$  is not determined in our model. However, very accurately measured  $Z$  properties at LEP1 put a constraint on the  $Z - Z'$  mixing to be  $\sim 10^{-3}$  or smaller [36, 30]. In our model, the  $Z'$  does not couple to any SM particle directly.  $Z - Z'$  mixing can take place at the one loop level with the new vectorlike fermions in the loop. The mixing angle is

$$\theta_{ZZ'} \sim \frac{g_Z g_E}{16\pi^2} \left( \frac{m_Z}{M} \right)^2, \quad (3.14)$$

where  $M$  is the mass of the vectorlike fermions with masses in the TeV scale. Even with  $g_E \sim 1$ , we get  $\theta_{ZZ'} \sim 10^{-4}$  or less. Thus there is no significant bound for the mass of this  $Z'$  from the LEP1. This  $Z'$  can couple to the SM particles via dimension six operators with the interaction of the form

$$L = \frac{\bar{\psi}_L \sigma^{\mu\nu} \psi_R H Z'^{\mu\nu}}{M^2} \quad (3.15)$$

As was shown in [31], no significant bound on  $m_{Z'}$  emerges from these interactions.

### 3.4 Phenomenological Implications: New physics signals

Motivated to explain the observed mass hierarchy in the fermion sector, we have constructed a model which has a complex singlet Higgs (in addition to the usual doublet), a new  $U(1)_S$  gauge symmetry at the EW scale, and a new set of vectorlike fermions at the TeV scale. Thus our model has new particles such as a scalar Higgs and a new  $Z'$  boson at the EW scale, and heavy vectorlike quarks and leptons. The model has many phenomenological implications for the production and decays of the Higgs bosons, top quark physics, a new scenario for  $Z'$  physics, and the production and decays of the vectorlike fermions.

#### 3.4.1 Higgs signals

##### Higgs coupling to the SM fermions

As can be seen from eq. (3.8), the couplings of the doublet Higgs  $h$  to the SM fermions are identical to that in the SM, whereas the couplings of the singlet Higgs  $s$  have a different flavor dependence. In particular, the singlet Higgs  $s$  does not couple to the top quark, whereas its coupling to  $(b, \tau; c, s, \mu; u, d, e)$  involve the flavor dependent factors  $2, 2; 2, 4, 4; 6, 6, 6)$  respectively. This is, of course, in the limit of zero mixing between  $h$  and  $s$ . Including the mixing, these factors will be modified. Thus our model will be distinguished from the SM by the fact that the Higgs couplings to fermions are predicted in terms of two model parameters: the ratio of vevs  $\alpha$  and the mixing angle  $\theta$ .

##### Higgs decays

The couplings of the Higgs bosons  $h$  and  $s$  to the fermions and the gauge bosons can be obtained from Eqs. (3.8) and (3.9), and are given in Table 3.1.

Interaction	Coupling	Interaction	Coupling
$s \rightarrow u\bar{u}$	$\frac{m_u}{v\sqrt{2}} \left( \sin \theta + \frac{6 \cos \theta}{\alpha} \right)$	$h \rightarrow u\bar{u}$	$\frac{m_u}{v\sqrt{2}} \left( \cos \theta - \frac{6 \sin \theta}{\alpha} \right)$
$s \rightarrow d\bar{d}$	$\frac{m_d}{v\sqrt{2}} \left( \sin \theta + \frac{6 \cos \theta}{\alpha} \right)$	$h \rightarrow d\bar{d}$	$\frac{m_d}{v\sqrt{2}} \left( \cos \theta - \frac{6 \sin \theta}{\alpha} \right)$
$s \rightarrow \mu^+ \mu^-$	$\frac{m_\mu}{v\sqrt{2}} \left( \sin \theta + \frac{4 \cos \theta}{\alpha} \right)$	$h \rightarrow \mu^+ \mu^-$	$\frac{m_\mu}{v\sqrt{2}} \left( \cos \theta - \frac{4 \sin \theta}{\alpha} \right)$
$s \rightarrow s\bar{s}$	$\frac{m_s}{v\sqrt{2}} \left( \sin \theta + \frac{4 \cos \theta}{\alpha} \right)$	$h \rightarrow s\bar{s}$	$\frac{m_s}{v\sqrt{2}} \left( \cos \theta - \frac{4 \sin \theta}{\alpha} \right)$
$s \rightarrow \tau^+ \tau^-$	$\frac{m_\tau}{v\sqrt{2}} \left( \sin \theta + \frac{2 \cos \theta}{\alpha} \right)$	$h \rightarrow \tau^+ \tau^-$	$\frac{m_\tau}{v\sqrt{2}} \left( \cos \theta - \frac{2 \sin \theta}{\alpha} \right)$
$s \rightarrow c\bar{c}$	$\frac{m_c}{v\sqrt{2}} \left( \sin \theta + \frac{2 \cos \theta}{\alpha} \right)$	$h \rightarrow c\bar{c}$	$\frac{m_c}{v\sqrt{2}} \left( \cos \theta - \frac{2 \sin \theta}{\alpha} \right)$
$s \rightarrow b\bar{b}$	$\frac{m_b}{v\sqrt{2}} \left( \sin \theta + \frac{2 \cos \theta}{\alpha} \right)$	$h \rightarrow b\bar{b}$	$\frac{m_b}{v\sqrt{2}} \left( \cos \theta - \frac{2 \sin \theta}{\alpha} \right)$
$s \rightarrow t\bar{t}$	$\frac{m_t}{v\sqrt{2}} \sin \theta$	$h \rightarrow t\bar{t}$	$\frac{m_t}{v\sqrt{2}} \cos \theta$
$s \rightarrow ZZ$	$\frac{2m_Z^2}{v\sqrt{2}} \sin \theta$	$h \rightarrow ZZ$	$\frac{2m_Z^2}{v\sqrt{2}} \cos \theta$
$s \rightarrow Z'Z'$	$\frac{m_{Z'}^2}{v\alpha\sqrt{2}} \cos \theta$	$h \rightarrow Z'Z'$	$\frac{m_{Z'}^2}{v\alpha\sqrt{2}} \sin \theta$
$s \rightarrow W^+W^-$	$\frac{2m_W^2}{v\sqrt{2}} \sin \theta$	$h \rightarrow W^+W^-$	$\frac{2m_W^2}{v\sqrt{2}} \cos \theta$
		$h \rightarrow ss$	$\lambda_{\text{hss}}$

Table 3.1: Yukawa and gauge couplings of  $h$  and  $s$ .

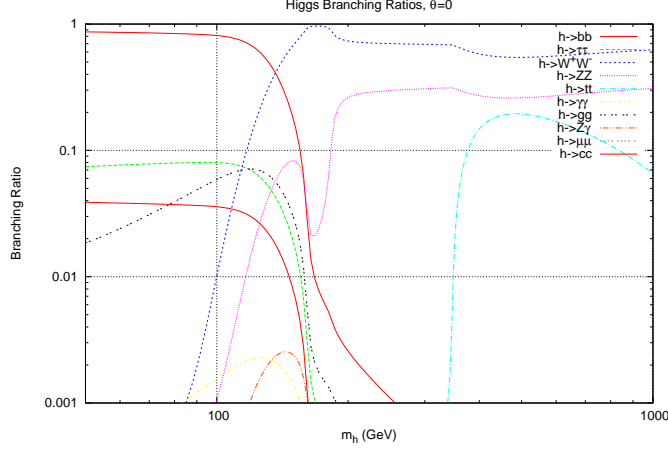


Figure 3.1: Branching ratio of  $h \rightarrow 2x$ , for  $\theta=0$  and  $\alpha=1$  [10].

The coupling of  $h$  to  $s$  given by:

$$\lambda_{hss} = \frac{m_h^2}{4v} \left\{ (1 - \mu) \sin 2\theta [\cos^3 \theta - \alpha \sin^3 \theta + \sin 2\theta (\alpha \cos \theta - \sin \theta)] + \right. \\ \left. 3 \sin 2\theta [\sin \theta (1 + \mu - (1 - \mu) \cos 2\theta) - \cos \theta (1 + \mu - (1 - \mu) \cos 2\theta) / \alpha] \right\}$$

where  $\mu = m_s^2/m_h^2$ .

Because of the flavor dependency of the couplings of  $s_0$  (and hence of  $s$  via mixing) to the fermions, the branching ratios (BR) for  $h$  to various final states are altered substantially from those in the SM. These branching ratios (BR) for  $h$  to the various final states are shown in Figs. 3.1, 3.2, 3.3, and 3.4 for the values of the mixing angle,  $\theta = 0, 20^\circ, 26^\circ$ , and  $40^\circ$  respectively.

For  $\theta = 0$ , i.e. no mixing, these BR's are the same as for the SM Higgs. Note that for both  $\theta = 20^\circ$  and  $26^\circ$ , the  $gg$  and the  $\gamma\gamma$  BR's are enhanced substantially compared to the SM. This is due to drastic reduction for the  $b\bar{b}$  mode from an approximate cancellation in the corresponding coupling as can be seen from Table 1. In particular, for  $\theta = 26^\circ$ , the effect is quite dramatic. For a light Higgs ( $m_h$  around 115 GeV), the usually dominant  $b\bar{b}$  mode is highly suppressed and the  $\gamma\gamma$  mode is enhanced by a factor of almost 10 compared to the SM. This is to be contrasted with the proposal of Refs. [25, 26] in which the  $h \rightarrow \gamma\gamma$  mode is reduced by about a factor of 10.

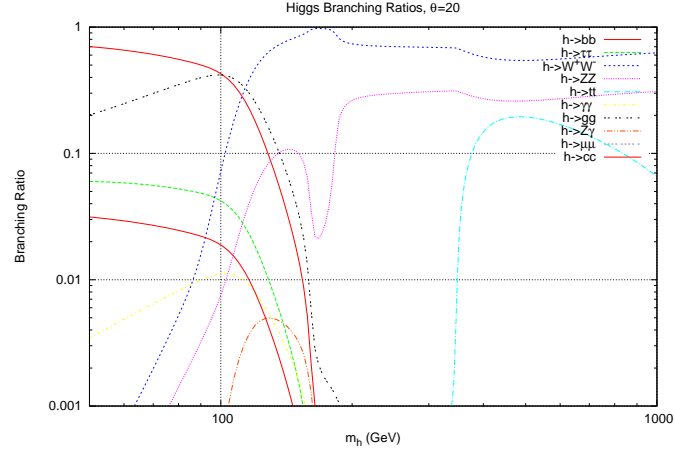


Figure 3.2: Branching ratio of  $h \rightarrow 2x$ , for  $\theta=20^\circ$  and  $\alpha=1$ .

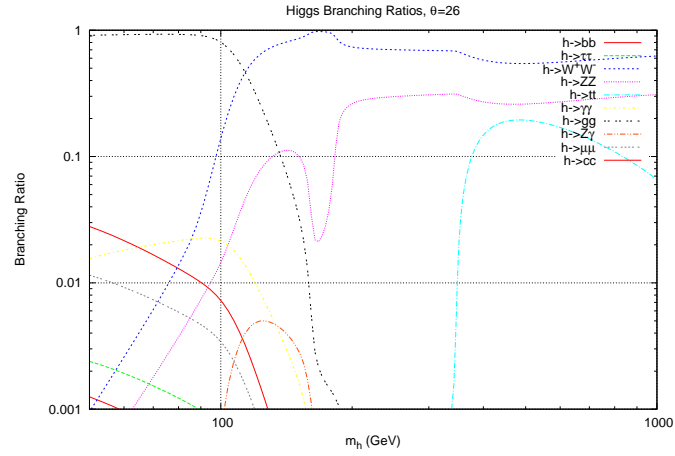


Figure 3.3: Branching ratio of  $h \rightarrow 2x$ , for  $\theta=26^\circ$  and  $\alpha=1$ .

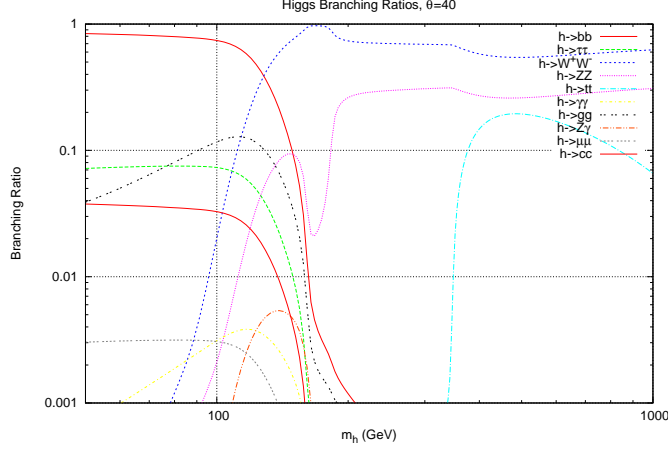


Figure 3.4: Branching ratio of  $h \rightarrow 2x$ , for  $\theta=40^\circ$  and  $\alpha=1$ .

Thus the Higgs signal in this mode for a Higgs mass of  $\sim 114 - 140$  GeV gets a big enhancement making its potential discovery via this mode much more favorable at the LHC. Such a signal may be observable at the Tevatron for a Higgs mass  $\sim 114$  as the luminosity accumulates, but would require about  $10 \text{ fb}^{-1}$  or more of data [32].

Another interesting effect is the Higgs signal via the  $WW^*$  for the light Higgs. In the SM, this mode becomes important for the Tevatron search for Higgs masses greater than about 135 GeV, where the BR to  $WW^*$  is approximate equal to that of  $b\bar{b}$ . Currently Tevatron experiments have excluded a SM Higgs with mass around 170 GeV (where the BR to  $WW^*$  is around 100 percent) for this mode [33]. In our framework, for  $\theta = 20^\circ$  for example, the crossover between the  $WW^*$  mode and the  $b\bar{b}$  mode takes place sooner than 135 GeV. Thus the Tevatron experiments will be more sensitive to the lower mass range than for a SM Higgs, and should be able to exclude masses much smaller than 160 GeV.

For a heavy Higgs,  $m_h > 200$  GeV, the Higgs will be accessible via the golden mode  $h \rightarrow ZZ$ . However, in this case, both  $h$  and  $s$  decay via this mode with comparable BR's (see Figs. 3.2 and 3.4 for  $\theta = 20^\circ$  and  $40^\circ$ ). So initially it will be hard to tell whether we are seeing  $h$  or  $s$ , a case of Higgs look-alikes. An accurate measurement

of this cross section times the BR, and the mass of the observed Higgs, we will be able to distinguish a heavy  $h$  from a heavy  $s$ , since the production cross sections depend on the mixing angle.

### 3.4.2 Top quark physics

In the SM,  $t \rightarrow ch$  mode is severely suppressed with a BR  $\sim 10^{-14}$  [34]. In our model, as can be seen from eqs.(3.8) and (3.9), although  $t \rightarrow ch$  is zero at tree level, we have a large coupling for  $t \rightarrow cs \sim 2\epsilon\beta$ . This gives rise to significant BR for the  $t \rightarrow cs$  mode for a Higgs mass of up to about 150 GeV. If the mixing between the  $h$  and  $s$  is substantial, both decay modes,  $t \rightarrow cs$  and  $t \rightarrow ch$  will have BR  $\sim 10^{-3}$ . With a very large  $t\bar{t}$  cross section,  $\sigma_{t\bar{t}} \sim 10^3$  pb at the LHC, this could be a significant production mode for Higgs bosons at the LHC. Observation of signals for two different Higgs masses will also show clear evidence for new physics beyond the SM.

### 3.4.3 $Z'$ physics

Our model has a  $Z'$  boson in the EW scale from the spontaneous breaking of the extra  $U(1)$  symmetry. As discussed before, since the  $Z - Z'$  mixing is very small  $\sim 10^{-4}$  or less, its mass is not constrained by the very accurately measured  $Z$  properties at LEP. Its mass can be as low as few GeV from the existing constraints. This  $Z'$  does not couple to the SM particles with dimension 4 operators. It does couple to  $s$  at tree level via the  $sZ'Z'$  interaction. Thus it can be produced via the decay of  $s$  (or  $h$  if there is a substantial mixing between  $h$  and  $s$ ). This gives an interesting signal for the Higgs decays,  $s \rightarrow Z'Z'$ ,  $h \rightarrow Z'Z'$  if allowed kinematically. In Figs. 3.5 and 3.6, we give the BR's for the  $h$  and  $s$  decays for a  $Z'$  mass of 40 GeV. The  $Z'$  will decay to the SM particles via the  $Z - Z'$  mixing with the same branching ratio as the  $Z$ . Thus the clear final state signal will be  $l^+l^-l^+l^-$  pairs ( $l = e, \mu$ ) with each pair having the invariant mass of the  $Z'$ . Such a signal will be easily detectable at the

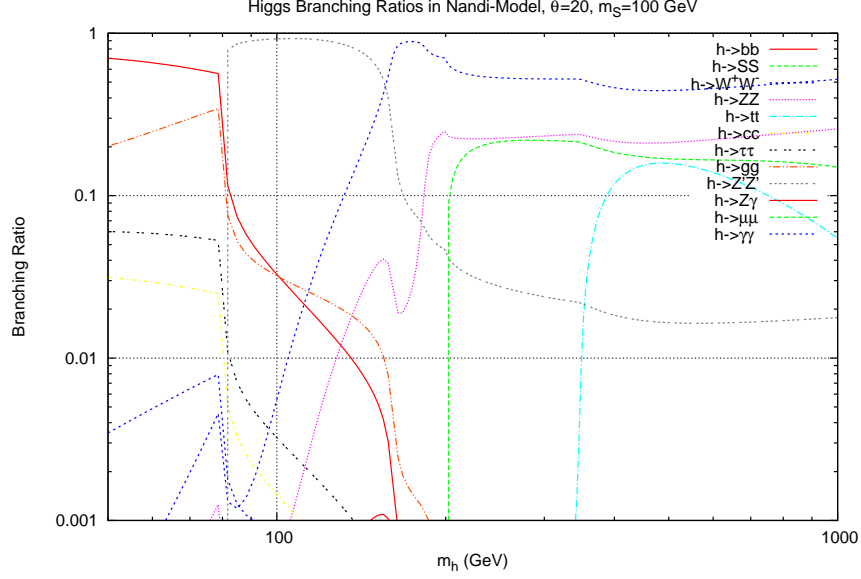


Figure 3.5: Branching ratio of  $h \rightarrow 2x$  including  $h \rightarrow ss$  and  $h \rightarrow Z'Z'$  where  $m_{Z'} = 40$  GeV and  $m_s = 100$  GeV. Here  $\alpha = 1$ .

LHC. If the  $Z'$  happens to be very light, (say a few GeV), and the mixing angle is extremely tiny, there is a possibility that the  $Z'$ 's may produce displaced vertices at the detector. Both of these will be very unconventional signals for Higgs bosons at the LHC.

#### 3.4.4 $B_s^0 \rightarrow \mu^+\mu^-$

In our model this decay gets a contribution from an FCNC interaction mediated by s-exchange. The amplitude for this decay is  $A \sim 4h_{22}^d h_{22}^\ell \epsilon^6 \beta^2$ . Taking  $\beta \sim \epsilon$ ,  $A \sim 4h_{22}^d h_{22}^\ell \epsilon^8$ , and with the couplings  $h_{22}^d, h_{22}^\ell \sim 1$ , we obtain the branching ratio,  $BR(B_s^0 \rightarrow \mu^+\mu^-) \sim 10^{-9}$ . Current experimental limit for this BR is  $4.7 \times 10^{-8}$  [36], and thus this decay could be observed soon at the Tevatron as the luminosity accumulates.



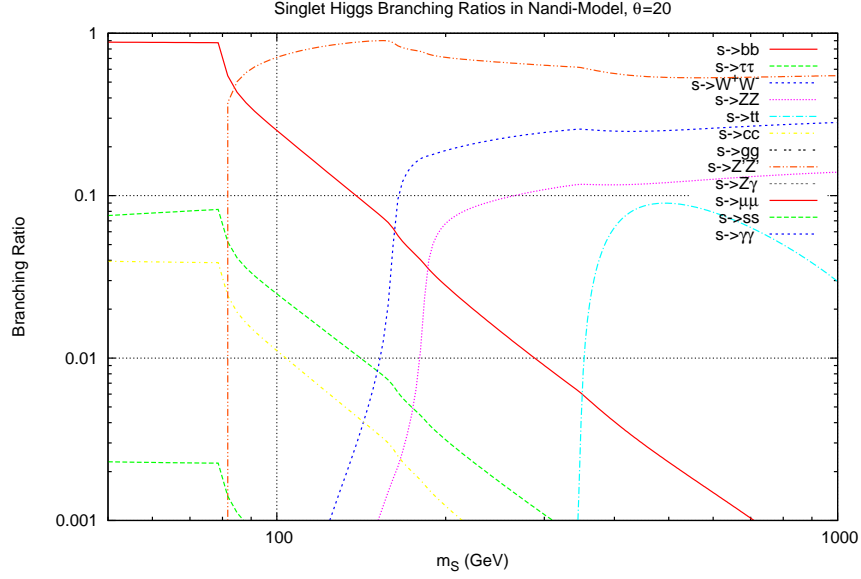


Figure 3.6: Branching ratio of  $s \rightarrow 2x$  including  $s \rightarrow Z'Z'$  where  $m_{Z'} = 40$  GeV. Here  $\alpha = 1$ .

### 3.4.5 Vectorlike fermions, productions and decays

Our model requires vectorlike quarks and leptons, both  $SU(2)$  doublets,  $P_i$  and singlets  $T_i$ , with masses at the TeV scale. These will be pair produced at high energy hadron colliders via the strong interaction. For example, for a 1 TeV vectorlike quark, the production cross section at the LHC is  $\sim 60$  fb [35]. We need several such vectorlike quarks for our model. So the total production cross section will be few hundred fb. These will decay to the light quarks of the same electric charge and Higgs bosons (h or s):  $P \rightarrow qh, qs$ . Thus the signal will be two high  $p_T$  jets together with the final states arising from the Higgs decay. For a heavy Higgs, in the golden mode ( $h \rightarrow ZZ, s \rightarrow ZZ$ , this will give rise to two high  $p_T$  jets plus four Z bosons. In the case of a light  $Z'$ , the final state signal will be two high  $p_T$  jets plus 8 charged leptons in the final state (with each lepton pair having the invariant mass of the  $Z'$ ).

### 3.5 UV Completion

We present two concrete examples of models from which an effective action like Eq. (3.1) can be derived. The first example only reproduces the second and third generation quark couplings, but its simplicity serves to introduce the basic issues and mechanisms. The second example is a complete three generation TeV scale model of quark flavor. The correct lepton couplings can be obtained from a copy of the same structure used for the down-type quarks. We assume that neutrino masses benefit from some additional see-saw mechanism, although it is not obvious that we can't obtain them by refining the TeV scale flavon model.

#### 3.5.1 Two generation model

For this pedagogical example we will employ two important simplifications:

- We only reproduce the second and third generation quark couplings. In the next subsection we extend this to include the first generation, but the model-building is more cumbersome.
- We will choose charge assignments such that the couplings  $h_{32}^u$ ,  $h_{32}^d$ , and  $h_{23}^d$  are higher order in  $\epsilon$ . As already mentioned nonzero values of these couplings are not needed to reproduce the observed SM quark masses and mixings.

With these simplifications we postulate a TeV scale model with the field content shown in Table 3.2, where the hypercharges are listed along with the charge assignments under  $U(1)_S$  and  $U(1)_F$ . The Higgs doublet  $H$  is the only scalar that carries hypercharge, while the SM singlet  $S$  is the only scalar carrying  $U(1)_S$  charge. The SM singlet flavon  $F$  is the only scalar carrying  $U(1)_F$  charge. The SM quarks are neutral under  $U(1)_S$ . The third generation up-type quark fields also carry no  $U(1)_F$  charge, while the other quark fields have flavor-dependent nonzero  $U(1)_F$  charges.

Field	U(1) <sub>Y</sub>	U(1) <sub>S</sub>	U(1) <sub>F</sub>	Field	U(1) <sub>Y</sub>	U(1) <sub>S</sub>	U(1) <sub>F</sub>
$H$	1/2	0	0	$U_{1L}$	2/3	1	0
$S$	0	1	0	$U_{1R}$	2/3	1	1
$F$	0	0	1	$U_{2L}$	2/3	-1	3
$q_{3L}$	1/6	0	0	$U_{2R}$	2/3	-1	3
$q_{2L}$	1/6	0	2	$D_{1L}$	-1/3	-1	-1
$u_{3R}$	2/3	0	0	$D_{1R}$	-1/3	-1	-1
$u_{2R}$	2/3	0	3	$D_{2L}$	-1/3	2	3
$d_{3R}$	-1/3	0	-1	$D_{2R}$	-1/3	2	2
$d_{2R}$	-1/3	0	3	$D_{3L}$	-1/3	1	3
$Q_{1L}$	1/6	-1	-1	$D_{3R}$	-1/3	1	3
$Q_{1R}$	1/6	-1	0				
$Q_{2L}$	1/6	1	1				
$Q_{2R}$	1/6	1	2				
$Q_{3L}$	1/6	-1	3				
$Q_{3R}$	1/6	-1	2				
$Q_{4L}$	1/6	2	2				
$Q_{4R}$	1/6	2	1				

Table 3.2: Charge assignments in the two generation model for the scalar fields  $H$ ,  $S$ ,  $F$ , and the SM quark fields  $q_{3L}$ ,  $q_{2L}$ ,  $u_{3R}$ ,  $u_{2R}$ ,  $d_{3R}$ , and  $d_{2R}$ . Also listed are the color triplet weak doublet heavy quark pairs  $Q_{iL}$ ,  $Q_{iR}$  and the color triplet weak singlet heavy quark pairs  $U_{iL}$ ,  $U_{iR}$ ,  $D_{iL}$ ,  $D_{iR}$ .

We introduce four pairs of new color triplet weak doublet fermion fields  $Q_{iL}$ ,  $Q_{iR}$ , two pairs of color triplet up-type weak singlets  $U_{iL}$ ,  $U_{iR}$ , and three pairs of color triplet down-type weak singlets  $D_{iL}$ ,  $D_{iR}$ . Each pair is vectorlike with respect to the SM gauge group and  $U(1)_S$ , thus no anomalies are introduced with respect to these gauge groups, and each vectorlike pair naturally acquires a Dirac mass of order  $M$  (when they have the same  $U(1)_F$  charge) or of order the vev of  $F$  (when their  $U(1)_F$  charges differ by one). We assume that both the vev of  $F$  and  $M$  are of order a TeV. Any residual anomaly in  $U(1)_F$  can be handled either by introducing more heavy fermions or using the Green-Schwarz mechanism at the TeV scale.

With these charge assignments the only dimension 4 couplings involving the second and third generation SM quarks are:

$$\begin{aligned} & f_1 \bar{q}_{3L} u_{3R} \bar{H} + f_2 \bar{q}_{3L} Q_{1R} S + f_3 \bar{D}_{1L} d_{3R} S^\dagger + f_4 \bar{q}_{2L} Q_{2R} S^\dagger \\ & + f_5 \bar{U}_{1L} u_{3R} S + f_6 \bar{q}_{2L} Q_{3R} S + f_7 \bar{U}_{2L} u_{2R} S^\dagger + f_8 \bar{D}_{3L} d_{2R} S + h.c. \quad , \end{aligned} \quad (3.16)$$

where the  $f_i$  are dimensionless coupling constants. Thus the top quark receives the correct mass from electroweak symmetry breaking for  $|f_1| \simeq 1$ . The other couplings involve the  $S$  scalar, but not the Higgs  $H$  or the flavon  $F$ . Both electroweak symmetry breaking and flavor symmetry breaking are communicated to the rest of the SM quark sector via a Froggatt-Nielsen type mechanism, integrating out the heavy TeV scale fermions from tree level diagrams that connect SM quark left doublets to SM quark right singlets and to  $H$  or  $\bar{H}$ .

The renormalizable couplings involving just the heavy fermions are:

$$\begin{aligned} & f_9 \bar{Q}_{1R} Q_{1L} F + f_{10} \bar{Q}_{1L} D_{1R} H + M \bar{D}_{1R} D_{1L} \\ & + f_{11} \bar{Q}_{2R} Q_{2L} F + f_{12} \bar{Q}_{2L} U_{1R} \bar{H} + f_{13} \bar{U}_{1R} U_{1L} F \\ & + f_{14} \bar{Q}_{3R} Q_{3L} F^\dagger + f_{15} \bar{Q}_{3L} U_{2R} \bar{H} + M \bar{U}_{2R} U_{2L} \\ & + f_{16} \bar{Q}_{2L} Q_{4R} S^\dagger + f_{17} \bar{Q}_{4L} Q_{2R} S + f_{18} \bar{Q}_{4R} Q_{4L} F^\dagger + f_{19} \bar{Q}_{4L} D_{2R} H \\ & + f_{20} \bar{D}_{2R} D_{2L} F^\dagger + f_{21} \bar{D}_{2L} D_{3R} S + M \bar{D}_{3L} D_{3R} + h.c. \quad . \end{aligned} \quad (3.17)$$

Thus, integrating out the heavy fermions in the tree level diagram composed from the couplings

$$f_2 \bar{q}_{3L} Q_{1R} S + f_9 \bar{Q}_{1R} Q_{1L} F + f_{10} \bar{Q}_{1L} D_{1R} H + M \bar{D}_{1R} D_{1L} + f_3 \bar{D}_{1L} d_{3R} S^\dagger \quad (3.18)$$

produces an effective coupling below the TeV scale proportional to

$$f_2 f_3 f_9 f_{10} \frac{F}{M} \frac{S^\dagger S}{M^2} \bar{q}_{3L} d_{3R} H + h.c. . \quad (3.19)$$

Integrating out the heavy fermions in the tree level diagram composed from the couplings

$$f_4 \bar{q}_{2L} Q_{2R} S^\dagger + f_{11} \bar{Q}_{2R} Q_{2L} F + f_{12} \bar{Q}_{2L} U_{1R} \bar{H} + f_{13} \bar{U}_{1R} U_{1L} F + f_5 \bar{U}_{1L} u_{3R} S \quad (3.20)$$

produces an effective coupling below the TeV scale proportional to

$$f_4 f_5 f_{11} f_{12} f_{13} \frac{F^2}{M^2} \frac{S^\dagger S}{M^2} \bar{q}_{2L} u_{3R} \bar{H} + h.c. . \quad (3.21)$$

Integrating out the heavy fermions in the tree level diagram composed from the couplings

$$f_6 \bar{q}_{2L} Q_{3R} S + f_{14} \bar{Q}_{3R} Q_{3L} F^\dagger + f_{15} \bar{Q}_{3L} U_{2R} \bar{H} + M \bar{U}_{2R} U_{2L} + f_7 \bar{U}_{2L} u_{2R} S^\dagger \quad (3.22)$$

produces an effective coupling below the TeV scale proportional to

$$f_6 f_7 f_{14} f_{15} \frac{F^\dagger}{M} \frac{S^\dagger S}{M^2} \bar{q}_{2L} u_{2R} \bar{H} + h.c. . \quad (3.23)$$

Finally, integrating out the heavy fermions in the tree level diagram composed from the couplings

$$\begin{aligned} & f_4 \bar{q}_{2L} Q_{2R} S^\dagger + f_{17}^* \bar{Q}_{2R} Q_{4L} S^\dagger + f_{19} \bar{Q}_{4L} D_{2R} H \\ & + f_{20} \bar{D}_{2R} D_{2L} F^\dagger + f_{21} \bar{D}_{2L} D_{3R} S + M \bar{D}_{3R} D_{3L} + f_8 \bar{D}_{3L} d_{2R} S \end{aligned} \quad (3.24)$$

produces an effective coupling below the TeV scale proportional to

$$f_4 f_8 f_{17}^* f_{19} f_{20} f_{21} \frac{F^\dagger}{M} \frac{(S^\dagger S)^2}{M^4} \bar{q}_{2L} d_{2R} H + h.c. . \quad (3.25)$$

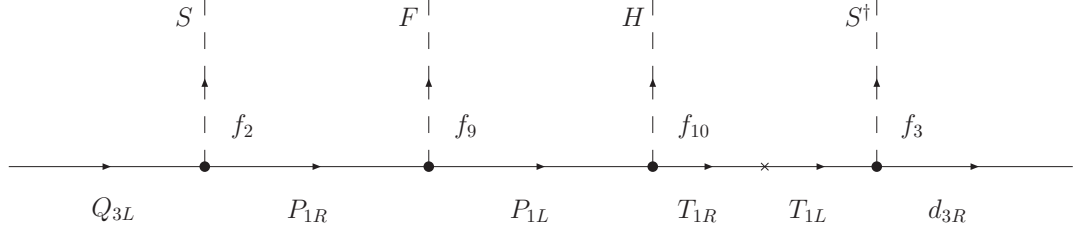


Figure 3.7: The Feynman diagram associated with Eq. (3.18)

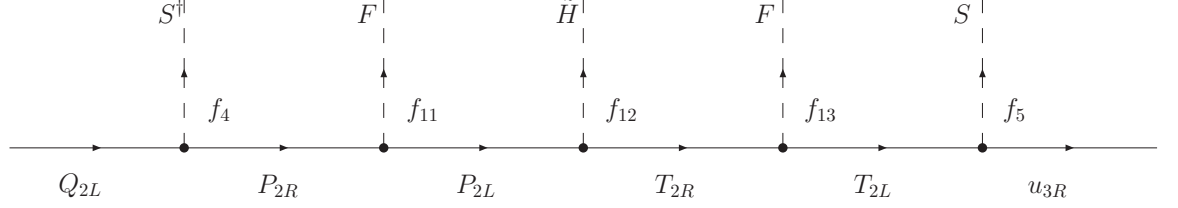


Figure 3.8: The Feynman diagram associated with Eq. (3.20)

There is an additional very similar tree level diagram contributing to  $h_{22}^d$  composed from the couplings

$$f_4 \bar{q}_{2L} Q_{2R} S^\dagger + f_{11} \bar{Q}_{2R} Q_{2L} F + f_{16} \bar{Q}_{2L} Q_{4R} S^\dagger + f_{18} \bar{Q}_{4R} Q_{4L} F^\dagger + f_{19} \bar{Q}_{4L} D_{2R} H + f_{20} \bar{D}_{2R} D_{2L} F^\dagger + f_{21} \bar{D}_{2L} D_{3R} S + M \bar{D}_{3R} D_{3L} + f_8 \bar{D}_{3L} d_{2R} S \quad (3.26)$$

which produces an effective coupling below the TeV scale proportional to

$$f_4 f_8 f_{11} f_{16} f_{18} f_{19} f_{20} f_{21} \frac{F(F^\dagger)^2}{M^3} \frac{(S^\dagger S)^2}{M^4} \bar{q}_{2L} d_{2R} H + h.c. \quad (3.27)$$

### 3.5.2 Three generation model

Here we present an concrete example of a full three generation TeV scale model that reproduces an effective action like Eq. (3.1) at the electroweak scale. This model uses

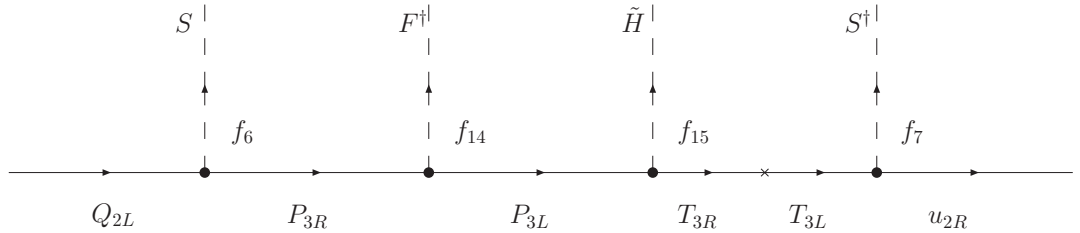


Figure 3.9: The Feynman diagram associated with Eq. (3.22)

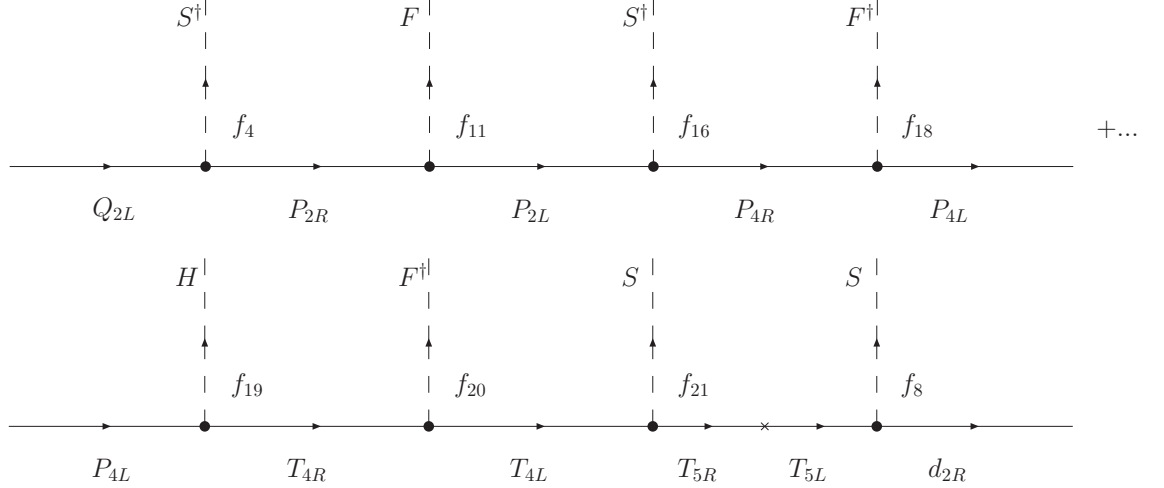


Figure 3.10: The Feynman diagram associated with Eq. (3.26)

a single electroweak messenger scalar  $S$ , but employs three TeV scale flavon scalars  $F_1$ ,  $F_2$ , and  $F_3$ , each corresponding to a different broken  $U(1)_{F_i}$  flavon symmetry. As before the SM quarks are neutral under  $U(1)_S$ . The third generation up-type quark fields also carry no  $U(1)_{F_i}$  charges, while the other quark fields have flavor-dependent nonzero  $U(1)_{F_i}$  charges.

The model has a rather large number of new heavy fermions: seven pairs of new color triplet weak doublet fermion fields  $Q_{iL}$ ,  $Q_{iR}$ , six pairs of color triplet up-type weak singlets  $U_{iL}$ ,  $U_{iR}$ , and eight pairs of color triplet down-type weak singlets  $D_{iL}$ ,  $D_{iR}$ . Each pair is vectorlike with respect to the SM gauge group and  $U(1)_S$ , thus no anomalies are introduced with respect to these gauge groups, and each vectorlike pair naturally acquires a Dirac mass of order  $M$  (when they have the same  $U(1)_{F_i}$  charges) or of order the vev of some  $F_i$  (when one of their  $U(1)_{F_i}$  charges differs by one). We assume that both the  $F_i$  vevs and  $M$  are of order a TeV. Any residual anomaly in the  $U(1)_{F_i}$  symmetries can be handled either by introducing more heavy fermions or using the Green-Schwarz mechanism at the TeV scale.

We do not suggest that this model is the most efficient one implementing the basic concepts of our proposal. We have made an explicit trade-off, in some sense, of

maximizing the number of the new heavy fermions required in order to minimize the complexity of the messenger sector and the charge assignments.

With the charge assignments listed in Table 3.3 the only dimension 4 couplings of fermions to the Higgs scalar are

$$\begin{aligned} & f_1 \bar{q}_{3L} u_{3R} \bar{H} + f_2 \bar{Q}_{2L} U_{2R} \bar{H} + f_3 \bar{Q}_{4R} U_{4L} \bar{H} + f_4 \bar{Q}_{6L} U_{3R} \bar{H} \\ & + f_5 \bar{Q}_{7L} U_{6R} \bar{H} + f_6 \bar{Q}_{3L} D_{3R} H + f_7 \bar{Q}_{4L} D_{4R} H + f_8 \bar{Q}_{7L} D_{7R} H + h.c. . \end{aligned} \quad (3.28)$$

The only dimension 4 couplings of fermions to the the  $S$  messenger scalar are

$$\begin{aligned} & f_9 \bar{q}_{1L} Q_{1R} S^\dagger + f_{10} \bar{q}_{2L} Q_{2R} S^\dagger + f_{11} \bar{q}_{3L} Q_{3R} S^\dagger + f_{12} \bar{U}_{1L} u_{1R} S \\ & + f_{13} \bar{U}_{2L} u_{2R} S + f_{14} \bar{D}_{1L} d_{1R} S + f_{15} \bar{D}_{2L} d_{2R} S + f_{16} \bar{D}_{3L} d_{3R} S \\ & + f_{17} \bar{Q}_{2L} Q_{4R} S^\dagger + f_{18} \bar{Q}_{1L} Q_{5R} S^\dagger + f_{19} \bar{Q}_{7L} Q_{5R} S^\dagger + f_{20} \bar{Q}_{5L} Q_{7R} S^\dagger \\ & + f_{21} \bar{U}_{4L} U_{2R} S + f_{22} \bar{U}_{5L} U_{1R} S + f_{23} \bar{U}_{6L} U_{5R} S + f_{24} \bar{D}_{4L} D_{3R} S \\ & + f_{25} \bar{D}_{3L} D_{4R} S^\dagger + f_{26} \bar{D}_{5L} D_{2R} S + f_{27} \bar{D}_{6L} D_{1R} S + f_{28} \bar{D}_{1L} D_{6R} S^\dagger \\ & + f_{29} \bar{D}_{7L} D_{5R} S + f_{30} \bar{D}_{8L} D_{6R} S + f_{31} \bar{D}_{6L} D_{8R} S^\dagger + h.c. . \end{aligned} \quad (3.29)$$

The direct fermion mass terms and mixings consistent with the flavon symmetries and SM gauge symmetries generated by operators of dimension 4 or less are

$$\begin{aligned} & f_{32} \bar{Q}_{1L} Q_{1R} F_3^\dagger + f_{33} \bar{Q}_{2L} Q_{2R} F_1 + f_{34} \bar{Q}_{3L} Q_{3R} F_1 + f_{35} \bar{Q}_{3L} Q_{3R} F_2^\dagger \\ & + f_{36} \bar{Q}_{4L} Q_{4R} F_2^\dagger + f_{37} \bar{Q}_{5L} Q_{5R} F_1 + f_{38} \bar{Q}_{5L} Q_{6R} F_2 + f_{39} \bar{Q}_{6L} Q_{6R} F_3^\dagger \\ & + f_{40} \bar{Q}_{7L} Q_{7R} F_1^\dagger + f_{41} \bar{U}_{1L} U_{1R} F_3 + f_{42} \bar{U}_{2L} U_{2R} F_2^\dagger + M \bar{U}_{3L} U_{3R} + f_{43} \bar{U}_{3L} U_{4R} F_3^\dagger \\ & + f_{44} \bar{U}_{4L} U_{4R} F_1^\dagger + f_{45} \bar{U}_{5L} U_{5R} F_2^\dagger + f_{46} \bar{U}_{6L} U_{6R} F_1^\dagger + f_{47} \bar{D}_{1L} D_{1R} F_3^\dagger \\ & + f_{48} \bar{D}_{2L} D_{2R} F_1^\dagger + M \bar{D}_{3L} D_{3R} + M \bar{D}_{4L} D_{4R} + f_{49} \bar{D}_{5L} D_{5R} F_3 \\ & + f_{50} \bar{D}_{4L} D_{5R} F_2^\dagger + f_{51} \bar{D}_{6L} D_{6R} F_3 + f_{52} \bar{D}_{7L} D_{7R} F_2^\dagger + M \bar{D}_{8L} D_{7R} + f_{53} \bar{D}_{8L} D_{8R} F_3^\dagger + h.c. , \end{aligned} \quad (3.30)$$

where for simplicity of notation we have used  $M$  to denote all the TeV scale mass parameters.



Field	U(1) <sub>Y</sub>	U(1) <sub>S</sub>	U(1) <sub>F<sub>1</sub></sub>	U(1) <sub>F<sub>2</sub></sub>	U(1) <sub>F<sub>3</sub></sub>	Field	Y	S	F <sub>1</sub>	F <sub>2</sub>	F <sub>3</sub>
$q_{1L}$	1/6	0	1	2	1	$U_{1L,R}$	2/3	1	0	1	1,0
$q_{2L}$	1/6	0	0	1	0	$U_{2L,R}$	2/3	1	1	0,1	0
$q_{3L}$	1/6	0	0	0	0	$U_{3L,R}$	2/3	2	2	1	-1
$u_{1R}$	2/3	0	0	1	1	$U_{4L,R}$	2/3	2	1,2	1	0
$u_{2R}$	2/3	0	1	0	0	$U_{5L,R}$	2/3	2	0	1,2	0
$u_{3R}$	2/3	0	0	0	0	$U_{6L,R}$	2/3	3	0,1	2	0
$d_{1R}$	-1/3	0	1	2	0	$D_{1L,R}$	-1/3	1	1	2	0,1
$d_{2R}$	-1/3	0	0	1	1	$D_{2L,R}$	-1/3	1	0,1	1	1
$d_{3R}$	-1/3	0	1	0	0	$D_{3L,R}$	-1/3	1	1	0	0
$H$	1/2	0	0	0	0	$D_{4L,R}$	-1/3	2	1	0	0
$S$	0	1	0	0	0	$D_{5L,R}$	-1/3	2	1	1	1,0
$F_1$	0	0	1	0	0	$D_{6L,R}$	-1/3	2	1	2	1,0
$F_2$	0	0	0	1	0	$D_{7L,R}$	-1/3	3	1	1,2	0
$F_3$	0	0	0	0	1	$D_{8L,R}$	-1/3	3	1	2	0,1
$Q_{1L,R}$	1/6	1	1	2	0,1	$Q_{5L,R}$	1/6	2	2,1	2	0
$Q_{2L,R}$	1/6	1	1,0	1	0	$Q_{6L,R}$	1/6	2	2	1	-1,0
$Q_{3L,R}$	1/6	1	1,0	1	0	$Q_{7L,R}$	1/6	2	1	0	0
$Q_{4L,R}$	1/6	2	1	0,1	0						

Table 3.3: Charge assignments in the three generation model for the scalar fields  $H$ ,  $S$ ,  $F_i$ , the SM quark fields  $q_{iL}$ ,  $u_{iR}$ ,  $d_{iR}$ , and the heavy quark pairs  $Q_{iL}$ ,  $Q_{iR}$ ,  $U_{iL}$ ,  $U_{iR}$ ,  $D_{iL}$ ,  $D_{iR}$ .

Thus, integrating out the heavy fermions in the tree level diagram composed from the couplings

$$f_{11}\bar{q}_{3L}Q_{3R}S^\dagger + f_{34}^*\bar{Q}_{3R}Q_{3L}F_1^\dagger + f_{10}\bar{Q}_{3L}D_{3R}H + M\bar{D}_{3R}D_{3L} + f_3\bar{D}_{3L}d_{3R}S \quad (3.31)$$

produces an effective coupling below the TeV scale proportional to

$$f_{11}f_{34}^*f_{10}f_3\frac{F_1^\dagger}{M}\frac{S^\dagger S}{M^2}\bar{q}_{3L}d_{3R}H + h.c. . \quad (3.32)$$

Integrating out the heavy fermions in the tree level diagram composed from the couplings

$$f_{10}\bar{q}_{2L}Q_{2R}S^\dagger + f_{33}^*\bar{Q}_{2R}Q_{2L}F_1^\dagger + f_2\bar{Q}_{2L}U_{2R}\bar{H} + f_{42}^*\bar{U}_{2R}U_{2L}F_2 + f_{13}\bar{U}_{2L}u_{2R}S \quad (3.33)$$

produces an effective coupling below the TeV scale proportional to

$$f_{10}f_{33}^*f_2f_{42}^*f_{13}\frac{F_1^\dagger F_2}{M^2}\frac{S^\dagger S}{M^2}\bar{q}_{2L}u_{2R}\bar{H} + h.c. . \quad (3.34)$$

Integrating out the heavy fermions in the tree level diagram composed from the couplings

$$\begin{aligned} & f_{10}\bar{q}_{2L}Q_{2R}S^\dagger + f_{33}^*\bar{Q}_{2R}Q_{2L}F_1^\dagger + f_{17}\bar{Q}_{2L}Q_{4R}S^\dagger + f_{36}^*\bar{Q}_{4R}Q_{4L}F_2 + f_7\bar{Q}_{4L}D_{4R}H \\ & + M\bar{D}_{4R}D_{4L} + f_{24}^*\bar{D}_{4L}D_{3R}S + M\bar{D}_{3R}D_{3L} + f_3\bar{D}_{3L}d_{3R}S \end{aligned} \quad (3.35)$$

produces an effective coupling below the TeV scale proportional to

$$f_{10}f_{33}^*f_{17}f_{36}^*f_7f_{24}^*f_3\frac{F_1^\dagger F_2}{M^2}\frac{(S^\dagger S)^2}{M^4}\bar{q}_{2L}d_{3R}H + h.c. . \quad (3.36)$$

Integrating out the heavy fermions in the tree level diagram composed from the couplings

$$\begin{aligned} & f_{11}\bar{q}_{3L}Q_{3R}S^\dagger + f_{34}^*\bar{Q}_{3R}Q_{3L}F_1^\dagger + f_{10}\bar{Q}_{3L}D_{3R}H + f_{24}^*\bar{D}_{3R}D_{4L}S^\dagger + f_{50}\bar{D}_{4L}D_{5R}F_2^\dagger \\ & + f_{49}^*\bar{D}_{5R}D_{5L}F_3^\dagger + f_{26}\bar{D}_{5L}D_{2R}S + f_{48}^*\bar{D}_{2R}D_{2L}F_1 + f_{15}\bar{D}_{2L}d_{2R}S \end{aligned} \quad (3.37)$$

produces an effective coupling below the TeV scale proportional to

$$f_{11}f_{34}^*f_{10}f_{24}^*f_{50}f_{49}^*f_{26}f_{48}^*f_{15}\frac{F_1^\dagger F_1 F_2^\dagger F_3^\dagger (S^\dagger S)^2}{M^4}\frac{1}{M^4}\bar{q}_{3L}d_{2R}H + h.c. . \quad (3.38)$$

There is also another tree level contribution to  $h_{32}^d$ , proportional to

$$f_{11}f_{34}^*f_{10}f_{24}f_{50}f_{49}^*f_{26}f_{48}^*f_{15}\frac{F_1^\dagger F_1 F_2^\dagger F_3^\dagger (S^\dagger S)^2}{M^4}\frac{1}{M^4}\bar{q}_{3L}d_{2R}H + h.c. . \quad (3.39)$$

Integrating out the heavy fermions in the tree level diagram composed from the couplings

$$f_{10}\bar{q}_{2L}Q_{2R}S^\dagger + f_{33}^*\bar{Q}_{2R}Q_{2L}F_1^\dagger + f_{17}\bar{Q}_{2L}Q_{4R}S^\dagger + f_{36}^*\bar{Q}_{4R}Q_{4L}F_2 + f_7\bar{Q}_{4L}D_{4R}H + M\bar{D}_{4R}D_{4L} \\ + f_{50}\bar{D}_{4L}D_{5R}F_2^\dagger + f_{49}^*\bar{D}_{5R}D_{5L}F_3^\dagger + f_{26}\bar{D}_{5L}D_{2R}S + f_{48}^*\bar{D}_{2R}D_{2L}F_1 + f_{15}\bar{D}_{2L}d_{2R}S \quad (3.40)$$

produces an effective coupling below the TeV scale proportional to

$$f_{10}f_{33}^*f_{17}f_{36}^*f_7f_{50}f_{49}^*f_{26}f_{48}^*f_{15}\frac{F_1^\dagger F_1 F_2^\dagger F_2 F_3^\dagger (S^\dagger S)^2}{M^5}\frac{1}{M^4}\bar{q}_{3L}d_{2R}H + h.c. . \quad (3.41)$$

Integrating out the heavy fermions in the tree level diagram composed from the couplings

$$f_9\bar{q}_{1L}Q_{1R}S^\dagger + f_{32}^*\bar{Q}_{1R}Q_{1L}F_3 + f_{18}^*\bar{Q}_{1L}Q_{5R}S^\dagger + f_{19}^*\bar{Q}_{5R}Q_{7L}S^\dagger + f_8\bar{Q}_{7L}D_{7R}H \\ + M\bar{D}_{7R}D_{8L} + f_{30}\bar{D}_{8L}D_{6R}S + f_{28}\bar{D}_{6R}D_{1L}S + f_{14}\bar{D}_{1L}d_{1R}S \quad (3.42)$$

produces an effective coupling below the TeV scale proportional to

$$f_9f_{32}^*f_{18}^*f_{19}^*f_8f_{30}f_{28}f_{14}\frac{F_3}{M}\frac{(S^\dagger S)^3}{M^6}\bar{q}_{1L}d_{1R}H + h.c. . \quad (3.43)$$

There are four other very similar tree level contributions to  $h_{11}^d$ .

Integrating out the heavy fermions in the tree level diagram composed from the couplings

$$f_9\bar{q}_{1L}Q_{1R}S^\dagger + f_{32}^*\bar{Q}_{1R}Q_{1L}F_3 + f_{18}^*\bar{Q}_{1L}Q_{5R}S^\dagger + f_{19}^*\bar{Q}_{5R}Q_{7L}S^\dagger + f_5\bar{Q}_{7L}U_{6R}\bar{H} + f_{46}^*\bar{U}_{6R}U_{6L}F_1 \\ + f_{23}\bar{U}_{6L}U_{5R}S + f_{45}^*\bar{U}_{5R}U_{5L}F_2 + f_{22}\bar{U}_{5L}U_{1R}S + f_{41}^*\bar{U}_{1R}U_{1L}F_3^\dagger + f_{12}\bar{U}_{1L}u_{1R}S \quad (3.44)$$

produces an effective coupling below the TeV scale proportional to

$$f_9 f_{32}^* f_{18}^* f_{19}^* f_5 f_{46}^* f_{23} f_{45}^* f_{22} f_{41}^* f_{12} \frac{F_1 F_2 F_3^\dagger F_3}{M^4} \frac{(S^\dagger S)^3}{M^6} \bar{q}_{1L} u_{1R} \bar{H} + h.c. . \quad (3.45)$$

Integrating out the heavy fermions in the tree level diagram composed from the couplings

$$\begin{aligned} & f_9 \bar{q}_{1L} Q_{1R} S^\dagger + f_{32}^* \bar{Q}_{1R} Q_{1L} F_3 + f_{18}^* \bar{Q}_{1L} Q_{5R} S^\dagger + f_{19}^* \bar{Q}_{5R} Q_{7L} S^\dagger + f_8 \bar{Q}_{7L} D_{7R} H + f_{52}^* \bar{D}_{7R} D_{7L} F_2 \\ & + f_{29} \bar{D}_{7L} D_{5R} S + f_{49}^* \bar{D}_{5R} D_{5L} F_3^\dagger + f_{26} \bar{D}_{5L} D_{2R} S + f_{48}^* \bar{D}_{2R} D_{2L} F_1 + f_{15} \bar{D}_{2L} d_{2R} S \end{aligned} \quad (3.46)$$

produces an effective coupling below the TeV scale proportional to

$$f_9 f_{32}^* f_{18}^* f_{19}^* f_8 f_{52}^* f_{29} f_{49}^* f_{26} f_{48}^* f_{15} \frac{F_1 F_2 F_3^\dagger F_3}{M^4} \frac{(S^\dagger S)^3}{M^6} \bar{q}_{1L} d_{2R} H + h.c. . \quad (3.47)$$

Integrating out the heavy fermions in the tree level diagram composed from the couplings

$$\begin{aligned} & f_9 \bar{q}_{1L} Q_{1R} S^\dagger + f_{32}^* \bar{Q}_{1R} Q_{1L} F_3 + f_{18}^* \bar{Q}_{1L} Q_{5R} S^\dagger + f_{19}^* \bar{Q}_{5R} Q_{7L} S^\dagger + f_8 \bar{Q}_{7L} D_{7R} H + f_{52}^* \bar{D}_{7R} D_{7L} F_2 \\ & + f_{29} \bar{D}_{7L} D_{5R} S + f_{50}^* \bar{D}_{5R} D_{4L} F_2 + f_{24}^* \bar{D}_{4L} D_{3R} S + M \bar{D}_{3R} D_{3L} + f_3 \bar{D}_{3L} d_{3R} S \end{aligned} \quad (3.48)$$

produces an effective coupling below the TeV scale proportional to

$$f_9 f_{32}^* f_{18}^* f_{19}^* f_8 f_{52}^* f_{29} f_{50}^* f_{24}^* f_3 \frac{(F_2)^2 F_3}{M^3} \frac{(S^\dagger S)^3}{M^6} \bar{q}_{1L} d_{3R} H + h.c. . \quad (3.49)$$

There is one other very similar tree level contribution to  $h_{13}^d$ .

Integrating out the heavy fermions in the tree level diagram composed from the couplings

$$\begin{aligned} & f_{11} \bar{q}_{3L} Q_{3R} S^\dagger + f_{34}^* \bar{Q}_{3R} Q_{3L} F_1^\dagger + f_{10} \bar{Q}_{3L} D_{3R} H + f_{24}^* \bar{D}_{3R} D_{4L} S^\dagger + f_{50} \bar{D}_{4L} D_{5R} F_2^\dagger + f_{29}^* \bar{D}_{5R} D_{7L} S^\dagger \\ & + f_{52}^* \bar{D}_{7L} D_{7R} F_2^\dagger + M \bar{D}_{7R} D_{8L} + f_{30} \bar{D}_{8L} D_{6R} S + f_{28} \bar{D}_{6R} D_{1L} S + f_{14} \bar{D}_{1L} d_{1R} S \end{aligned} \quad (3.50)$$

produces an effective coupling below the TeV scale proportional to

$$f_{11} f_{34}^* f_{10} f_{24}^* f_{50} f_{29}^* f_{52}^* f_{30} f_{28} f_{14} \frac{F_1^\dagger (F_2^\dagger)^2}{M^3} \frac{(S^\dagger S)^3}{M^6} \bar{q}_{3L} d_{1R} H + h.c. . \quad (3.51)$$

The following effective couplings are not generated or are generated at higher order in  $\epsilon$  and/or  $\beta$ :  $h_{23}^u$ ,  $h_{32}^u$ ,  $h_{12}^u$ ,  $h_{21}^u$ ,  $h_{13}^u$ ,  $h_{31}^u$ , and  $h_{21}^d$ . As already indicated these couplings are not needed to reproduce the observed SM quark masses and mixings. For illustration,  $h_{32}^u$  arises from the effective coupling

$$f_{11}f_{34}^*f_6f_{25}f_7^*f_{36}f_{17}^*f_2f_{42}^*f_{13}\frac{F_1^\dagger F_2 F_2^\dagger}{M^3}\frac{(S^\dagger S)^2}{M^4}\frac{H^\dagger H}{M^2}\bar{q}_{3L}u_{2R}\bar{H} + h.c. , \quad (3.52)$$

so the extra suppression relative to Eq. (3.1) is by an additional factor of  $\beta$  as well as an additional factor of  $\epsilon$ .

Since  $h_{12}^u$  and  $h_{21}^u$  have extra suppression in this model,  $D^0 - \bar{D}^0$  mixing also has extra suppression. This weakens the lower bound on  $m_s$  derived in Section 3.3.2. Similarly since  $h_{23}^u$  and  $h_{32}^u$  have extra suppression the relatively large BR for  $t \rightarrow cs$  discussed in Section 3.4.2 will not occur for this particular realization.

### 3.6 Conclusion

We have presented a proposal in which only the top quark obtains its mass from the Yukawa interaction with the SM Higgs boson via dimension four operators. All the other quarks receive their masses from operators of dimension six or higher involving a complex scalar Higgs  $S$  whose VEV is at the EW scale. The successive hierarchy of light quark masses is generated via the expansion parameter  $\left(\frac{S^\dagger S}{M^2}\right) \sim \epsilon^2$ , where  $\epsilon \equiv \frac{v_s}{M} \sim 0.15$ . All the couplings of the higher dimensional operators are of order one. We are able to generate the appropriate hierarchy of fermion masses with this small parameter  $\epsilon$ . Since  $v_s$  is at the EW scale, the physics of the new scale,  $M$  is not far above a TeV. Because of the new degree of freedom at the EW scale, we predict a neutral scalar  $s$ , which gives rise to signals that could be detected at the LHC or at the Tevatron. We make new predictions for Higgs decays and for top quark physics. The model has a light  $Z'$  that has very weak couplings to SM fermions, but could be light enough to be produced via mixing in Higgs decays at the LHC; this could give

rise to invisible Higgs decays, displaced vertices from the  $Z'$  decays, or multilepton final states, depending on the mass and lifetime of the  $Z'$ .

We have presented a model in which an effective interaction given in Eq. (3.1) can be realized. This involves extending the SM gauge symmetry by an abelian gauge symmetry  $U(1)_S$  and a local flavon symmetry group  $U(1)_{F_1} \times U(1)_{F_2} \times U(1)_{F_3}$ . The flavon symmetry is spontaneously broken at the TeV scale by a complex flavon scalars  $F_1, F_2, F_3$ , whereas the  $U(1)_S$  symmetry is broken at the electroweak scale by the complex scalar  $S$ , which is a SM singlet extension of the SM Higgs sector.  $S$  acts as the messenger of both flavor and electroweak symmetry breaking. The model requires the existence of vectorlike quarks and leptons, both EW doublets and singlets, at the TeV scale. These can be probed at the LHC. Their decays will be a new source for Higgs production and give rise to final states with 4  $Z$ 's or 4  $Z'$ 's and other interesting new physics signals at the LHC.

We have restricted ourselves to models where all of the hierarchies of the SM quark and charged lepton masses and mixings arise from powers of the vev of a single messenger field. In [25], a framework was suggested in which all of these hierarchies arise from powers of  $\beta = \left(\frac{H^\dagger H}{M^2}\right)$ . As we saw in the previous section, in explicit models it is natural to generate powers of both  $\epsilon$  and  $\beta$ . Thus the model presented here and the framework of [25] are two extremes of a more general class of models. Obviously one could also generalize by introducing a more complicated messenger sector, i.e. further extending the Higgs sector.

A truly viable model should have fewer species of heavy fermions than were required in our example, ameliorating what is otherwise a dramatic worsening of the little hierarchy problem of the standard model. This could be achieved by a more efficient construction of the messenger sector and its interplay with the flavon sector. Another interesting direction is to attempt to generate some of the higher order effective couplings from the top quark Yukawa, as was done successfully with

leptoquark-generated loop diagrams in [23].

### 3.7 Extension of the Model

After this work was done we continued it in [19]. In this paper we explore models in which we add a singlet scalar Higgs to the Standard Model. All of these models explain the origin of the mass hierarchy amongst the fermion masses and mixing angles. We discuss 24 different variations on this model, and explore the different phenomenological possibilities. We find that the phenomenological implications of all the models are very similar except in the Higgs sector. Higgs decays and signals can be altered very significantly in all the models, but break up into two distinct classes. We also describe a systematic method for generating these models from higher order interactions involving vector-like quarks and flavon scalars.

## CHAPTER 4

### PERTURBATIVITY AND A FOURTH GENERATION IN THE MSSM

#### 4.1 Introduction

The repetition of the quark-lepton families is one of the great mysteries of particle physics. Despite its great success in describing the nature of strong and electroweak (EW) interactions, the Standard Model (SM) does not predict the number of families. What is the principle limiting the number of chiral families? Why not have a fourth generation or even more? The masses of the three observed families have a strong hierarchical pattern. Only the top quark mass ( $m_t \simeq 172.6$  GeV) lies close to the EW symmetry breaking scale. This, within the SM, suggests the Yukawa coupling of the top quark should be,  $\lambda_t \simeq 1$ . All remaining Yukawa couplings are suppressed. Thus, with only three observed families,  $\lambda_t$  and the three gauge couplings  $g_{1,2,3}$  would play an essential role in dynamics upon performing renormalization group (RG) studies. The situation may be modified within a two Higgs doublet SM and MSSM. In these models, due to the parameter  $\tan \beta = v_u/v_d$  (the ratio of the VEVs of the up type to the down type Higgses)  $\lambda_b$  and  $\lambda_\tau$  can also be large ( $\sim 1$  for  $\tan \beta \approx 60$ ). How would the picture change if there were a fourth family?

Current lower limits on the masses of the 4th generation fermions at 95% C.L. are [36]:

$$m_{t'} \geq 220 \text{ GeV} , \quad m_{b'} \geq 190 \text{ GeV} , \quad m_{\tau'} \geq 100 \text{ GeV} , \quad m_{\nu'} \geq 50 \text{ GeV} . \quad (4.1)$$

When these masses are translated to the values of their Yukawa couplings, we find the possibility of couplings larger than  $\lambda_t$ . Moreover, the bound on  $m_{\nu'}$  indicates the



existence of at least one massive neutrino with mass near the EW scale.

Due to the possible existence of large new Yukawa couplings, a study should be performed and the validity of the perturbative treatment must be examined. As we will show, within the MSSM with a 4th family, there is no value of  $\tan \beta$  that allows the perturbativity of the couplings up to the GUT scale. This fact suggests a lower cutoff scale. If there is such a cutoff scale, it should be related to new physics which take care of the self consistent ultraviolet (UV) completion. Can such a completion be constructed? A positive answer would be encouraging for model building as well as for further investigations with various phenomenological implications.

Even without focusing on UV completion of the theory, any extension of the SM or MSSM should be in accord with low energy observables. Some previous works [37]-[40] have focused on the effect of a 4th generation on the EW precision parameters  $S$ ,  $T$  and  $U$ . These constrain the masses of  $t'$  and  $b'$  quarks.

Assuming that the mixings of the fourth family matter with the observed three generations are minimal, most of the constraints come from the self energy diagrams of  $W^\pm$  and  $Z^0$  gauge bosons. In Ref. [40] it was found that with  $m_{t'} - m_{b'} \simeq (1 + \frac{1}{5} \ln \frac{M_h}{115 \text{ GeV}}) \times 50 \text{ GeV}$ , the new contributions to the parameters  $S$  and  $T$  get minimized. In particular, with  $M_h = 115 \text{ GeV}$  one obtains  $m_{t'} - m_{b'} \simeq 50 \text{ GeV}$ . However, this study did not consider the 4th family's effect on the parameter  $U$ . It is useful to analyze the impact of a 4th generation on all three quantities  $S$ ,  $T$  and  $U$ . Using analytical expressions given in Ref. [39] and the experimentally allowed ranges of  $S$ ,  $T$ ,  $U$  at  $1\sigma$  [36]:

$$\begin{aligned} S &= -0.13 \pm 0.10 , \\ T &= -0.13 \pm 0.11 , \\ U &= 0.20 \pm 0.12 , \end{aligned} \tag{4.2}$$

we can derive further constraints on  $m_{t'}$  and  $m_{b'}$ . In Fig. 4.1 we show the allowed

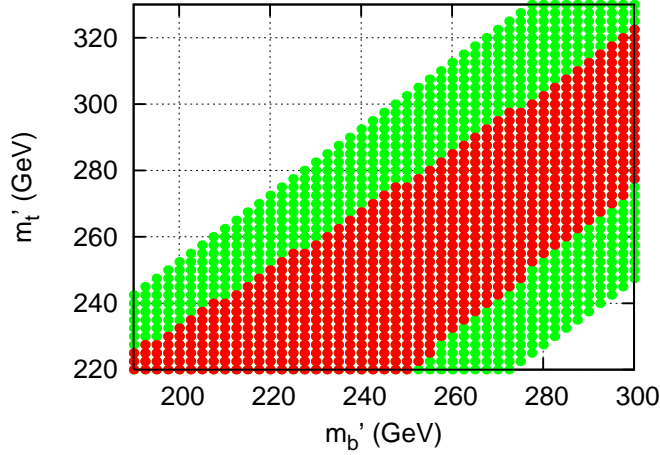


Figure 4.1: Plotting allowed quark masses using  $3\sigma$  limits of  $S$  and  $T$  in green. Superimposed in red are constraints from all 3 parameters,  $S$ ,  $T$ , and  $U$ , while more wide, green, area corresponds to the analysis with ignoring  $U$ . Here,  $M_h = 115$  GeV,  $m_{\tau'} = 150$  GeV, and  $m_{\nu'} = 100$  GeV.  $(\Delta S, \Delta T, \Delta U)$  for the leptons are  $(0.01, 0.045, 0.11)$ . regions for  $m_{t'}$  and  $m_{b'}$ . For these analysis we have allowed  $3\sigma$  deviations in Eq. 4.2.

A fourth generation of chiral matter would also affect the Higgs sector. This will give more interesting insights [41, 42] within a SUSY framework. As is well known, in MSSM the value  $\tan\beta \approx 1$  is disfavored due to the LEP lower bound on a lightest CP even Higgs boson mass  $M_h \geq 114.4$  GeV. In the MSSM, at tree level  $M_h^2 = M_Z^2 \cos^2 2\beta$ . Taking  $\tan\beta \simeq 1$ , the tree level mass vanishes. Loop corrections are not sufficient to raise  $M_h$ . When a 4th generation is added, the situation is even more drastic because in order to preserve perturbativity  $\tan\beta$  cannot be much greater than 1. This is an additional motivation for new physics.

This leads us to believe that the MSSM with a 4th family should be extended further. In this paper we suggest one such extension with vector like states having masses at the TeV scale. As an outcome of the proposed model, we obtain perturbativity of the couplings all the way up to the GUT scale with  $\tan\beta \sim 2$ . This avoids the difficulties discussed above, and is promising for the possibility of embedding the

whole scenario in a grand unified theory.

The paper is organized as follows. In section 4.2 we discuss theoretical bounds: problems arising from perturbativity considerations that limit  $\tan\beta$  and implications on Higgs physics. In section 4.3 we present our model which allows perturbativity of all couplings up to the GUT scale and extends  $\tan\beta$  up to  $\sim 2$  such that the LEP bound on  $M_h$  can easily be satisfied. The model has extra vector-like states which can be detected at the LHC. The summary of our work and conclusions are presented in section 4.4.

## 4.2 Theoretical Bounds and Some Implications

In this section we discuss bounds coming from theoretical considerations and discuss some implications of theories with a new heavy chiral fermion family.

### 4.2.1 Bounds from Tree Level Unitarity

The upper bound on a heavy chiral fermion's mass comes from the unitarity of scattering amplitudes. We assume that fermion mass is generated through the Yukawa coupling of the fermion with a fundamental Higgs doublet. In this case, for the heavy quark doublet  $Q$  with mass  $m_Q$  the  $Q\bar{Q} \rightarrow Q\bar{Q}$  scattering  $J = 0$  partial wave amplitude at tree level (at energies  $\sqrt{s} \gg m_Q$ ) is given by [43]:

$$|a_0| \approx \frac{5}{4\sqrt{2}\pi} G_F m_Q^2, \quad (4.3)$$

and the unitarity requirement  $|a_0| < 1$  gives the upper bound

$$m_Q^2 < \frac{4\sqrt{2}\pi}{5G_F} \simeq (552 \text{ GeV})^2, \quad (4.4)$$

as was first obtained in [43]. The analogous bound for the leptonic doublet  $L$

$$m_L^2 < \frac{4\sqrt{2}\pi}{G_F} \simeq (1.23 \text{ TeV})^2, \quad (4.5)$$

is higher. As we see, the current experimental direct bounds in Eq. (4.1) are not in conflict with the theoretical upper bounds of (4.4) and (4.5) derived at tree level. As we discuss below, the inclusion of loop corrections and the requirement of perturbativity will imply stringent theoretical bounds on Yukawa couplings.

## 4.2.2 Bounds from Perturbative RGE

Here we focus on MSSM with a 4th generation. The reason for the SUSY framework is twofold. First of all, low scale SUSY is the most appealing extension of SM in order to solve the gauge hierarchy problem. Second, as it turns out, more stringent bounds are obtained in the SUSY setup and for demonstrative purposes it is most useful. The discussed mechanisms (presented in the next section) for solving various problems could be also applied for SM and on two Higgs doublet SM.

The superpotential couplings involving 4th generation matter superfields are

$$W_4 = \lambda_{t'} q_4 u_4^c h_u + \lambda_{b'} q_4 d_4^c h_d + \lambda_{\tau'} l_4 e_4^c h_d + \lambda_{\nu_{\tau'}} l_4 N h_u, \quad (4.6)$$

where  $N$  is a right handed neutrino (complete singlet of MSSM) responsible for the Dirac mass generation of  $\nu_{\tau'}$ . Yukawa couplings defined at corresponding mass scales can be expressed as

$$\begin{aligned} \lambda_{t'}(m_{t'}) &= \frac{m_{t'}}{|1 + \delta_{t'}|v \sin \beta}, & \lambda_{b'}(m_{b'}) &= \frac{m_{b'}}{|1 + \delta_{b'}|v \cos \beta}, \\ \lambda_{\tau'}(m_{\tau'}) &= \frac{m_{\tau'}}{|1 + \delta_{\tau'}|v \cos \beta}, & \lambda_{\nu_{\tau'}}(m_{\nu_{\tau'}}) &= \frac{m_{\nu_{\tau'}}}{|1 + \delta_{\nu_{\tau'}}|v \sin \beta}, \end{aligned} \quad (4.7)$$

where  $\delta_\alpha$  ( $\alpha = t', b', \tau', \nu_{\tau'}$ ) exhibit the 1-loop finite corrections emerging after SUSY breaking [44]. Since we are dealing with large Yukawa couplings ( $\sim 2$ ), these corrections can be as large as 25% and should be taken into account. For examining the RG perturbativity, one should take the values for masses satisfying the bounds in Eq. (4.1) and run each Yukawa coupling from the corresponding mass scales up to higher scales. In Ref. [45] this analysis was done with the fourth generation fermion

masses smaller than the top mass. This was in accord with the experimental bounds that existed at that time. They found that if  $\tan\beta < 3$  all Yukawa couplings could be perturbative up to the GUT scale. Given the current lower bounds on quark and lepton masses, we find this is no longer the case. When one uses the renormalization group equations for evolving the Yukawa couplings from low scale up to higher energy scales, the couplings rapidly grow and blow up. For example for  $\tan\beta = 2$ ,  $\lambda_{b'}$  becomes non-perturbative at about 1 TeV. As  $\tan\beta$  increases, it is more difficult to tame the Yukawa coupling. This is shown in Fig. 4.2.

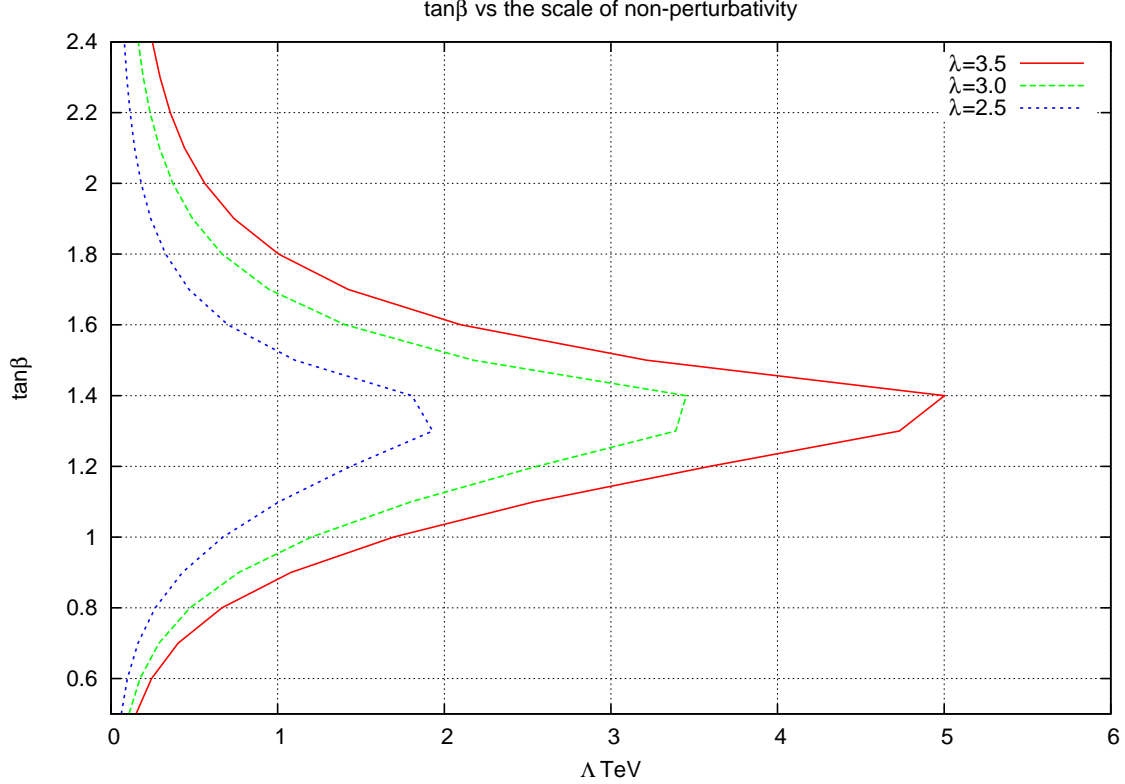


Figure 4.2: Plotting  $\tan\beta$  vs.  $\Lambda$ , the scale at which  $y_{b'}$  becomes non-perturbative. For masses we took the lowest allowed values from Eq. 4.1.

We have assumed the validity of the perturbative RG for Yukawa couplings  $< 2.5$ . For this analysis we set  $\delta_\alpha = 0$ , keeping in mind that unknown soft breaking terms allow more flexibility. The values  $\delta_a \sim 1/4$  will allow slightly relaxed bounds, however

do not change the situation much.

It is clear from this figure that *no* value of  $\tan\beta$  allows perturbative calculation all the way up to the GUT scale. Perturbativity puts a strict upper bound on the mass of the  $b'$  quark. For  $\tan\beta = 1.5$  we calculate this limit to be about  $\approx 100$  GeV. This value is below the experimental lower bound of 190 GeV. If a fourth generation exists, this provides a strong reason to introduce new physics at the TeV scale. In order for this to work, the cutoff scale of the theory should be near the TeV scale. Without any UV completion we have a strongly coupled theory at the TeV scale. What are the solutions to this problem? In section 4.3 we will introduce a specific model with new physics at the TeV scale that will allow values of  $\tan\beta$  up to  $\sim 2$  with perturbativity all the way up to the GUT scale  $\approx 2 \cdot 10^{16}$  GeV.

### 4.2.3 Implications for Higgs Physics

In the MSSM with large  $\tan\beta$  the lightest Higgs boson mass has an upper bound  $M_h \lesssim 125$  GeV. Even if  $\tan\beta$  is large, the mass at tree level can be no larger than  $M_Z$ . This is an even bigger problem when one introduces a fourth family. The new quarks limit  $\tan\beta$  to small values, thus reducing the tree level contribution for the lightest Higgs mass. Luckily at the same time they provide additional loop corrections to the lightest Higgs mass. The one-loop top-stop radiative corrections to the Higgs mass squared can be simplified as:

$$\Delta(M_h^2) \simeq \frac{3}{4\pi^2} \frac{m_t^4}{v^2} \ln \frac{m_{\tilde{t}_1} m_{\tilde{t}_2}}{m_t^2} . \quad (4.8)$$

The new  $t'$  and  $b'$  quarks and their superpartners will also contribute to the Higgs mass. These corrections can enhance the Higgs mass [47, 48]. When  $\tan\beta > 1$ , the correction from the  $b'$  quark has a similar form, but it is negative. If  $m_{b'} > m_{t'}$  then there is a problem, as the overall correction will be negative. When  $m_{t'} > m_{b'}$ , with constrained mass splitting displayed in Fig. 4.1, there is still a sizable positive

correction of about  $(60 \text{ GeV})^2$ . With  $\tan\beta \sim 2$  this puts an upper bound,  $M_h \lesssim 130 \text{ GeV}$ , greater than the LEP lower bound of  $114 \text{ GeV}$ .

The existence of a 4th chiral family in the mass range of  $(200 - 300) \text{ GeV}$  will have a significant impact on the Higgs signals at the LHC [40]. The most dominant production mechanism for the light Higgs boson is its production from gluon-gluon fusion via a top quark loop [46]. With the 4th chiral family, there will be additional contributions from the non-degenerate  $t'$  and  $b'$  loops. Thus the Higgs productions will be significantly enhanced. Also, for the light Higgs with mass below  $130 \text{ GeV}$ , the Higgs decaying to two photons is the most clean channel for detection at the LHC. With the additional contributions from the  $t'$  and  $b'$  quarks in the loops, the two photon branching ratio will also be enhanced. The other possible mode for the light Higgs detection is the  $t\bar{t}h$  mode, and the subsequent decay of the Higgs to  $b\bar{b}$ . This mode has been downgraded by recent studies mainly due to low production rate and large SM background. However, with the 4th family quarks, there will be additional contributions to the Higgs production via the  $t'\bar{t}'h$  and  $b'\bar{b}'h$  modes. Thus the Higgs detection via this channel may become viable.

### 4.3 The Model with Perturbative UV Completion

If the LHC discovers a fourth chiral family, it will be a great challenge for theorists to build self consistent models. There are several reasons for this. First of all, from existing experimental bounds it follows that the Yukawa couplings for  $t'$  and  $b'$  should be large. Let us be more specific. If the theory is one Higgs doublet Standard Model (SM), then the bounds  $m_{t'} \geq 220 \text{ GeV}$  and  $m_{b'} \geq 190 \text{ GeV}$  imply that near these mass scales we have  $\lambda_{t'} \geq 1.26$  and  $\lambda_{b'} \geq 1.1$ . The situation is more drastic within the MSSM. The above bound for the  $m_{b'}$  gives  $\lambda_{b'} \geq 1.1\sqrt{1 + \tan^2\beta}$  which for  $\tan\beta \simeq 3$  gives  $\lambda_{b'}(m_{b'}) \geq 3.45$ , a non-perturbative value. Therefore, the (tree level) perturbativity suggests the upper bound  $\tan\beta \leq 2.5$ . However, as we saw in the previous

section, after taking into account RGE effects, the requirement of perturbativity up to higher scales prefers even lower ( $\lesssim 1.5$ ) values of  $\tan\beta$ . This may lead to clash with the LEP bound on the lightest Higgs boson mass  $M_h \geq 114$  GeV. For  $\tan\beta \sim 1$ , in MSSM with three families it is difficult to satisfy this bound. As RGE studies discussed in section 4.2 show, no value of  $\tan\beta$  allows perturbativity up to the GUT scale for  $M_{\text{GUT}} \simeq 2 \cdot 10^{16}$  GeV. What are the possibilities to overcome these difficulties? The solution is some reasonable extension which modifies RG running above the TeV scale. Here we suggest one simple extension which allows perturbativity up to the  $M_{\text{GUT}}$  with less constraint on  $\tan\beta$ .

Our proposal is the following. The couplings  $\lambda_{t'}$ ,  $\lambda_{b'}$  and  $\lambda_{\tau'}$  are derived quantities in a low energy effective theory. They are generated after decoupling of additional vector like states with mass  $\Lambda_4 \sim \text{few} \cdot \text{TeV}$ . Above  $\Lambda_4$ , new interactions appear in the RGE and this makes the theory perturbative all the way up to  $M_{\text{GUT}}$ . We discuss the realization of this idea within the framework of the MSSM, however, non-SUSY models can be constructed with equal success.

We introduce two additional vector like pairs  $(H_u + H_d)$ ,  $(H_u' + H_d')$  of Higgs superfields, where  $H_u, H_u'$  and  $H_d, H_d'$  have the same quantum numbers under the MSSM gauge group as the up type ( $h_u$ ) and the down type ( $h_d$ ) Higgs superfields. These  $H$ -states are accompanied by two pairs of vector like quarks  $(D^c + \bar{D}^c)$ ,  $(D'^c + \bar{D}'^c)$ , where  $D^c$  has the quantum numbers of the down type quark  $d^c$ . Introduction of  $D$ -states are suggestive: they, together with  $H$ -states, effectively constitute complete  $SU(5)$  multiplets and therefore gauge coupling unification can be maintained at 1-loop approximation.

We will consider the following superpotential couplings

$$\begin{aligned}
W_4 = & \lambda_{t'}^{(1)} q_4 u_4^c h_u + \lambda_U q_4 u_4^c H_u + \lambda_{b'}^{(1)} q_4 d_4^c h_d + \lambda_D q_4 d_4^c H_d + \lambda'_{D'} q_4 D'^c h_d + \lambda_{\tau'}^{(1)} l_4 e_4^c h_d \\
& + \lambda_E l_4 e_4^c H_d - M_H H_u H_d - M_{H'} H_u' H_d' + M H_u h_d + M' H_d' h_u + M_D \bar{D}^c D^c - M'_D \bar{D}'^c D'^c .
\end{aligned}$$



For simplicity we do not couple  $D'^c, \bar{D}'^c$  states with chiral matter and assume that they have mass  $\simeq M_D$ . After integrating out the  $H$  and  $D$ -states one can easily verify that the effective Yukawa interactions are

$$W_4^{\text{eff}} = \lambda_{t'} q_4 u_4^c h_u + \lambda_{b'} q_4 d_4^c h_d + \lambda_{\tau'} l_4 e_4^c h_d ,$$

where:

$$\lambda_{t'} = \lambda_{t'}^{(1)} + \lambda_U \cos \gamma' \quad (4.9)$$

$$\lambda_{b'} = \lambda_{b'}^{(1)} + \lambda_D \cos \gamma + \lambda'_D \cos \gamma_D \quad (4.10)$$

$$\lambda_{\tau'} = \lambda_{\tau'}^{(1)} + \lambda_E \cos \gamma \quad (4.11)$$

$$\tan \gamma' \simeq \frac{M_{H'}}{M'} , \quad \tan \gamma \simeq \frac{M_H}{M} , \quad \tan \gamma_D \simeq \frac{M_D}{M_D'} . \quad (4.12)$$

The relevant diagrams are shown in Fig. 4.3. With all the mass scales of the same order ( $\simeq \Lambda_4$ ) the effective superpotential given above is valid below the scale  $\Lambda_4$ . With  $\cos \gamma \approx \cos \gamma_D \approx \cos \gamma' \approx 1$ , we can see that the effective (derived) Yukawas can be non-perturbative ( $\approx 3$ ) while the original Yukawa couplings remain perturbative; for example,  $\lambda_{t'} \simeq 2.4$  with  $\lambda_{t'}^{(1)} \simeq \lambda_U \simeq 1.2$ . Above the scale  $\Lambda_4$  we are dealing with the couplings  $\lambda_{t',b',\tau'}^{(1)}$  and  $\lambda_{U,D,E}, \lambda'_D$ . By making proper choice for the values of these couplings at  $\Lambda_4$ , we can have a perturbative regime up to the GUT scale. To demonstrate this we take  $\Lambda_4 = 1$  TeV and set up all RG equations valid above this

scale. At 1-loop they are given by

$$16\pi^2 \frac{d}{dt} \lambda_{t'}^{(1)} = \lambda_{t'}^{(1)} (S_q + S_{u^c} + S_{h_u} - c_i^u g_i^2) \quad (4.13)$$

$$16\pi^2 \frac{d}{dt} \lambda_{b'}^{(1)} = \lambda_{b'}^{(1)} (S_q + S_{d^c} + S_{h_d} - c_i^d g_i^2) \quad (4.14)$$

$$16\pi^2 \frac{d}{dt} \lambda_{\tau'}^{(1)} = \lambda_{\tau'}^{(1)} (S_l + S_{h_d} - c_i^e g_i^2) \quad (4.15)$$

$$16\pi^2 \frac{d}{dt} \lambda_t = \lambda_t \left( 6\lambda_t^2 + 3 \left( \lambda_{t'}^{(1)} \right)^2 - c_i^u g_i^2 \right) \quad (4.16)$$

$$16\pi^2 \frac{d}{dt} \lambda_U = \lambda_U (S_q + S_{u^c} + 3\lambda_U^2 - c_i^u g_i^2) \quad (4.17)$$

$$16\pi^2 \frac{d}{dt} \lambda_D = \lambda_D (S_q + S_{d^c} + 3\lambda_D^2 + \lambda_E^2 - c_i^d g_i^2) \quad (4.18)$$

$$16\pi^2 \frac{d}{dt} \lambda'_D = \lambda'_D (S_q + S_{h_d} + 2\lambda_D'^2 - c_i^d g_i^2) \quad (4.19)$$

$$16\pi^2 \frac{d}{dt} \lambda_E = \lambda_E (S_l + 3\lambda_D^2 + \lambda_E^2 - c_i^e g_i^2) \quad (4.20)$$

where

$$S_q = \left( \lambda_{t'}^{(1)} \right)^2 + \left( \lambda_{b'}^{(1)} \right)^2 + \lambda_U^2 + \lambda_D^2 + \lambda_D'^2 \quad (4.21)$$

$$S_{u^c} = 2 \left( \lambda_{t'}^{(1)} \right)^2 + 2\lambda_U^2 \quad (4.22)$$

$$S_{d^c} = 2 \left( \lambda_{b'}^{(1)} \right)^2 + 2\lambda_D^2 \quad (4.23)$$

$$S_l = 3 \left( \lambda_{\tau'}^{(1)} \right)^2 + 3\lambda_E^2 \quad (4.24)$$

$$S_{h_u} = 3 \left( \lambda_{t'}^{(1)} \right)^2 + 3\lambda_t^2 \quad (4.25)$$

$$S_{h_d} = 3 \left( \lambda_{b'}^{(1)} \right)^2 + \left( \lambda_{\tau'}^{(1)} \right)^2 + 3\lambda_D^2 \quad (4.26)$$

$$c_i^u = \left( \frac{13}{15}, 3, \frac{16}{3} \right), \quad c_i^d = \left( \frac{7}{15}, 3, \frac{16}{3} \right), \quad c_i^e = \left( \frac{9}{5}, 3, 0 \right), \quad (4.27)$$

and  $t = \ln \mu$ . We have ignored bottom and tau Yukawa couplings because we still work in a low  $\tan \beta$  regime. Also the Dirac Yukawa coupling of the fourth left handed neutrino with the ‘right handed’ singlet  $N$  is neglected, because assuming  $m_{\nu'} \simeq 50$  GeV we get  $\lambda_{\nu'} \simeq 0.25$  which is small.

At scale  $\Lambda_4 = 1$  TeV, for boundary conditions we take

$$\text{at } \mu = \Lambda_4 = 1 \text{ TeV : } \quad \lambda_{t'}^{(1)} = \lambda_U = 0.62,$$

$$\lambda_{b'}^{(1)} = \lambda_D = \lambda'_D = 0.813, \quad \lambda_{\tau'}^{(1)} = 0.564, \quad \lambda_E = 0.632, \quad (4.28)$$

and run the couplings up to  $\mu = M_{\text{GUT}}$ . The numerical solutions are displayed in Fig. 4.4. For completeness we have also included 2-loop contributions. As we see from Fig. 4.4, all couplings remain perturbative. Note that the boundary values in (4.28) with  $\cos \gamma \approx \cos \gamma' \approx 1$  for  $\tan \beta \simeq 2$  give values for  $m_{t'}, m_{b'}, m_{\tau'}$  (evaluated at their own mass scales) satisfying current experimental bounds. Thus, our solution is fully consistent.

We have demonstrated that with a simple extension one can make the MSSM with four chiral generations perturbative all the way up to the GUT scale. This gives firm ground for embedding the whole scenario in a Grand Unified Theory. Other variations of the construction of the effective Yukawa sector are possible, however, we have limited ourselves here with one example because it solves the problems in a simple and efficient way. We hope that our studies will motivate others in further investigations.

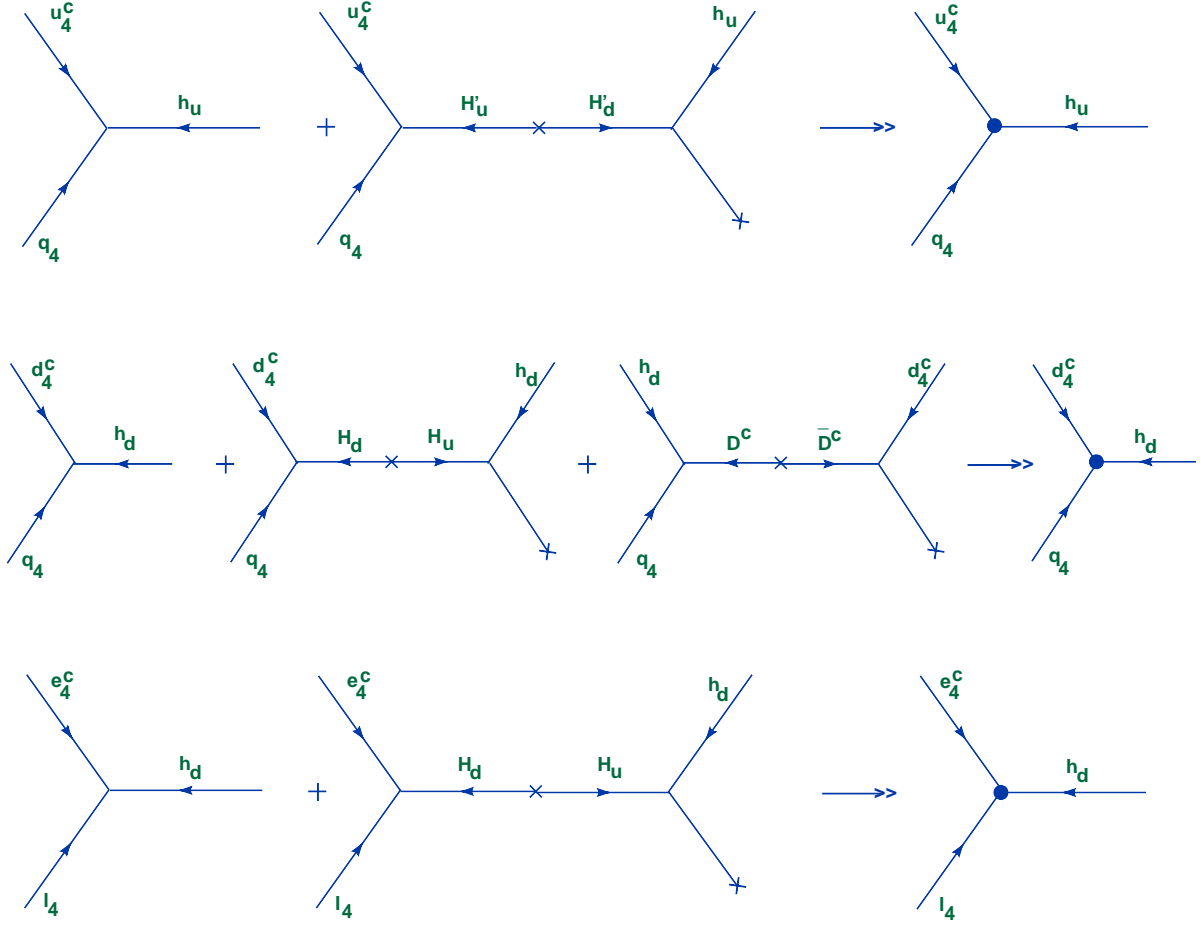


Figure 4.3: Diagrams generating Yukawa couplings  $\lambda_{t'}$ ,  $\lambda_{b'}$  and  $\lambda_{\tau'}$ .

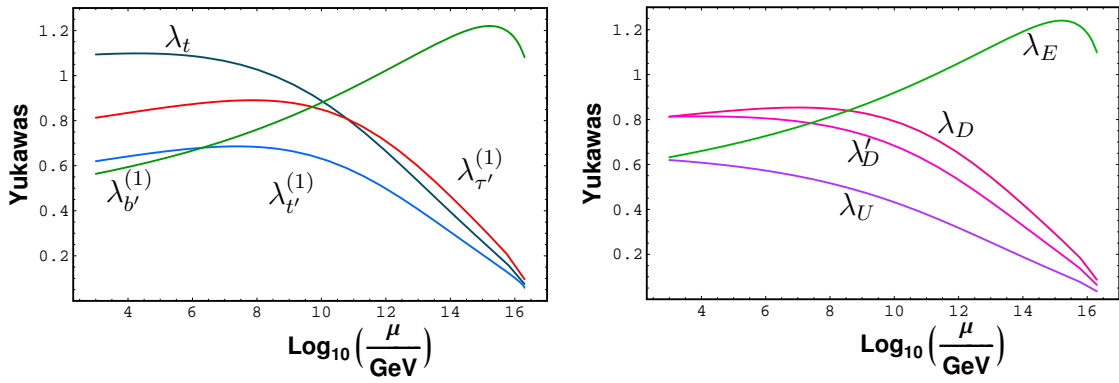


Figure 4.4: Plots at left hand side: running of Yukawa couplings  $\lambda_t$ ,  $\lambda_{t'}^{(1)}$ ,  $\lambda_{b'}^{(1)}$  and  $\lambda_{\tau'}^{(1)}$ . Right hand side: running of couplings  $\lambda_U$ ,  $\lambda_D$ ,  $\lambda_D'$ ,  $\lambda_E$ .

## 4.4 Conclusions

We have investigated the implications of the presence of a 4th chiral family of fermions in the MSSM as well as the SM. Previous work used the experimental values of the precision EW parameters,  $S$ ,  $T$  to set constraints on the masses of the 4th family and their splitting between the up and down type quarks ( $t'$  and  $b'$ ). In our analysis, we have included the parameter  $U$  and derived further constraints. This result is shown in Fig. (4.1).

We also investigated the constraint on the 4th family from the perturbativity condition on the corresponding Yukawa couplings, and found that in MSSM, there is no allowed value of  $\tan\beta$  for which the couplings remain perturbative all the way up to the GUT scale. As a result, if a 4th family is discovered at the LHC, then for the theory to make sense perturbatively, there must be additional new physics with a suitable ultraviolet completion. We have presented such a model with additional vector-like states, at the TeV scale. In our model, only the very narrow range of  $\tan\beta < 2$  is allowed.

In addition to observing the 4th chiral family of fermions at the LHC, the model has several predictions, such as the existence of vector-like down type quarks at the TeV scale which can be pair produced by gluon-gluon fusion, enhanced decay of the lightest Higgs boson to two photons, and enhanced Higgs production from gluon-gluon fusion due to the  $t'$  and  $b'$  quarks. These predictions of the model can be tested at the LHC.

## CHAPTER 5

### NEUTRINO MASSES FROM FINE-TUNING

#### 5.1 Introduction

In the past decade, the existence of tiny neutrino masses of the order of one hundredth to one tenth of an electron volt has been firmly established through atmospheric, solar and reactor neutrino experiments [50][49][51]. These masses are a million or more times smaller than the corresponding charged lepton masses. While the quark and charged lepton masses span many orders of magnitude, the neutrino masses are do not. The square root of the neutrino mass square differences, as obtained from the neutrino oscillation experiments, lies within a factor of five. Also the quark mixing angles are very small, whereas two of the neutrino mixing angles are large [36]. These observations have led to several unanswered questions. Why are the neutrino masses so small compared to the corresponding charged lepton or quark masses? Why is there such a large hierarchy among the charged fermion masses, while there is practically no hierarchy among the neutrino masses? Also, unlike the quark sector why are the mixing angles in the neutrino sector large? Another related fundamental question is whether neutrinos are Majorana or Dirac particles, and whether the light neutrino spectrum exhibit a normal hierarchy or an inverted hierarchy.

The most popular idea proposed so far for understanding the tiny neutrino mass is the famous see-saw mechanism [52]. One postulates the existence of a very massive Standard Model (SM) singlet right handed neutrinos with Majorana masses of order of  $M \sim 10^{14}\text{GeV}$ . The Yukawa coupling of the left-handed neutrino to this heavy right-handed neutrino then gives a Dirac mass of the order of the charged lepton

masses,  $m_l$ . As a result, the left-handed neutrino obtains a tiny mass of the order of  $m_l^2/M$ . Although there are several indirect benefits for its existence, there is no direct experimental evidence for such a heavy particle. The mass scale is so high that no connection can be made with the physics to be explored at the high energy colliders such as the Tevatron and the LHC. It is important to explore other possibilities to explain the tiny neutrino masses. Also, the see-saw mechanism does not naturally lead to lack of hierarchy among the light neutrino masses, though such an hierarchy can be accommodated with the appropriate choice of the right handed Majorana sector.

Recent astrophysical observation requires a tiny but non-zero value of the cosmological constant,  $\Lambda^{1/4} \simeq (10^{-4} \text{ eV})$ . This value is surprisingly close to the value of the light neutrino masses required from the neutrino oscillation experiments,  $\simeq 10^{-2} - 10^{-1} \text{ eV}$ . It has been exceedingly difficult to derive such a tiny value of the cosmological constant, and there is some acceptance that it may be fine tuned. The idea of Higgs mass also being fine tuned has been explored leading to the so called ‘‘Split Supersymmetry’’ [53] with interesting implications at the TeV scale that can be explored at the LHC. Neutrino masses being in the same ballpark as the cosmological constant, it is not unreasonable to assume that their values are also fine tuned. The objective in this project is to adopt this philosophy, build a concrete model realizing this scenario, and explore its phenomenological implications, specially for the LHC.

In this work, we present a model in which the light neutrinos get their masses from the usual see-saw mechanism, except the right handed neutrino masses are at the TeV scale. The neutrino Dirac masses get contributions from two different Higgs doublets with their vacuum expectation values (vevs) at the electroweak scale. The neutrino masses are small not because of tiny Yukawa couplings, or not because of a tiny vev of a new Higgs doublet [54]. In fact, we take the Yukawa couplings to be of order one. The smallness of the light neutrino masses are due to the cancellation in

the Dirac neutrino mass matrix, making it of the order of  $m_D \sim 10^{-4}$  GeV giving rise to light neutrino masses  $m_\nu \sim m_D^2/M$  where  $M$  is the RH Majorana neutrino mass. Thus with  $M$  in the TeV scale, we get the light neutrino mass in the correct range of  $10^{-2} - 10^{-1}$  eV range.

Our work is presented as follows: In section 2, we present the model and the formalism. In section 3, we discuss the phenomenological implications of the model, especially how it alters the usual Standard Model Higgs decay modes, and its implications for the Higgs search at the LHC. Section 4 contains our conclusions.

## 5.2 Model and the formalism

### 5.2.1 Our model

Our model is based on the SM gauge symmetry,  $SU(3)_C \times SU(2)_L \times U(1)_Y$ , supplemented by a discrete  $Z_2$  symmetry. In addition to the SM fermions and the Higgs doublet,  $H$ , we introduce three RH neutrinos,  $N_{Ri}$  where,  $i = 1, 2, 3$ , and two additional Higgs doublets,  $H_1$  and  $H_2$ , with vevs at the EW scale. All the SM particles are even under the  $Z_2$  symmetry, while the three RH neutrinos and the two new Higgs doublets  $H_1$  and  $H_2$  are odd under  $Z_2$ . The  $Z_2$  symmetry is softly broken by the bilinear Higgs terms. With this symmetry, the Yukawa interactions are given by

$$\mathcal{L}_{\text{SM Yukawa}} = \bar{q}_L y_u u_R \tilde{H} + \bar{q}_L y_d d_R H + \bar{l}_L y_L e_R H + h.c., \quad (5.1)$$

where the fermion fields represent three families, and  $y_d, y_u$  and  $y_l$  represent three corresponding Yukawa coupling matrices.

$$\mathcal{L}_{\text{New Yukawa}} = \bar{l}_L f_{1\nu} N_R \tilde{H}_1 + \bar{l}_L f_{2\nu} N_R \tilde{H}_2 + h.c., \quad (5.2)$$

$$\mathcal{L}_{\text{Maj}} = \frac{1}{2} M_{\text{Maj}} N_R^T C^{-1} N_R. \quad (5.3)$$



Note that from the above equations, the  $6 \times 6$  neutrino mass matrix is obtained to be

$$M_\nu = \begin{pmatrix} 0 & m_D \\ (m_D)^T & M_{\text{Maj}} \end{pmatrix} \quad (5.4)$$

The  $3 \times 3$  Dirac mass matrix is given by

$$m_D = \frac{1}{\sqrt{2}} (f_{1\nu} v_1 + f_{2\nu} v_2) \quad (5.5)$$

Here  $v_1$  and  $v_2$  are the vevs of the new Higgs fields  $H_1$  and  $H_2$ . For the mass scales in which  $m_D \ll M_{\text{Maj}}$ , the  $3 \times 3$  light neutrino mass matrix is given by

$$m_\nu^{\text{light}} = -m_D M_{\text{Maj}}^{-1} (m_D)^T \quad (5.6)$$

Note that experimentally masses of the light neutrinos are in the  $10^{-1}$  eV range. Thus with  $M_{\text{Maj}}$  in the EW scale, the matrix  $m_D$  needs to be in the scale of  $10^{-4}$  GeV. Since the vevs  $v_1$  and  $v_2$  are in the EW scale, we can get  $m_D$  in the  $10^{-4}$  GeV scale by assuming the Yukawa couplings to be very tiny, of order  $10^{-6}$ . Such a path, similar to the usual see-saw, will not lead to any interesting implications for neutrino physics in the TeV scale. Instead we assume that the Yukawa couplings,  $f_{1\nu}$  and  $f_{2\nu}$  are of  $\sim \mathcal{O}(1)$ , and these Yukawa couplings and vevs  $v_1$  and  $v_2$  are fine tuned to get  $m_D$  in the  $10^{-4}$  GeV. This is our approach to the smallness of the light neutrino mass scale. As we will see, this gives interesting implication for the neutrino physics at the TeV scale, and can be explored at the LHC.

### 5.2.2 Higgs potential

Now we discuss the Higgs sector of the model. In addition to the usual SM Higgs  $H$  two other Higgs doublets  $H_1$ ,  $H_2$  are required in this model. These two new Higgs doublets couple only to the neutrinos, and this is imposed using the  $Z_2$  symmetry. It is the cancelation of contributions to the Dirac neutrino mass from these two new doublets that enable the use of fine tuning.

We assume that the  $Z_2$  symmetry is softly broken by the bilinear terms in the Higgs Potential. The two new doublets will mix with the SM Higgs doublet, and as we will see, this will produce entirely new signals for the SM Higgs boson decays. The Higgs potential is given by

$$V_{\text{Higgs}} = V_{\text{Higgs}}^{(2)\text{even}} + V_{\text{Higgs}}^{(2)\text{odd}} + V_{\text{Higgs}}^{(4)\text{even}} \quad (5.7)$$

$$V_{\text{Higgs}}^{(2)\text{even}} = \mu_H^2 H^\dagger H + \mu_1^2 H_1^\dagger H_1 + \mu_2^2 H_2^\dagger H_2 + \mu_{12}^2 (H_1^\dagger H_2 + H_2^\dagger H_1) \quad (5.8)$$

$$V_{\text{Higgs}}^{(2)\text{odd}} = \mu_{H1}^2 (H^\dagger H_1 + H_1^\dagger H) + \mu_{H2}^2 (H^\dagger H_2 + H_2^\dagger H) \quad (5.9)$$

Note that the odd part of the potential breaks the  $Z_2$  symmetry softly, and as a result, SM Higgs bosons can mix with the two new Higgs doublets. This will have interesting implications for the SM Higgs boson decays.

$$\begin{aligned} V_{\text{Higgs}}^{(4)\text{even}} = & \lambda (H^\dagger H)^2 + \lambda_1 (H_1^\dagger H_1)^2 + \lambda_2 (H_2^\dagger H_2)^2 \\ & + \lambda_{1122} (H_1^\dagger H_1) (H_2^\dagger H_2) + \lambda_{HH12} (H^\dagger H) (H_1^\dagger H_2 + H_2^\dagger H_1) \\ & + \lambda_{HH22} (H^\dagger H) (H_2^\dagger H_2) + \lambda_{1112} (H_1^\dagger H_1) (H_1^\dagger H_2 + H_2^\dagger H_1) \\ & + \lambda_{HH11} (H^\dagger H) (H_1^\dagger H_1) + \lambda_{2212} (H_2^\dagger H_2) (H_1^\dagger H_2 + H_2^\dagger H_1) \\ & + \lambda_{12} (H_1^\dagger H_2)^2 + \lambda_{H1} (H^\dagger H_1)^2 + \lambda_{H2} (H^\dagger H_2)^2 \\ & + \lambda_{H1H2} (H^\dagger H_1 + H_1^\dagger H) (H^\dagger H_2 + H_2^\dagger H) \end{aligned} \quad (5.10)$$

Since there are three Higgs doublets, after EW symmetry breaking, there will remain a pair of charged Higgs ( $H^\pm, H'^\pm$ ), five neutral scalar Higgses ( $h', h'_1, h'_2, H'_1, H'_2$ ), and two neutral pseudoscalar Higgses ( $A'_1, A'_2$ ). Due to the breaking of the  $Z_2$  symmetry, there is mixing within each of these three groups of Higgses (but not between groups). We denote the mass eigenstates of the five neutral Higgses by  $h, h_{10}, H_{10}, h_{20}$ , and  $H_{20}$ .

### 5.2.3 Mixing between the light and heavy neutrinos

In our model, we are considering a scenario in which the three RH handed neutrinos have masses in the EW scale with  $\sim \mathcal{O}(1)$  Yukawa couplings with the light left handed

neutrinos. They will also mix with the light neutrinos, and thus will participate in the gauge interactions. LEP has searched for such RH neutrinos. Before we discuss these constraints, let us first consider the mixing between the light neutrinos and the RH neutrinos. Using the observed values of the light neutrino masses and mixings, we can make a reasonable estimate of the mixing between the LH and RH neutrino as follows. We use the normal hierarchy for the light neutrino masses with the values

$$m_{\nu\text{Eigenvalues}}^{\text{light}} = \text{Diag}(m_{\nu_1}, m_{\nu_2}, m_{\nu_3}) = \text{Diag}(0, 8.71, 49.3) \times 10^{-12} \text{ GeV} \quad (5.11)$$

The mixing matrix  $R_{\nu\nu}$  follows the standard parametrization. The angles  $\theta_{12}, \theta_{23}$  are the central values, and  $\theta_{13}$  is the maximal value allowed by current experiment [Ref Choze].

$$(\theta_{12}, \theta_{23}, \theta_{13}) = (0.601, 0.642, 0.226) \quad (5.12)$$

$$R_{\nu\nu} = \begin{pmatrix} 0.804 & 0.551 & 0.223 \\ -0.563 & 0.585 & 0.584 \\ 0.190 & -0.595 & 0.781 \end{pmatrix} \quad (5.13)$$

The three possible CP-violating phases are assumed to be zero. From the above mass eigenvalues and the mixing matrix, we can calculate the light neutrino mass matrix using

$$(R_{\nu\nu})^T m_{\nu}^{\text{light}} R_{\nu\nu} = m_{\nu\text{Eigenvalues}}^{\text{light}} \quad (5.14)$$

For simplicity, we assume that the  $3 \times 3$  RH Majorana mass matrix  $M_{\text{Maj}}$  to be proportional to the unit matrix,

$$M_{\text{Maj}} = \text{Diag}(M, M, M), \quad (5.15)$$

and we use  $M = 100 \text{ GeV}$ . As a consequence of this choice for  $M_{\text{Maj}}$  and having a symmetric  $m_D$ , the mixing matrix among only the generations of heavy neutrinos is equivalent to the mixing matrix among only the generations of light neutrinos

$R_{NN} = R_{\nu\nu}$ . Using the above numbers, we can now calculate numerically the  $3 \times 3$  Dirac neutrino mass matrix from the equation

$$m_{\nu}^{\text{light}} = -m_{\text{D}} M_{\text{Maj}}^{-1} m_{\text{D}}^{\text{T}} \quad (5.16)$$

There are four sets of real solutions for  $m_{\text{D}}$ . Only two sets of solutions are presented in Table 5.1. The other two are just the negatives of these two sets.

$\times 10^{-5} \text{ GeV}$	$m_{\text{D}}^{11}$	$m_{\text{D}}^{12}$	$m_{\text{D}}^{13}$	$m_{\text{D}}^{22}$	$m_{\text{D}}^{23}$	$m_{\text{D}}^{33}$
Set 1	-1.25	-1.87	-0.267	-3.42	-2.20	-5.36
Set 2	-.543	-0.0280	2.20	1.40	4.25	3.27

Table 5.1: Solution values for the matrix  $m_{\text{D}}$ .

Using the solutions for  $m_{\text{D}}$  and  $M_{\text{Maj}}$ , we can now use the full  $6 \times 6$  neutrino mass matrix and calculate the full mixing matrix  $Q$  and the mixing angles between the heavy and light neutrinos.

$$M^{\text{Full}} = \begin{pmatrix} 0_{3 \times 3} & m_{\text{D}} \\ m_{\text{D}}^{\text{T}} & M_{\text{Maj}} \end{pmatrix}, \quad Q^{-1} M^{\text{Full}} Q = M_{\text{Eigenvalues}}^{\text{Full}}. \quad (5.17)$$

It turns out that

$$Q \approx \begin{pmatrix} R_{\nu\nu} & Q_{\nu N} \\ Q_{N\nu} & R_{NN} \end{pmatrix}, \quad Q_{\nu N} \approx Q_{N\nu}. \quad (5.18)$$

$\times 10^{-7}$	$\theta_{14}$	$\theta_{15}$	$\theta_{16}$	$\theta_{24}$	$\theta_{25}$	$\theta_{26}$	$\theta_{34}$	$\theta_{35}$	$\theta_{36}$
Set 1	1.2	1.9	0.26	1.9	3.4	2.2	0.26	2.2	5.3
Set 2	0.55	0.36	-2.2	0.034	-1.4	-4.2	-2.2	-4.2	-3.2

Table 5.2: Mixing angles between the light neutrinos (subscripts 1, 2, 3) and the heavy neutrinos (subscripts 4, 5, 6).

For solution set 1, the full rotation matrix is

$$Q = \begin{pmatrix} \begin{pmatrix} 0.80 & 0.55 & 0.22 \\ -0.56 & 0.59 & 0.58 \\ 0.19 & -0.60 & 0.78 \end{pmatrix} & \begin{pmatrix} 3.1 \times 10^{-3} & 1.6 & 1.6 \\ 3.513 \times 10^{-3} & 1.7 & 4.1 \\ -2.5 \times 10^{-3} & -1.8 & 5.5 \end{pmatrix} \times 10^{-7} \\ \begin{pmatrix} 1.1 \times 10^{-4} & -1.6 & -1.6 \\ 1.3 \times 10^{-4} & -1.7 & -4.1 \\ -8.8 \times 10^{-5} & 1.8 & -5.5 \end{pmatrix} \times 10^{-7} & \begin{pmatrix} 0.81 & 0.55 & 0.22 \\ -0.56 & 0.59 & 0.58 \\ 0.19 & -0.60 & 0.78 \end{pmatrix} \end{pmatrix}. \quad (5.19)$$

For solution set 2, the full rotation matrix is

$$Q = \begin{pmatrix} \begin{pmatrix} 0.80 & 0.55 & 0.22 \\ -0.56 & 0.59 & 0.58 \\ 0.19 & -0.60 & 0.78 \end{pmatrix} & \begin{pmatrix} 4.1 \times 10^{-3} & 1.6 & -1.6 \\ 3.9 \times 10^{-3} & 1.7 & -4.1 \\ -5.7 \times 10^{-3} & -1.8 & -5.5 \end{pmatrix} \times 10^{-7} \\ \begin{pmatrix} -8.9 \times 10^{-4} & -1.6 & 1.6 \\ -7.9 \times 10^{-4} & -1.7 & 4.1 \\ 1.4 \times 10^{-3} & 1.8 & 5.5 \end{pmatrix} \times 10^{-7} & \begin{pmatrix} 0.80 & 0.55 & 0.22 \\ -0.56 & 0.590 & 0.58 \\ 0.19 & -0.60 & 0.78 \end{pmatrix} \end{pmatrix}. \quad (5.20)$$

As can be seen on Table 5.2, the mixing between the heavy and light neutrinos is extremely small.

### 5.3 Phenomenological implications

In this section, we discuss the phenomenological implications of our model. We are considering RH neutrinos at the EW scale. Their mass can be below the  $W$  boson mass. Thus they can be searched for at LEP, Tevatron, and at the LHC. First we discuss the constraints that already exist from the search at LEP.

#### 5.3.1 LEP constraints

Searches for  $N_R$  have been conducted at LEP in the channel  $e^+e^- \rightarrow Z \rightarrow N_R\nu_l$ , with  $N_R$  subsequently decaying to  $W^+e^-$  or  $Z\nu$ . This experiment puts limit on the mixing angle,  $\theta$  between the heavy and the light neutrinos  $\sin^2\theta < 10^{-4}$  for  $3\text{ GeV} < M_N < 80\text{ GeV}$ , and  $\sin^2\theta < 0.1$  for  $M_N > 80\text{ GeV}$  [55]. As we discussed in previous section, the mixing angles,  $\theta$  between the light and heavy neutrinos are extremely small, ranging between  $\sim 10^{-6}$  to  $10^{-8}$ . Thus, in our model, LEP constraints allows small masses for the heavy Majorana neutrinos.

#### 5.3.2 Higgs decays and Higgs signals

In our model, the Yukawa couplings between the light neutrinos, the heavy Majorana neutrinos and the new Higgs fields  $H_1$  and  $H_2$  are of  $\sim \mathcal{O}(1)$ . The Standard model Higgs,  $H$  mixes with the new Higgses, and these mixings are naturally large. Thus, for  $M_N < M_h$ , the standard model Higgs will dominantly decay to a light  $\nu$  and  $N_R$ , as soon as this decay mode becomes kinematically allowed, because the coupling for this decay mode is much larger than the usually dominant  $\bar{b}b$  mode, or even the  $WW$  mode. The branching ratios for the various Higgs decay modes are shown in Fig.1 for  $M_N = 80\text{ GeV}$ . As can be seen from the plot, as soon as the decay mode  $h \rightarrow \nu N_R$  becomes kinematically allowed, this mode totally dominates over the usual  $\bar{b}b$  mode, and larger than the usually dominant  $WW$  mode even beyond the  $WW$  threshold. Thus in our model, the SM Higgs decay mode is greatly altered.

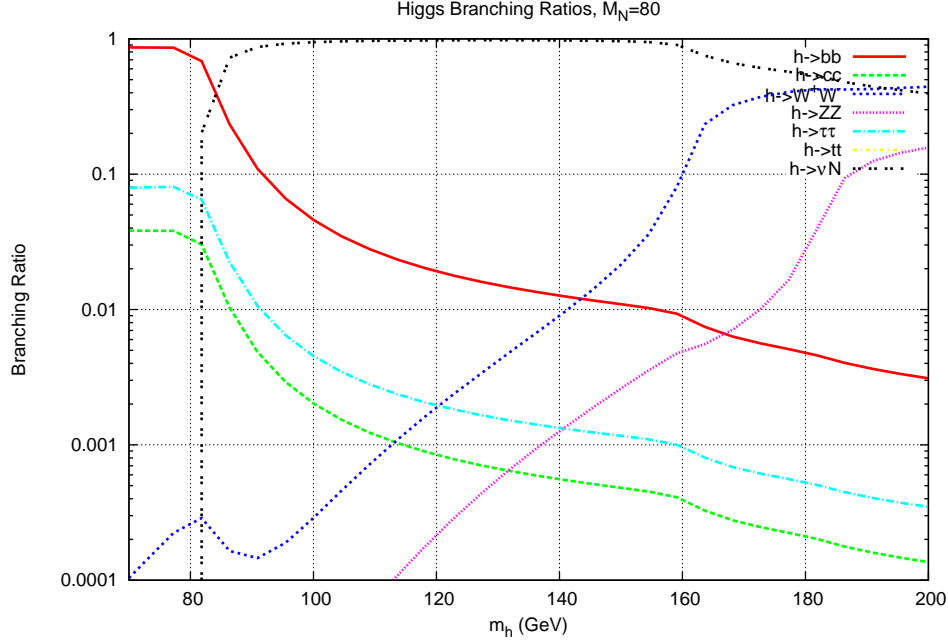


Figure 5.1: Branching ratio of  $h \rightarrow 2x$ .

At hadron colliders, the SM Higgs boson is dominantly produced via gluon fusion with the top quark in the loop. In our model, because of the mixing of  $H$  with  $H_1$  and  $H_2$ , the lightest mass neutral scalar Higgs decays dominantly to  $h \rightarrow \nu N_R$ . The final state signal will depend on the decay modes of  $N_R$ . Two of the allowed decay modes of  $N_R$  are shown in Fig. 5.3. The 3-body decay mode  $N_R \rightarrow \nu \bar{b} b$  is completely dominant over the 2-body decay mode  $lW$  or  $\nu Z$ . This is because the 2-body decay is suppressed by the tiny mixing angle,  $\theta \sim 10^{-6}$  or smaller. Thus the final state signals for the Higgs bosons at the LHC, in our model, is  $\bar{\nu} \nu \bar{b} b$ . Collider signals will include large missing energy and 2 hard b-jets.

Using Madgraph, we generated events for  $pp \rightarrow \bar{\nu} \nu \bar{b} b$  in the SM for LHC at 14 TeV, 7 TeV, and Tevatron. Using the cuts  $\cancel{E}_T = 30$  GeV, and the  $p_T$  for each b-jet to be greater than 20 GeV, we find the cross section to be  $\sim 13$  pb. The cross section for Higgs production at the LHC at 14 TeV is  $\sim 50$  pb for a 120 GeV Higgs. For a large mass range of the Higgs boson in our model, the branching ratio,

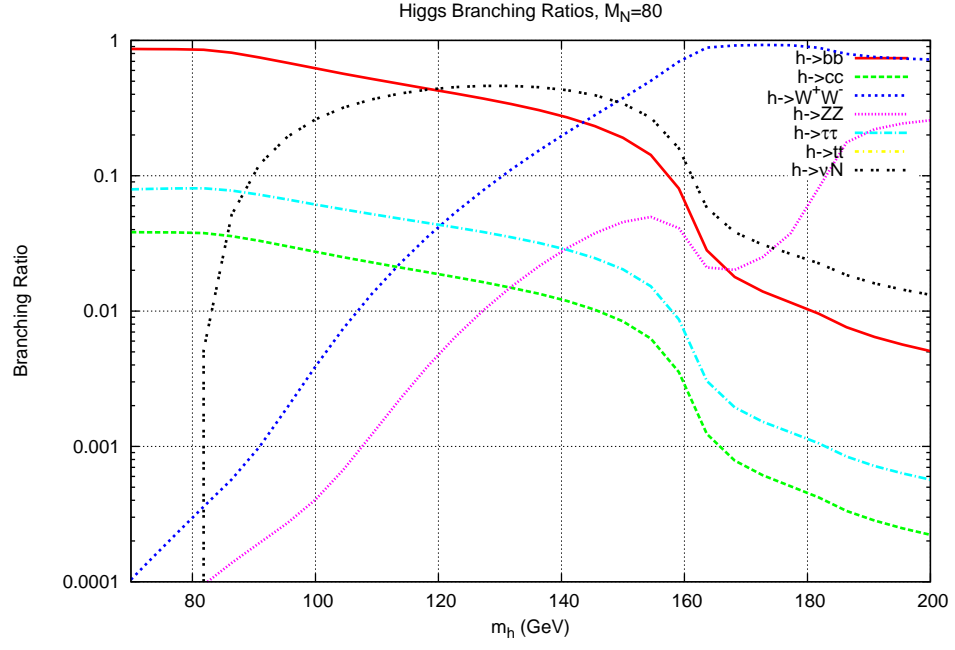


Figure 5.2: Branching ratio of  $h \rightarrow 2x$  with the coupling between  $N_R$  and  $\nu_L$ ,  $y = \frac{1}{7}$

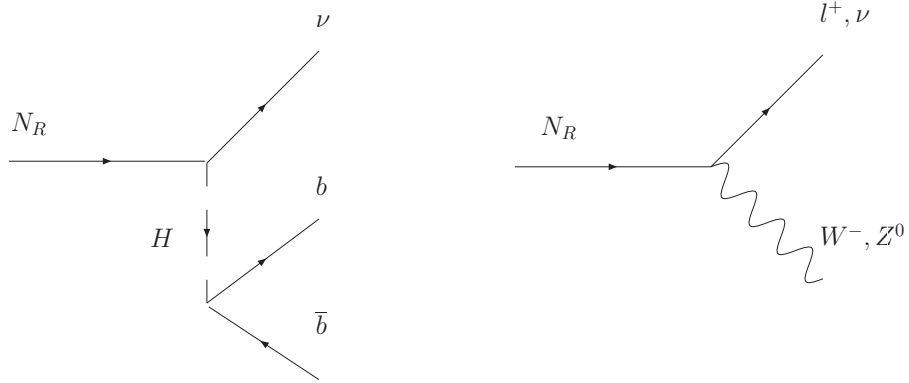


Figure 5.3: Decay modes of  $N_R$



$BR(h \rightarrow \nu N_R) \sim 100\%$ . Thus this Higgs signal in our model is observable at the LHC, and stands out over the SM background. A summary for different energies is given in Table 5.3.

Collider	$\sqrt{s}$ Energy	Background	Signal
LHC	14 TeV	13 pb	50 pb
LHC	7 TeV	2.4 pb	30 pb
Tevatron	2 TeV	240 fb	1 pb

Table 5.3: Collider Searches for  $m_h = 120\text{GeV}$

The Higgs production at the Tevatron is taken from [56]. For the LHC we used [57]

### 5.3.3 $ZH \rightarrow \nu\bar{\nu}b\bar{b}$ Search at Tevatron

Searches for the standard model higgs in the channel  $ZH \rightarrow \nu\bar{\nu}b\bar{b}$  have been made at the Tevatron [58]. With  $5.2\text{ fb}^{-1}$  of data they see nothing and are able to place a limit on this mode in the standard model. Since our final state and cuts are virtually identical, this search places a limit on the branching ratios of  $h$  and  $N_R$  in our model. The number of events we expect to see is:

$$\# \text{ of events} = \sigma(pp \rightarrow h) \times BR(h \rightarrow N_R \nu) \times BR(N_R \rightarrow \nu b\bar{b}) \times \epsilon_{b\text{-tag}}^2 \quad (5.21)$$

Where  $\epsilon_{b\text{-tag}}$  is the b-tagging efficiency. One of these branching ratios needs to be smaller to accomodate the results of  $ZH \rightarrow \nu\bar{\nu}b\bar{b}$  searches. Other possibilities for our model are that the right handed neutrino's could decay via a charged higgs.

### 5.3.4 $N_R$ Decays via Charged Higgs

For a sufficiently light,  $m_{H^\pm} < 250\text{ GeV}$ , the decay of  $N_R \rightarrow \nu_\tau \tau^+ \tau^-$  via a charged Higgs becomes important. Taking the yukawa couplings to be order one, and the

mixing to be maximal between the three higgs doublets, the decay rates for the  $N_R$  decays are shown in table 5.4. Taking the tau  $p_T > 20\text{GeV}$  and missing  $E_T > 30\text{GeV}$  the cross section for  $pp \rightarrow \nu\bar{\nu}\tau^+\tau^-$  at the Tevatron is 45 fb (123 pb the LHC for 7 TeV collisions). This background is much smaller than  $pp \rightarrow \bar{b}b\nu\bar{\nu}$  background, as it is a leptonic (not QCD) process. This signature, two high  $p_T$  tau's plus missing energy, may be easier to see.

Decay Mode	$\Gamma(N_R \rightarrow 3x)$ (GeV)	$m_{H^\pm}$ (GeV)	BR
$N_R \rightarrow \nu b\bar{b}$	$1.56 * 10^{-9}$	200	43.8%
$N_R \rightarrow \nu_\tau \tau^+ \tau^-$	$1.32 * 10^{-9}$	200	37.0%
$N_R \rightarrow \tau c\bar{s}$ (or $\bar{c}s$ )	$5.80 * 10^{-10}$	200	16.3%
$N_R \rightarrow \nu c\bar{c}$	$6.60 * 10^{-11}$	200	1.85%
$N_R \rightarrow \nu_\mu \mu^+ \mu^-$	$4.00 * 10^{-11}$	200	1.12%
$N_R \rightarrow \nu b\bar{b}$	$1.56 * 10^{-9}$	250	63.6%
$N_R \rightarrow \nu_\tau \tau^+ \tau^-$	$5.62 * 10^{-10}$	250	22.9%
$N_R \rightarrow \tau^- c\bar{s}$ (or $\tau^+ \bar{c}s$ )	$2.26 * 10^{-10}$	250	9.21%
$N_R \rightarrow \nu c\bar{c}$	$6.60 * 10^{-11}$	250	2.69%
$N_R \rightarrow \nu_\mu \mu^+ \mu^-$	$2.45 * 10^{-11}$	250	1.65%

Table 5.4: Decay Rates for  $N_R$ ,  $M_N = 80$  GeV,  $M_h = 120$  GeV

## 5.4 Conclusions

We have proposed a new approach for the understanding of the tinyness of the light neutrino masses. We extend the Standard Model gauge symmetry by a discrete  $Z_2$  symmetry, and the particle content by adding three right handed neutrinos and two

additional Higgs doublets. These new Higgs doublets couple only to the neutrinos. The tiny neutrino masses are generated via the see-saw mechanism with the right handed neutrino mass matrix at the EW scale, and the Dirac neutrino mass matrix at the  $10^{-4}$  GeV scale. The Dirac neutrino mass matrix gets contribution from the two new EW Higgs doublets with vevs at the EW scale. The Yukawa couplings are of order one, and the two EW contributions are fine tuned to achieve the Dirac neutrino mass matrix at the  $10^{-4}$  level. The model links neutrino physics to collider physics at the TeV scale. The SM Higgs decays are drastically altered. For a wide range of the Higgs mass, it decays dominantly to  $\nu_L N_R$  mode giving rise to the final state  $\bar{\nu}\nu\bar{b}b$ , or  $\bar{\nu}\nu\tau^+\tau^-$ . This can be tested at the LHC and possibly at the Tevatron.

## CHAPTER 6

### CONCLUSIONS

Modifying the Yukawa sector of the Standard model can lead to some interesting physical results. We showed how the recent exclusion plot from the Tevatron can be extended significantly if we change our fundamental assumption that the Yukawa interactions of the Higgs with the fermions are dimension 4. This allows the use of dimension 6 operators to give mass to the fermions.

The use of vector-like quarks, flavon symmetries, and an additional singlet Higgs were used to generate the fermion mass hierarchy. This simultaneously alters the phenomenology of Higgs decays substantially. In particular when the mixing between the singlet Higgs and the Standard Model Higgs doublet is  $\theta = 26^\circ$ , the commonly dominant  $b\bar{b}$  mode is heavily suppressed. This increases modes such as the two photon mode. This is the so-called golden mode of the LHC as it has a very distinct signal for a light Higgs.

Adding a fourth generation of fermions to the MSSM can produce some interesting challenges. In the MSSM with a fourth generation only a very small range of values of  $\tan\beta$  are allowed by perturbativity. The main issue is that when the Yukawa couplings are evolved via RGEs, they become non-perturbative very quickly. While this is only a theoretical issue it hints that there is a problem with trying to add a fourth generation. We showed that this problem can be resolved if we introduce some new vector-like quarks that alter the Yukawa couplings by making them an effective coupling coming from a higher order interaction.

Finally we addressed the problem of neutrino mass. The standard way to give

neutrino mass is the seesaw mechanism. It predicts that there is a very heavy ( $M_{GUT}$ ) right-handed neutrino that gives mass to the light neutrinos of the standard model via a seesaw relationship that drives the light mass down to the eV scale. It is hard to find any experimental evidence of these right-handed neutrinos because their mass is so high. In this work we have described a model that produces right-handed neutrinos that are able to be produced at colliders. The phenomenology of Higgs decays changes because the dominant mode becomes  $h \rightarrow N_R \nu \rightarrow \nu \nu b \bar{b}$ . This provides an interesting way to see the neutrino mass mechanism at the LHC.

## BIBLIOGRAPHY

- [1] F. Mandl and G. Shaw, *Quantum Field Theory, Revised Edition*. John Wiley and Sons, 1993.
- [2] D. Griffiths, *Introduction to Elementary Particles*. John Wiley and Sons, 1987.
- [3] T. Cheng and L. Li, *Gauge Theory of Elementary Particle Physics*, Oxford University Press, 1984.
- [4] W. A. Bardeen, C. T. Hill and M. Lindner, Phys. Rev. D **41**, 1647 (1990).  
V. A. Miransky, M. Tanabashi and K. Yamawaki, Phys. Lett. B **221**, 177 (1989);  
V. A. Miransky, M. Tanabashi and K. Yamawaki, Mod. Phys. Lett. A **4**, 1043 (1989);
- [5] C. T. Hill, M. A. Luty and E. A. Paschos, Phys. Rev. D **43**, 3011 (1991).
- [6] C. T. Hill and E. H. Simmons, Phys. Rept. **381**, 235 (2003) [Erratum-ibid. **390**, 553 (2004)]; R. Contino, arXiv:1005.4269 [hep-ph], *and references therein*.
- [7] C. Grojean, G. Servant and J. D. Wells, Phys. Rev. D **71**, 036001 (2005).
- [8] V. Barger, T. Han, P. Langacker, B. McElrath and P. Zerwas, Phys. Rev. D **67**, 115001 (2003).
- [9] W. Buchmuller and D. Wyler, Nucl. Phys. B **268**, 621 (1986); B. Grzadkowski, M. Iskrzynski, M. Misiak and J. Rosiek, arXiv:1008.4884 [hep-ph].
- [10] M. Spira, Nucl. Instrum. Meth. A **389**, 357 (1997); A. Djouadi, J. Kalinowski and M. Spira, Comput. Phys. Commun. **108**, 56 (1998).

- [11] T. Aaltonen *et al.* [CDF and D0 Collaborations], Phys. Rev. Lett. **104**, 061802 (2010).
- [12] [The TEVNPH Working Group of the CDF and D0 Collaborations], arXiv:1007.4587 [hep-ex].
- [13] R. Barate *et al.* Phys. Lett. B **565**, 61 (2003).
- [14] W. Beenakker, S. Dittmaier, M. Kramer, B. Plumper, M. Spira and P. M. Zerwas, Phys. Rev. Lett. **87**, 201805 (2001).
- [15] F. Maltoni, D. L. Rainwater and S. Willenbrock, Phys. Rev. D **66**, 034022 (2002).
- [16] D. A. Dicus, C. Kao and S. S. D. Willenbrock, Phys. Rev. D **38**:1088 (1988).
- [17] E. W. N. Glover and J. J. van der Bij, Nucl. Phys. B **309**, 282 (1988).
- [18] T. Plehn, M. Spira and P. M. Zerwas, Nucl. Phys. B **479**, 46 (1996) [Erratum-  
ibid. B **531**, 655 (1998)].
- [19] B. Grossmann, Z. Murdock, S. Nandi “Fermion Mass Hierarchy from Symmetry Breaking at the TeV Scale”, arXiv:1011.5256.
- [20] C. D. Froggatt and H. B. Nielsen, Nucl. Phys. B **147**, 277 (1979).
- [21] There is a vast literature on the fermion mass hierarchy problem; see for example:  
A. De Rujula, H. Georgi and S. L. Glashow, Annals Phys. **109**, 258 (1977);  
H. Georgi and C. Jarlskog, Phys. Lett. B **86**, 297 (1979);  
S.M. Barr, Phys. Rev. **D21**, 1424 (1980);  
C. T. Hill, Phys. Rev. D **24**, 691 (1981);  
H. Georgi, A. Manohar and A. Nelson, Phys. Lett. **126B**, 169 (1983);  
S. Dimopoulos, Phys. Lett. B **129**, 417 (1983);  
J. Bagger, S. Dimopoulos, E. Masso and M. H. Reno, Nucl. Phys. B **258**, 565

- (1985);
- K.S. Babu and R.N. Mohapatra, Phys. Rev. Lett. **64**, 2747 (1990);
- M. Leurer, Y. Nir and N. Seiberg, Nucl. Phys. B **398**, 319 (1993);
- Z. Berezhiani and R. Rattazzi, Nucl.Phys. **B407**, 249 (1993);
- Y. Nir and N. Seiberg, Phys. Lett. **B309**, 337 (1993);
- L. E. Ibanez and G. G. Ross, Phys. Lett. B **332**, 100 (1994).
- P. Binetruy and P. Ramond, Phys. Lett. B **350**, 49 (1995);
- E. Dudas, S. Pokorski and C. A. Savoy, Phys. Lett. B **356**, 45 (1995);
- C. H. Albright and S. Nandi, Mod. Phys. Lett. A **11**, 737 (1996);
- D. J. Muller and S. Nandi, Phys. Lett. B **383**, 345 (1996).
- [22] S. Nandi and Z. Tavartkiladze, arXiv:0804.1996 [hep-ph].
- [23] B. A. Dobrescu and P. J. Fox, JHEP **0808**, 100 (2008) [arXiv:0805.0822 [hep-ph]].
- [24] B. S. Balakrishna, Phys. Rev. Lett. **60**, 1602 (1988); B. S. Balakrishna, A. L. Kagan and R. N. Mohapatra, Phys. Lett. B **205**, 345 (1988); B. S. Balakrishna and R. N. Mohapatra, Phys. Lett. B **216**, 349 (1989).
- [25] K. S. Babu and S. Nandi, Phys. Rev. D **62**, 033002 (2000) [arXiv:hep-ph/9907213].
- [26] G. F. Giudice and O. Lebedev, Phys. Lett. B **665**, 79 (2008) [arXiv:0804.1753 [hep-ph]].
- [27] I. Dorsner and S. M. Barr, Phys. Rev. D **65**, 095004 (2002) [arXiv:hep-ph/0201207].
- [28] T. Aaltonen *et al.* [CDF Collaboration], Phys. Rev. Lett. **100**, 121802 (2008) [arXiv:0712.1567 [hep-ex]].



- K. Abe *et al.* [BELLE Collaboration], Phys. Rev. Lett. **99**, 131803 (2007) [arXiv:0704.1000 [hep-ex]].
- [29] LEP Electroweak Working Group, <http://lepewwg.web.cern.ch>
- [30] P. Langacker, arXiv:0801.1345 [hep-ph].
- [31] B. A. Dobrescu, Phys. Rev. Lett. **94**, 151802 (2005) [arXiv:hep-ph/0411004].
- [32] S. Mrenna and J. D. Wells, Phys. Rev. D **63**, 015006 (2001) [arXiv:hep-ph/0001226].
- A. Melnitchouk [D0 Collaboration], Int. J. Mod. Phys. A **20**, 3305 (2005) [arXiv:hep-ex/0501067].
- [33] G. Bernardi *et al.* [Tevatron New Phenomena Higgs Working Group and CDF Collaboration and D], arXiv:0808.0534 [hep-ex].
- [34] J. A. Aguilar-Saavedra and G. C. Branco, Phys. Lett. B **495**, 347 (2000) [arXiv:hep-ph/0004190].
- [35] M. Cacciari, S. Frixione, M. M. Mangano, P. Nason and G. Ridolfi, arXiv:0804.2800 [hep-ph].
- [36] W.-M. Yao et al. (Particle Data Group), J. Phys. G **33**, 1 (2006)
- [37] P. H. Frampton, P. Q. Hung and M. Sher, Phys. Rept. **330**, 263 (2000).
- [38] M. Maltoni, V. A. Novikov, L. B. Okun, A. N. Rozanov and M. I. Vysotsky, Phys. Lett. B **476**, 107 (2000).
- [39] H. J. He, N. Polonsky and S. f. Su, Phys. Rev. D **64**, 053004 (2001).
- [40] G. D. Kribs, T. Plehn, M. Spannowsky and T. M. P. Tait, Phys. Rev. D **76**, 075016 (2007) [arXiv:0706.3718 [hep-ph]].

- [41] E. Arik, M. Arik, S. A. Cetin, T. Conka, A. Mailov and S. Sultansoy, Eur. Phys. J. C **26**, 9 (2002);  
E. Arik, O. Cakir, S. A. Cetin and S. Sultansoy, Acta Phys. Polon. B **37**, 2839 (2006).
- [42] R. Fok and G. D. Kribs, arXiv:0803.4207 [hep-ph].
- [43] M. S. Chanowitz, M. A. Furman and I. Hinchliffe, Phys. Lett. B **78**, 285 (1978);  
M. S. Chanowitz, M. A. Furman and I. Hinchliffe, Nucl. Phys. B **153**, 402 (1979).
- [44] L. J. Hall, R. Rattazzi and U. Sarid, Phys. Rev. D **50** (1994) 7048.
- [45] J. F. Gunion, D. W. McKay and H. Pois, Phys. Lett. B **334**, 339 (1994) [arXiv:hep-ph/9406249].
- [46] H. M. Georgi, S. L. Glashow, M. E. Machacek and D. V. Nanopoulos, Phys. Rev. Lett. **40**, 692 (1978).
- [47] H. E. Haber and R. Hempfling, Phys. Rev. Lett. **66**, 1815 (1991).
- [48] J. R. Ellis, G. Ridolfi and F. Zwirner, Phys. Lett. B **257**, 83 (1991).
- [49] SNO Collaboration, S.N. Ahmed et al., nucl-ex/0309004; SNO Collaboration, Q.R. Ahmad et al., Phys. Rev. Lett. **89** (2002) 011301; Super-Kamiokande Collaboration, S. Fukuda et al., Phys. Lett. B **539** (2002) 179; Super-Kamiokande Collaboration, M.B. Smy et al., Phys. Rev. D **69** (2004) 011104.
- [50] Super-Kamiokande Collaboration, Y. Ashie et al., Phys. Rev. D **71** (2005) 11205; Super-Kamiokande Collaboration, Y. Ashie et al., Phys. Rev. Lett. **93** (2004) 101801.
- [51] For a recent comprehensive review, see for example, R.N. Mohapatra et al., hep-ph/0510213.

- [52] P. Minkowski, Phys. Lett. B **67** (1977) 421, M. Gell-Mann, P. Ramond, and R. Slansky, Supergravity (P. van Nieuwenhuizen et al. eds.), North Holland, Amsterdam, 1980, p. 315; T. Yanagida, in Proceedings of the Workshop on the Unified Theory and the Baryon Number in the Universe (O. Sawada and A. Sugamoto, eds.), KEK, Tsukuba, Japan, 1979, p. 95; S. L. Glashow, The future of elementary particle physics, in Proceedings of the 1979 Cargèse Summer Institute on Quarks and Leptons (M. Levy et al. eds.), Plenum Press, New York, 1980, pp. 687-71. R. N. Mohapatra and G. Senjanovic, Phys. Rev. Lett. **44** (1980) 912.
- [53] N. Arkani-Hamed and S. Dimopoulos, JHEP **0506**, 073 (2005) [arXiv:hep-th/0405159].
- [54] S. Gabriel and S. Nandi, Phys. Lett. B **655**, 141 (2007) [arXiv:hep-ph/0610253]. S. Gabriel, B. Mukhopadhyaya, S. Nandi and S. K. Rai, Phys. Lett. B **669**, 180 (2008) [arXiv:0804.1112 [hep-ph]].
- [55] P. Achard *et al.* [L3 Collaboration], Phys. Lett. B **517**, 67 (2001) [arXiv:hep-ex/0107014].
- [56] J. Baglio and A. Djouadi, arXiv:1003.4266 [hep-ph].
- [57] F. Stockli and R. Suarez, <http://wwweth.cern.ch/HiggsCrossSections/HiggsCrossSection.html>
- [58] V. M. Abazov *et al.* [D0 Collaboration], Phys. Rev. Lett. **104**, 071801 (2010) [arXiv:0912.5285 [hep-ex]].

## VITA

Zeke Murdock

Candidate for the Degree of  
Doctor of Philosophy

Dissertation: NEW IDEAS FOR YUKAWA INTERACTIONS AND THE ORIGIN  
OF MASS

Major Field: Physics

Biographical:

Personal Data: Born in Stillwater, OK, January, 8, 1981.

Education:

Received a B.A. degree from St. John's College, Santa Fe, NM, 2003, in  
Liberal Arts

Completed the requirements for the degree of Doctor of Philosophy with a  
major in Physics from Oklahoma State University in July, 2011.

### Teaching Experience

- Teaching Assistant, General Physics, 6 semesters, Oklahoma State University
- Teaching Assistant, Astronomy, 3 semesters, Oklahoma State University
- Mathematics Tutor/Teacher at St. John's College for 2 years.
- Remarkable evaluations for all teaching from students.

### Technical Skills

- Familiarity with MadGraph, HDecay, Fortran
- Thorough Experience with CalcHEP, Excel, Mathematica

## Conferences/Workshops

- Attended Pheno 2007, and TASI 2009
- Presented “Fourth Generation in the MSSM” at Pheno 2008 in Madison, WI
- Presented “A Light Scalar as the Messenger of Electroweak and Flavor Symmetry Breaking” at:
  - Pheno 2009 in Madison, WI
  - “Particle Physics and Cosmology” 2009 in Norman, OK
- Presented “Neutrino Masses from Fine Tuning” at Pheno 2010

## Publications

- \* Z. Murdock, S. Nandi and Z. Tavartkiladze, “Perturbativity and a Fourth Generation in the MSSM,” *Phys. Lett. B* **668**, 303 (2008).
- \* J. D. Lykken, Z. Murdock and S. Nandi, “A light scalar as the messenger of electroweak and flavor symmetry breaking,” *Phys. Rev. D* **79**, 075014 (2009).
- \* B. N. Grossmann, Z. Murdock and S. Nandi, “Neutrino Masses from Fine Tuning,” *Phys. Lett. B* **693**, 274 (2010).
- \* Z. Murdock, S. Nandi and S. K. Rai, “Non-renormalizable Yukawa Interactions and Higgs Physics,” arXiv:1010.1559 [hep-ph].
- \* B. N. Grossmann, Z. Murdock and S. Nandi, “Fermion Mass Hierarchy from Symmetry Breaking at the TeV Scale,” arXiv:1011.5256 [hep-ph].

Name: Zeke Murdock

Date of Degree: July, 2011

Institution: Oklahoma State University

Location: Stillwater, Oklahoma

Title of Study: NEW IDEAS FOR YUKAWA INTERACTIONS AND THE ORIGIN OF MASS

Pages in Study: 97

Candidate for the Degree of Doctor of Philosophy

Major Field: Physics

I explore new ideas in the Yukawa sector of the Standard Model. Very little is known experimentally about the Yukawa sector. We have yet to discover the Higgs boson. We have not experimentally measured the Yukawa couplings. Because so little is known, this is a good area to explore changes to the Standard Model. The gauge sector has been extremely successful in predicting experimental results. This makes any modifications severely constrained. I discuss four ways in which modifying the Yukawa sector can produce interesting results that can be tested experimentally at colliders.

In chapter 2 dimension 6 operators, instead of the usual dimension 4 operators, are used to give mass to the fermions. If this theory is correct, it broadens the recent exclusion range for the mass of the Higgs boson from the Tevatron and also increases the double Higgs production.

In chapter 3 a Froggatt-Nielsen mechanism is used to generate the masses and mixings of the quarks in the Standard Model. The Yukawa couplings in this model are all of a similar order. The hierarchy of masses in the Standard Model is generated through higher order interactions involving vector-like quarks and singlet scalars. I show that in one parameterization the  $h \rightarrow \gamma\gamma$  signal is increased by a factor of 10. This mode is very good for early Higgs searches at the LHC.

In chapter 4 a fourth generation is added to the MSSM. Limits are placed on the masses of fourth generation particles based on the perturbativity of their Yukawa couplings. We place very stringent limits on the parameter  $\tan\beta$  and the masses for the  $b'$  and  $t'$  quarks. In order to broaden these limits we construct a model in which the Yukawa couplings are modified by the introduction of new heavy vector-like quarks.

In chapter 5 the problem of Neutrino mass is discussed. We introduce a new way to give masses to neutrinos by fine tuning the values of two different Yukawa coupling matrices. This allows us to have a right handed neutrino that has a mass of about 100 GeV. The new Yukawa interactions change the decay modes of the Higgs drastically, and can be tested at the LHC.

ADVISOR'S APPROVAL: \_\_\_\_\_